

**Circadian regulation of innate immunity and microRNAs
in *Drosophila melanogaster***

by

Jung-Eun Lee

A Dissertation submitted to the
Graduate School-New Brunswick
Rutgers, The State University of New Jersey
and
The Graduate School of Biomedical Sciences
University of Medicine and Dentistry of New Jersey
in partial fulfillment of the requirements
for the degree of Doctor of Philosophy
Graduate Program in Biochemistry
written under the direction of
Professor Isaac Edery
and approved by

New Brunswick, New Jersey

October, 2008

ABSTRACT OF THE DISSERTATION

Circadian regulation of innate immunity and microRNAs in *Drosophila melanogaster*

by

Jung-Eun Lee

Dissertation Director: Dr. Isaac Edery

The main parts of my thesis are studies aimed at investigating circadian regulation of innate immunity using *Drosophila* as a model system. In unrelated work, I also participated in a collaborative study showing circadian regulation of microRNAs (miRNAs) in *Drosophila*.

We sought to determine if the innate immune response is under circadian regulation and whether this impacts overall health status. To this end, *Drosophila* was infected with the human opportunistic pathogenic bacteria *Pseudomonas aeruginosa* as a model system. The results show that the survival rates of wild-type flies vary as a function of when during the day they are infected, peaking in the middle of the night. Also the kinetics of bacterial growth and the expression of a limited number of innate immunity genes correlate with time-of-day effects on survival. Our findings suggest that medical intervention strategies incorporating chronobiological considerations could enhance the innate immune response, boosting the efficacy of combating pathogenic infections. This study also led us to

a second study where we characterized the innate immune response in the *Drosophila* head. We showed that the innate immunity pathway in the head is similar to the well described pathway in the body. Furthermore, the pericerebral fat body in the head or neurons are sufficient to combat bacterial infections, independent of the abdominal fat body. Our findings suggest that the pericerebral fat body may provide a fast and local immune response in the head, improving the survival outcome of *Drosophila*.

A minor aspect of my thesis work was unrelated to host defense. In this study, we used *Drosophila* to investigate the possibility that circadian clocks regulate the expression of miRNAs. From the analysis of microarray data, we found two miRNAs (dme-miR-263a and -263b) that exhibit robust daily changes in abundance in adult heads of wild-type flies that are abolished in the *cyc*⁰¹ mutant. Our results suggest that cycling miRNAs contribute to daily changes in mRNA and/or protein levels in *Drosophila*.

ACKNOWLEDGEMENTS

I'd like to forward my gratitude to the following people for their support in many ways, not only helping me through but also shaping my life here during the last 8 years.

Isaac Edery as my advisor for giving me absolute freedom as to where to head my research, providing the best critique of my work, and guiding me through the publication processes.

My colleagues in the lab: Eun Young Kim and Hyuk Wan Ko for sharing my concerns, their encouragement and exemplary love for family, Kwang Huei Low for being such an inspirational altruist and a portal to his eccentric friends (Guannan Wang, Xiongying Tu), Evrim Yildirim for challenging me with his very original, refreshing, and resourceful perspectives, Joanna Chiu for her lovely styles and sensible optimism, Cecilia Lim for her administrative assistance.

My beloved brother, Jae-Hyeok Lee for being the best example of the true love for science and his witty perspectives for life.

Kwi-Hye Kim, Ji-Yeon Choi and Gye-Hwa Shin for their friendship and all those happy hours together at CABM.

Many scientists in *Drosophila* community for sharing their valuable materials, inspiring advice, useful communication, and practical help: Dmitry Karahentsev, Svetlana Minakhina, Laurence Rahme, Brian Lazzaro, Bruno Lemaitre, Dan Hultmark, Ron Davis, Heig Keshishian, Amita Sehgal, Jeff Hall, Ravi Allada, Shoichiro Kurata and Michael Young.

Maocheng Yang and Richard Padgett for a great collaborative work on the

microRNA study.

My thesis committee members: Ruth Steward, Julie Williams and Celine Gelinas for serving my committee and their helpful advice.

Special thanks to Martin C. Moore-Ede, Frank M. Sulzman, and Charles A. Fuller for writing such an insightful and comprehensive book “The clocks that time us”: It has been an eye-opening reminder to me as to how deeply our environment and circadian timing systems can impact on a wide range of physiological parameters and hence how important it is for a biologist to take relevant physiological contexts into account.

DEDICATION

To my mother, Yoo-Seon Yoon, who has always believed in me

TABLE OF CONTENTS

ABSTRACT OF THE DISSERTATION	ii
ACKNOWLEDGEMENTS	iv
DEDICATION	vi
TABLE OF CONTENTS	vii
LIST OF FIGURES	xi
LIST OF TABLES	xiii
Chapter 1. Introduction	1
Overview.....	1
Circadian Clock	1
<i>Drosophila</i> Circadian Clock.....	3
Innate immunity	8
<i>Drosophila</i> humoral immune response	11
Chapter 2. Circadian regulation in the ability of <i>Drosophila</i> to combat	
pathogenic infections.....	20
Summary	20
Introduction.....	21
Results	23
Time-of-day and clock mutant effects on the survival rates	
of <i>Drosophila</i> infected with <i>P. aeruginosa</i>	23
Bacterial growth kinetics correlate with survival rates in	
rhythmic and clock mutant flies	35

Clock regulation in the induced profiles of innate immunity genes is highly selective and restricted to the early phase of the infection	39
Discussion	46
Materials and Methods	49
Fly strains	49
<i>P. aeruginosa</i> culture.....	49
<i>S. aureus</i> culture	50
Survival experiment.....	50
Bacterial growth assay	51
Quantitative RT-PCR.....	52
Statistical analysis	53
Chapter 3. The immune response in the pericerebral fat body is sufficient to protect the animals from bacterial infections	56
Summary	56
Introduction.....	57
Results	59
RELISH activation in the head follows a similar pathway as that in the body.....	59
The C-terminal fragment of RELISH accumulates faster in the head, which correlates with the extent of posttranscriptional modification	61

A more robust induction of <i>PGRP-SA</i> and <i>drosocin</i> mRNAs in the head, compared with the body.....	64
Processing of RELISH in <i>tim</i> -expressing cells of the head.....	66
RELISH overexpressed mainly in the pericerebral fat body is sufficient to improve the survival of <i>relish</i> null mutants in response to bacterial infections	68
Discussion	71
Materials and Methods.....	74
Fly strains	74
Bacterial culture.....	74
Western blot analysis	75
Survival experiment.....	76
Chapter 4. Circadian regulation of a limited set of conserved microRNAs in <i>Drosophila</i>	77
Summary	77
Introduction.....	79
Results	82
A limited number of miRNAs exhibit circadian regulation in <i>Drosophila</i> heads	82
Possible circadian-relevant targets of dme-miR-263a and 263b	88
Discussion	94
Materials and Methods.....	100

Fly strains and treatment	100
RNA preparation and labelling.....	100
MiRNA microarrays	101
Statistical analysis for microarrays	102
Quantitative RT-PCR.....	102
Chapter 5. Summary.....	104
Circadian regulation in the ability of <i>Drosophila</i> to combat	
pathogenic infections	104
The head immune response in <i>Drosophila</i>	106
References	110
CURRICULUM VITAE.....	126

LIST OF FIGURES

Figure 1.1. Molecular circuitry operating in a <i>Drosophila</i> pacemaker neuron	5
Figure 1.2. Schematic overview of invertebrate innate immunity	10
Figure 1.3. The IMD pathway in adult <i>Drosophila melanogaster</i>	16
Figure 1.4. The Toll pathway in adult <i>Drosophila melanogaster</i>	18
Figure 2.1. Time of infection during a daily cycle and mutations in clock genes modulate the survival outcomes of flies infected with <i>P. aeruginosa</i>	24
Figure 2.2. Time-of-day differences in the survival rates of <i>yw</i> flies infected with <i>P. aeruginosa</i> are observed over a wide range of bacterial doses	29
Figure 2.3. Night-time infections lead to higher survival rates in a variety of wild-type <i>D. melanogaster</i> strains infected with either <i>P. aeruginosa</i> or <i>S. aureus</i>	33
Figure 2.4. Bacterial growth correlates with time of infection and clock mutant effects on survival rates	36
Figure 2.5. <i>Clk^{Jrk}</i> flies exhibit higher survival rates compared to <i>per⁰¹</i> flies even when infected with approximately twice the bacterial dose as that used for <i>per⁰¹</i> flies	38
Figure 2.6. Night-time infection leads to early and transient clock-regulated increases in the mRNA induction profiles of a limited number of immune response genes	40

Figure 2.7. Time-of-day effects on the post-infection profiles for <i>PGRP-SA</i> and <i>drosocin</i> are also observed in the body	42
Figure 2.8. No time-of-day effects on the induction kinetics for <i>attacin A</i> , <i>defensin</i> , <i>diptericin</i> , <i>drosomycin</i> , <i>imd</i> , <i>PGRP-LC</i> , and <i>PGRP-LB</i>	43
Figure 3.1. Cleavage of RELISH in the head depends on <i>dredd</i>	60
Figure 3.2. Comparison of RELISH in the head and body following bacterial infection	62
Figure 3.3. <i>tim</i> -expressing cells are capable of processing RELISH in the head.	67
Figure 3.4. RELISH overexpressed mainly in the pericerebral fat body is sufficient to rescue <i>relish</i> null mutant (<i>Rel^{E20}</i>) in response to <i>E.cloacae</i> β 12 or PA14 <i>plcs</i>	70
Figure 4.1. Heatmap of <i>Drosophila</i> miRNA expression as a function of daily time and in <i>cyc</i> ⁰¹ flies.	83
Figure 4.2. MiRNAs showing significant differences in levels as a function of daily time within the <i>yw</i> control group.....	86
Figure 4.3. MiRNAs showing significant differences in overall daily levels between <i>yw</i> and <i>cyc</i> ⁰¹ flies	89
Figure 4.4. Similarity between some of the miRNAs identified in this study and recently described miRNAs that cycle in mammals.....	97

LIST OF TABLES

Table 2.1. Percent survival of mock-injury groups	27
Table 2.2. Power analysis of the survival rates for <i>yw</i> and clock mutant flies infected in DD	28
Table 2.3. Power analysis of the survival rates of <i>per</i> ⁰¹ and <i>Clk</i> ^{Jrk} flies infected at CT5 or CT17	31
Table 2.4. Sequences of the primers used for quantitative RT-PCR.....	55
Table 3.1. Relative <i>PGRP-SA</i> and <i>drosocin</i> mRNA levels at time 0hr and 2hrs post infection in response to PA14 <i>plcs</i>	65
Table 3.2. Induction fold of <i>PGRP-SA</i> and <i>drosocin</i> mRNAs between 0hr and 2hrs post infection in response to PA14 <i>plcs</i>	65
Table 4.1. Predicted clock-relevant targets for miRNAs identified in this study.....	91

Chapter 1. Introduction

Overview

My thesis work is mostly related to circadian regulation of innate immunity in *Drosophila*. Therefore, I will briefly summarize circadian rhythms and more specifically the mechanism of circadian clock operating in *Drosophila*. Then, I will give an overview of innate immunity in general and its humoral components in *Drosophila*.

Circadian Clock

One of the most obvious and everlasting features of our environment is the daily cycles of light and temperature. Due to the rotation of the earth on its own axis, most creatures on this planet are under the influence of the light-dark cycles. The daily patterns of food availability and predator activities could be critical information for the survival of animals. For example, bees can minimize unfruitful foraging trips by concentrating their visits to flowers at restricted times of day when the nectar and pollens can be offered [1].

The circadian clock is such a timing mechanism that measures the passage of time with about 24-hr period and allows us to adjust to the daily cycles in the environment (circa=about; dies=day). The time cues that provide information regarding the environmental cycling parameters are called zeitgebers ("time

givers” in German). The zeitgebers that can entrain mammals are cycles of light-dark, temperature, food availability, and social cues to name a few, although light is the most prominent entraining cue. The circadian clock is a pacemaker that free-runs with its own endogenous period in the absence of zeitgebers and universally found in animals and plants. Zeitgebers function by synchronizing clocks to local time. The timing information of the circadian clock is ultimately expressed as overt circadian rhythms (output component). The human activity-rest cycle shows 24.2 hr free-running period on average, for example [2]. Due to the difference between the free-running periods of circadian clocks and the 24-hr period of their environment, circadian clocks have to be reset every day. This daily synchronization process is called entrainment.

The importance of entrainment cannot be overstated when it comes to maintaining a good quality of life. Some totally blind people who cannot get any photic input necessary for entrainment suffer from frequent episodes of insomnia and daytime sleepiness due to circadian dysynchrony to the daily light-dark cycles [3]. Frequent shift works and jetlags can also cause a decline in the cognitive performance, quality of sleep, and digestive function as a result of maladaptation of human circadian system to the solar light-dark cycles [1].

The most prominent circadian rhythm studied in humans is the sleep-wake cycle. In addition, there are daily oscillations in body temperature, the level of hormones including insulin, plasma catecholamine, gonadal steroids, cortisol, melatonin, and immune function [1]. Since our cognitive, metabolic, endocrine, and immune functions show circadian variation, time-of-day effects becomes

especially important in medical perspectives: First, any diagnosis should consider the sampling or measurement time to improve its precision. Second, drug administration timing can be optimized to maximize its efficacy and minimize its toxicity [4]. Temporarily optimized drug delivery has proven effective for anesthetics, corticosteroids, antihistamines, and cancer chemotherapeutic agents. For instance, the cure rate of leukemic mice improved by 2-folds, depending on the time of peak dose of cytosine arabinoside, a cancer chemotherapeutic agent [1].

Thus, a key challenge is to understand the basic clock mechanism and how the circadian clock regulates a myriad of physiological and behavioral processes. My work focused on using *Drosophila* as a model system to study the interaction between the circadian clock and host defense.

***Drosophila* Circadian Clock**

Drosophila melanogaster has been one of the best model organisms used to study a range of behaviors such as circadian rhythms, courtship, learning and memory, benefitting from its shorter life span and easier genetic manipulations as compared to mammals. Highly conserved mechanisms generating circadian rhythms between *Drosophila* and mammals add to the merits of using *Drosophila* as a model organism [5].

Although the initial findings regarding circadian rhythms can go back to 1950's, the molecular makeup of intracellular pacemakers has been extensively studied only during the last twenty years. Circadian rhythms rely on daily oscillations in one or more "clock proteins" that are at the core of the timing

mechanism. In *Drosophila*, at least 15 genes have been identified, generating a self-sustaining pacemaker: transcriptional activators [*Clock (Clk)*, *cycle (cyc)*, *Par domain protein 1 ϵ (pdp1 ϵ)*], transcriptional repressors [*period (per)*, *timeless (tim)*, *vri* (*vri*), *clockwork orange (cwo)*], posttranslational modifiers [*doubletime (dbt)*, *casein kinase 2 (CK2)*, *shaggy (sgg)*, *protein phosphatase 1 (PP1)*, *protein phosphatase 2A (PP2A)*, *slimb*, *jetlag (jet)*] and a circadian photoreceptor [*cryptochrome (cry)*]. These clock components participate in two interconnected transcriptional feedback loops collaborated with posttranslational regulatory circuits [6] (Figure 1.1).

CLK and CYC form heterodimers and activate the transcription of many genes including *per* and *tim*. The levels of *per* and *tim* mRNA starts to rise in the early-to-mid day and peaks in the early night. However, PER and TIM levels reach their peak in the middle of night due to the instability of PER and TIM in the presence of light. During the day, PER is phosphorylated by a casein kinase 1 ϵ homologue, DBT, ubiquitinated via F-box protein SLIMB, and degraded by 26S proteasome in the absence of TIM [7, 8]. TIM is also phosphorylated by Tyr kinase or glycogen synthase kinase 3 β homologue SGG, ubiquitinated via F-box protein JET, and degraded by 26S proteasome [9-11]. Light signal is transduced by CRY, contributing to TIM degradation [12]. In the early night, TIM starts to build up in the cytoplasm and heterodimerizes with PER, protecting it from DBT-mediated degradation.

PER-TIM complexes go to the nucleus and inhibit the transcriptional activity of CLK-CYC, leading to the decrease in the levels of *per* and *tim* (negative

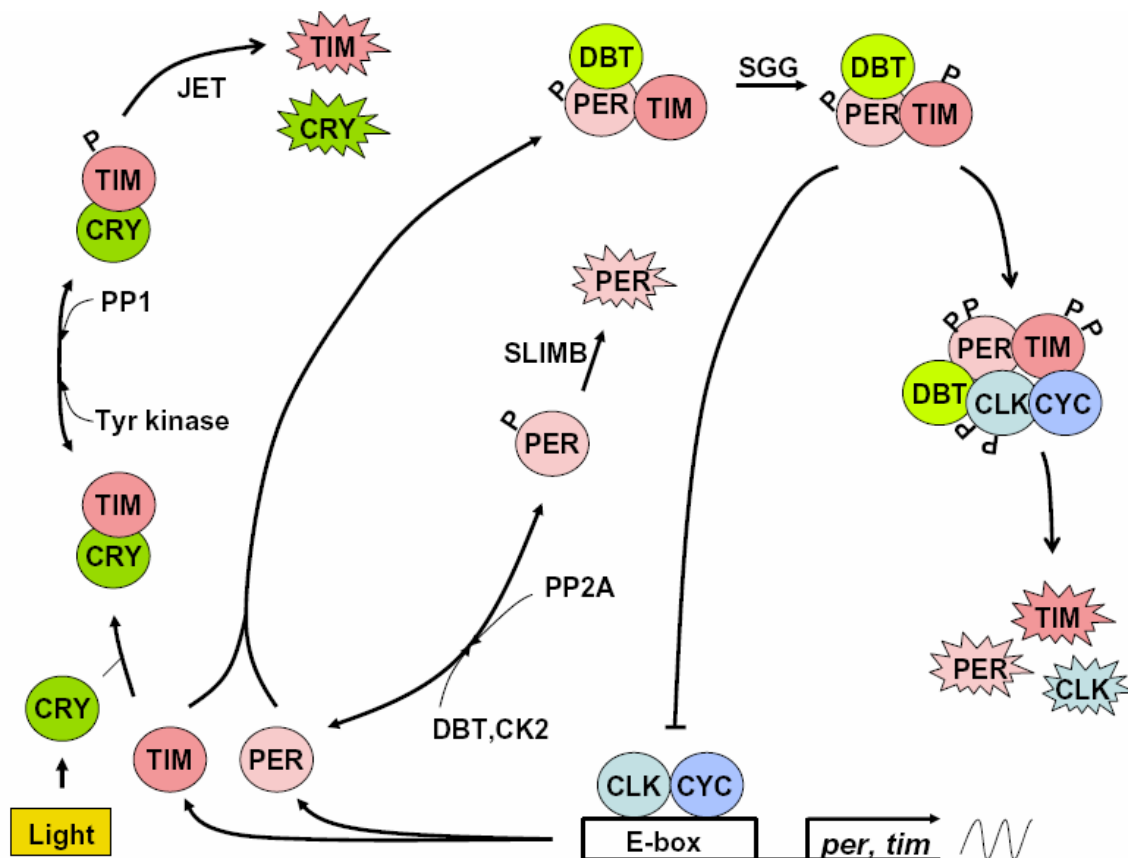



Figure 1.1. Molecular circuitry operating in a *Drosophila* pacemaker neuron

CLK and CYC form heterodimers and activate the transcription of *per* and *tim*. The levels of *per* and *tim* mRNA starts to rise in the early-to-mid day. During the day, CRY binds to TIM in the presence of light, stimulating TIM phosphorylation by an unknown Tyr kinase. On the other hand, PP1 dephosphorylates and stabilizes TIM. Phosphorylated TIM becomes susceptible to proteosomal degradation via JET. JET also expedites CRY degradation. DBT and CK2 phosphorylate and destabilize PER whereas PP2A dephosphorylates and stabilizes PER. Phosphorylated PER becomes susceptible to proteosomal degradation via SLIMB. Due to the instability of PER in the absence of TIM, accumulation of PER and TIM lags several hours behind

Figure Legend 1.1 Continued

that of *per* and *tim* mRNAs. TIM stabilizes PER bound to DBT and this complex translocates to the nucleus, which is expedited by TIM phosphorylation by SGG. In the nucleus, PER-TIM binds to CLK-CYC. DBT recruited by PER-TIM now phosphorylates CLK as well in the same complex, which reduces the transcriptional activity of CLK-CYC. During the mid-night and early morning, without further de novo synthesis of *per* and *tim* mRNAs, the levels of PER and TIM decrease as hyperphosphorylated PER, TIM, and CLK are degraded. It relieves the suppression of CLK-CYC-mediated transcription and starts up another round of feedback loop. For clarity, CLK-CYC feedback loop is not shown. E-box, target cis-acting element of CLK-CYC; wavy line, *per* and *tim* mRNA; P, phosphorylation; , degraded protein.

transcriptional feedback). During the mid-night and early morning, without further de novo synthesis, PER and TIM undergo hyperphosphorylation and subsequently get degraded in the nucleus, which relieves the suppression of CLK-CYC-mediated transcription and starts up another round of feedback loops. Of note, DBT is not the only kinase that phosphorylates PER. CK2 also phosphorylates PER and is involved in the nuclear accumulation of PER [13, 14]. Protein phosphatases as well as protein kinases affect the dynamics of PER stability and subcellular localization. PP2A dephosphorylates and stabilizes PER, expediting its nuclear translocation [15]. On the other hand, PP1 dephosphorylates and stabilizes TIM [16]. DBT and PP2A target CLK as well as PER, keeping the CLK level in a narrow range presumably to tightly control the amplitude of the pacemaker [17, 18].

Circadian pacemakers responsible for the daily rhythm of rest-activity are located in ~ 150 clock neurons of the *Drosophila* brain, which can be categorized into two classes: lateral and dorsal neurons [19]. Especially, lateral neurons are considered major clock neurons that harbor the oscillators governing the timing of locomotor activity peaks in a cell-autonomous manner [20-23]. These multiple rhythmic centers in the brain feature a certain level of interaction and hierarchy among them [19]. Circadian oscillators have also been found outside the brain: eyes, Malpighian tubules [24], and antennae [25]. Antennal neurons contain circadian clocks that are necessary and sufficient to drive olfactory rhythms in *Drosophila* [26].

Compared to the mechanistic studies focusing on the pacemaker

components, little is known about circadian output rhythms in *Drosophila*. Fruit flies show circadian rhythms in locomotor activity, eclosion (emergence of adult flies from their pupal cases), mating, olfactory sensitivity, and feeding [25, 27] (K. Xu, unpublished data). It is very likely that many more physiological behaviors are under circadian regulation in *Drosophila*. It would be informative to get a phase map for every circadian behavior of *Drosophila*: not only would it add much to our general understanding of behavior, but it could also serve as our guide we can refer to when designing or interpreting any physiological experiment.

Innate immunity

Immune systems can be broadly categorized into two classes: innate (natural) and adaptive (acquired) immunity [28]. Innate immunity is an ancient form of first-line defense mechanism and originated early during the evolution of multicellular organisms. It consists of germline-coded factors, recognizes the context of invading microorganisms and instructs the adaptive immune system for appropriate T-cell response or antibody production. On the other hand, adaptive immunity originated much later in the history of evolution and has become a hallmark of vertebrate immunity. It generates receptors that are products of somatic rearrangement and features antigen-specificity and immunological memory [28].

Invertebrates constitute 95% of animals and solely depend on innate immunity to safeguard their health. They have developed the following strategies to survive some hostile environments rich in microorganisms (Figure 1.2): First,

their external cuticles provide an efficient physical barrier. Their digestive tracts, a main entry of pathogens, are also armed with acids and enzymes that can kill microbes. Second, antimicrobial peptides (AMPs), reactive intermediates of oxygen or nitrogen, blood clotting and melanization comprise the humoral defense. Melanization is the deposition of melanin on the blood clots generated upon injury. It occurs via the activation of prophenoloxidase, which catalyzes the oxidation of phenolic compounds to quinones. Quinones then polymerize to form melanin around the wound. Not only the melanized clots can retain the invading microorganisms, but the melanin and the intermediates produced during melanization are toxic to them [29]. Third, hemocytes (blood cells) are responsible for cellular defense. It is composed of phagocytosis, encapsulation, opsonization and free radicals produced by hemocytes. Encapsulation is the process of trapping microbes too large for phagocytosis in hemocyte aggregates, another mechanism devised to limit the spreading of pathogens from their original entry site. Opsonization, on the other hand, is the process to mark the foreign invaders in a way to facilitate the phagocytosis.

Melanization and encapsulation are unique to invertebrates, but there are mammalian counterparts for all the other components of the invertebrate innate immunity. In addition, the roles of the innate immunity do not seem to be functionally redundant with those of adaptive immunity in mammals. For example, disrupted skin normally equipped with AMPs and macrophages puts severely burned patients at high risks of infection. People inheriting mutations in genes coding for complement proteins that play a role in opsonization also suffer from

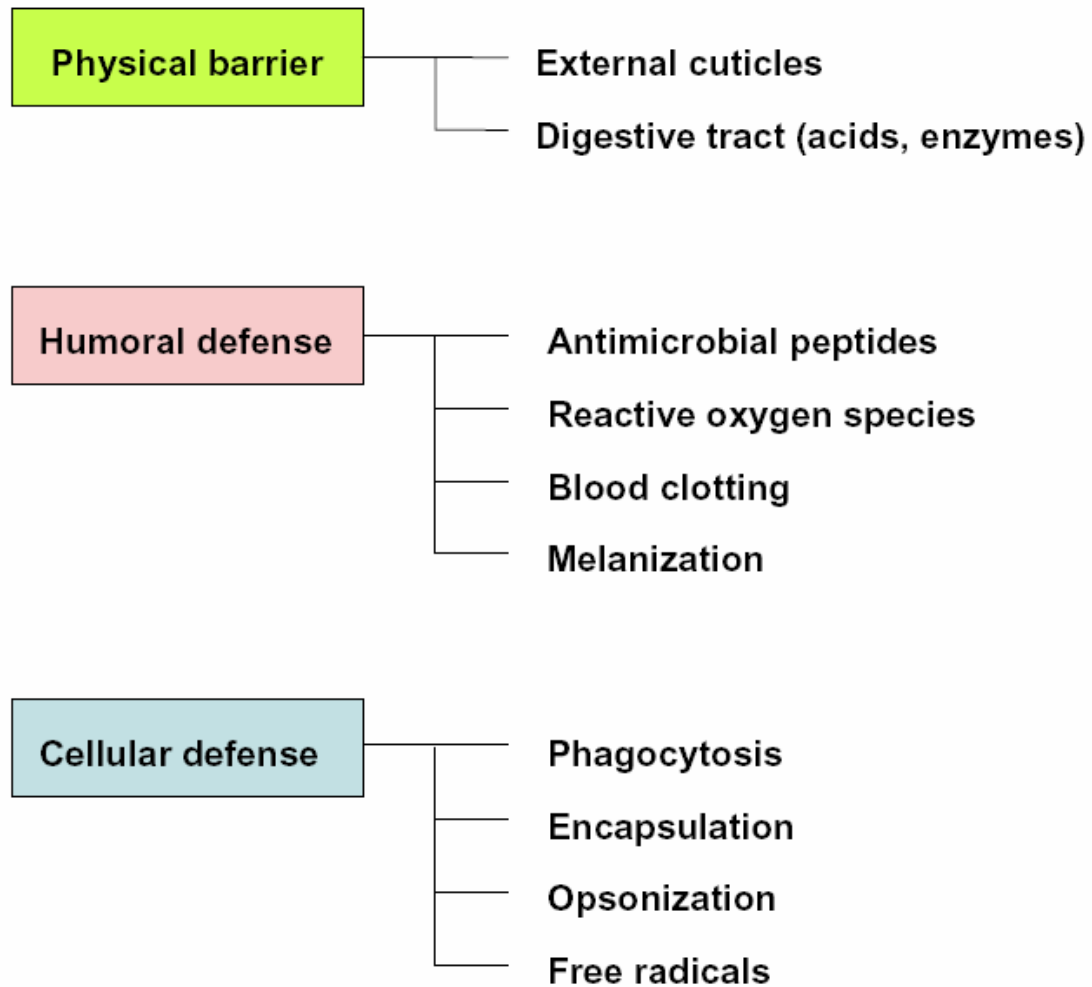


Figure 1.2. Schematic overview of invertebrate innate immunity

Invertebrates are equipped with physical barriers to prevent the entry of microorganisms. They also use a variety of strategies comprising humoral or cellular defense. See text for details.

recurrent infections [30].

In innate immunity, specificity at the level of sensing invading microorganisms is provided by pattern recognition receptors (PRR). They recognize pathogen-associated microbial patterns (PAMPs) shared among groups of pathogens but absent in higher organisms: lipopolysaccharides (LPS) of gram-negative bacteria, glycolipids of mycobacteria, lipoteichoic acids of gram-positive bacteria, mannans of yeasts and double-stranded RNA present in viruses [30]. In mammals, PRRs signaled by PAMPs stimulate the expression of costimulatory molecules in the antigen-presenting cells and the production of cytokines such as IL-1 and TNF- α . The costimulatory molecules and the processed antigens displayed by antigen-presenting cells connect the innate and adaptive immunity by activating T cells essential to adaptive immune responses [30]. The pro-inflammatory cytokines produced as a result of activated PRRs play important roles in clearing the invading pathogens. However, their excessive activation can also lead to septic shock, a leading cause of mortality in patients infected with bacteria [31].

***Drosophila* humoral immune response**

Drosophila has been used as a favorite model organism to study the innate immune response, motivated by the realization of its functional similarities with the system operating in mammals [32, 33]. The availability of powerful genetics approaches and the simplicity of *Drosophila* immune system have benefited mammalian studies, exemplified by the fact work using *Drosophila* led to the

discovery of Toll-like receptors in mammals [32]. Findings from *Drosophila* studies have also revealed numerous insights into understanding host-pathogen interactions [34].

Experimental setups to study *Drosophila* immune response often involve a septic injury method to deliver microbes into flies via wounding, inducing a rapid and massive synthesis of AMPs by the fat body, equivalent to the mammalian liver. The fat body consists of individual cells scattered in patches. It stores glycogen, fats, and proteins and metabolizes sugars, lipids, and proteins. It also regulates blood sugar and synthesizes the major blood proteins. During periods of feeding and growth, it synthesizes and releases proteins into the hemolymph (blood). On the other hand, it reabsorbs and stores accumulated proteins during nonfeeding stages [35]. Being able to control the traffic of metabolites and produce AMPs, the fat body is considered the center of metabolism and humoral immune response in *Drosophila*.

AMPs were the first innate immune player characterized in *Drosophila*. Once synthesized in the fat body, AMPs are released into the hemolymph and accumulate, reaching their overall concentrations as high as 300 μ M [36]. In addition to this systemic response, AMPs are also produced locally in barrier tissues such as the tracheal and gut epithelium [37, 38]. So far 400 AMPs have been reported in several multicellular organisms including insects, plants, and humans. Among these, seven AMPs have been characterized in *Drosophila*: Attacin, Cecropin, Defensin, Diptericin, Drosocin, Drosomycin, and Metchinikowin. Drosomycin and Metchinikowin show anti-fungal activity whereas all the other

AMPs are anti-bacterial [39]. AMPs can lyse bacteria very quickly by permeabilizing bacterial membranes. Resistance of higher eukaryotic membranes to AMPs and their rapid action make AMPs an attractive subject for new classes of antibiotics as well [39].

During the last decade, there has been an explosion in research towards deciphering genetic pathways of *Drosophila* innate immunity. The majority of these studies have been focusing on the humoral immune response culminating in the production of AMPs partly because they provide an easy readout for screening genetic mutants defective in *Drosophila* immunity. These efforts led to the identification of two major signaling pathways leading to the production of AMPs, depending on the types of invading microorganisms: the immune deficiency (IMD) pathway to gram-negative bacteria (Figure 1.3) and the Toll pathway mainly responding to fungi and gram-positive bacteria and (Figure 1.4) [32].

PRRs identified so far in *Drosophila* can be categorized into 3 classes: receptor, scavenger or phagocytic PRR. Eater expressed in hemocytes recognizes bacterial pathogens and mediates phagocytosis [40]. Therefore, it is qualified as a phagocytic PRR. Peptidoglycan recognition proteins (PGRP) and gram-negative binding proteins (GNBP) provide examples of receptor PRRs mediating the IMD/Toll signaling or scavenger PRRs downregulating the immunestimulatory activity of PAMPs. *Drosophila* genome contains 13 genes belonging to the PGRP family and 3 genes to the GNBP family. The GNBP family members have an N-terminal β -(1,3)-glucan binding domain and a C-terminal β -glucanase-like domain [32]. On the other hand, the PGRP family members

harbor PGRP domains some of which retain amidase activity cleaving peptidoglycans (catalytic PGRP) and others have lost it due to the changes in essential amino acids for catalysis (non-catalytic PGRP). Catalytic PGRPs serve as scavenger PRRs whereas some of the non-catalytic PGRPs have been shown to function as receptor PRRs.

Scavenger PRRs such as PGRP-SC1, PGRP-SC2, and PGRP-LB downregulate the immunostimulatory activity of peptidoglycan (PGN). In the gut where there is an endogenous bacterial flora, PGRP-SC1 and PGRP-SC2 are constitutively expressed and keep the level of PGN coming from the gut flora low so that it will not provoke systemic immune response [41]. However, when a large amount of gram-negative bacteria proliferate in the hemolymph, PGRP-LB is induced as a result of the IMD signaling, bringing the host immune system back to the resting state after systemic immune response has been turned on for long enough to clear the invading bacteria [42].

On the other hand, PGRP-LC and PGRP-LE belong to the non-catalytic PGRP members and detect diaminopimelic acid (DAP) peptidoglycan commonly found in the inner cell layer of gram-negative bacteria. They seem to synergize to activate the IMD pathway, possibly as PGRP-LC/PGRP-LE heterodimers [43, 44]. PGRP-SA, another receptor PGRP, cooperates with either PGRP-SD or GNBP1 to activate the Toll pathway in response to gram-positive bacteria [45]. In a proposed model, GNBP1, a catalytic PGRP, hydrolyzes Lys-type peptidoglycan of gram-positive bacteria into muropeptides, presenting them to PGRP-SA so that PGRP-SA can activate downstream Toll signaling pathway [46].

The IMD signaling pathway goes through IMD, *Drosophila* receptor-interacting protein (RIP) homologue (Figure 1.3). Activated PGRP-LC binds to IMD [47], which leads to the activation of TGF β -activated kinase 1 (dTAK1) [48] and I κ B kinase (IKK) complex [49, 50] in one arm. IMD can also recruit Fas-associated death domain (dFADD) [51, 52] and death-related ced-3/Nedd2-like protein (DREDD) [53] in another arm. Activated IKK complex phosphorylates RELISH [54], a *Drosophila* NF- κ B homologue, while DREDD is required for RELISH cleavage [55, 56]. On the other hand, Caspar suppresses the DREDD-dependent cleavage of RELISH, participating in the downregulation of the IMD pathway [57]. Then, the phosphorylated C-terminal I κ B-like fragment of RELISH remains in the cytosol and its N-terminal fragment containing a DNA-binding REL homology domain goes to the nucleus, transactivating its downstream target genes such as AMP genes [55].

The Toll signaling pathway begins with the activation of proteolytic cascades triggered by PRRs such as GGBP3 for fungi [58] and PGRP-SA/PGRP-SD/GGBP1 for gram-positive bacteria (Figure 1.4). It ultimately leads to the activation of Spatzle-processing enzyme (SPE), which in turn cleaves Spatzle [59]. The processed form of Spatzle binds to Toll, receptor of the Toll pathway [60]. The Toll dimerized by Spatzle recruits two adaptor molecules, myeloid differentiation primary response gene 88 (dMyD88) [61] and Tube, and the *Drosophila* homologue of interleukin 1 receptor-associated kinase (IRAK), Pelle. In turn, Cactus, *Drosophila* homologue of I κ B, becomes phosphorylated by unknown kinase(s), ubiquitinated, and degraded rapidly. Phosphorylation of Cactus relieves Dorsal and Dorsal-related immunity factor (DIF), *Drosophila* NF- κ B

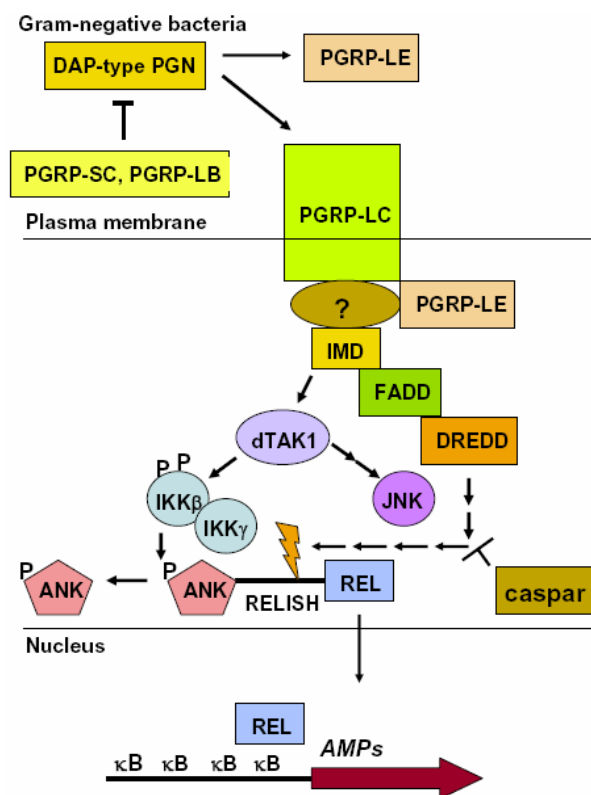


Figure 1.3. The IMD pathway in adult *Drosophila melanogaster*

DAP-type PGN from gram-negative bacteria or gram-positive bacilli binds to either PGRP-LCa/PGRP-LCx, heterodimers consisting of two isoforms of PGRP-LC, or possibly PGRP-LCx/PGRP-LE heterodimers. It triggers the activation of IMD, mediated by an unknown molecule, followed by the recruitment of FADD and DREDD in one arm. In the second arm, IMD also activates dTAK1, followed by the activation of the JNK pathway and the IKK complex. Active IKK complex in turn phosphorylates RELISH, which primes it for the DREDD-dependent proteolytic cleavage. Once cleaved, The N-terminal fragment of RELISH goes to the nucleus and transactivates its target genes, including AMP genes such as *dipthericin*. Activation of the JNK pathway also contributes to the *AMP* induction. On the other

Figure Legend 1.3 Continued

hand, scavenger molecules PGRP-SC1, PGRP-SC2, and PGRP-LB cleave PGN to downregulate its immunostimulatory activity. Caspar also participates in the downregulation of the IMD pathway by suppressing the DREDD-dependent cleavage of RELISH. P, phosphorylation; ⚡, proteolytic cleavage.

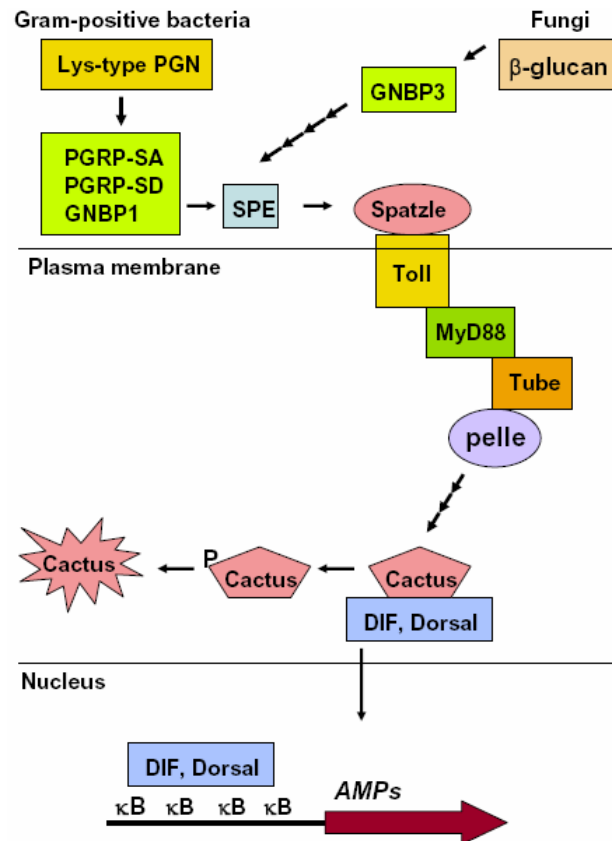


Figure 1.4. The Toll pathway in adult *Drosophila melanogaster*

Lys-type PGN from gram-positive bacteria binds to PGRP-SA/GNB1 or PGRP-SA/PGRP-SD complex whereas β -glucan from fungi binds to GNB3. These activated PRRs triggers the activation of proteolytic cascades, leading to the processing of Spatzle by SPE. The processed form of Spatzle binds to Toll. The Toll dimerized by Spatzle in turn recruits dMyd88, tube and pelle. Cactus becomes phosphorylated by unknown kinase(s) and degraded in the cytosol. DIF and Dorsal are released upon phosphorylation of Cactus, go to the nucleus and transactivate their target genes, including AMP genes such as *drosomycin*. P, phosphorylation.

homologues, allowing them to translocate to the nucleus and activate their target genes such as *drosomycin*. In adult flies, DIF plays a major role for the Toll-mediated immune response [62]. However, Gordon et al showed that Dorsal regulates the expression of *diptericin* and *wntD*, Wnt inhibitor of Dorsal, whose mutation affects the mortality of adult flies in response to pathogenic gram-positive bacteria [63].

My work described in this thesis provides the first evidence to show that a part of *Drosophila* innate immune response is under circadian regulation and it is correlated with the survival outcomes of adult flies in response to pathogenic bacterial infections. This study led us to a finding that the head immune response appears to show a sharper initial induction to bacterial stimuli as compared to the body one. Moreover, as tissues participating in the head immune response, the pericerebral fat body and neurons are sufficient to protect *relish* null mutant flies from pathogenic gram-negative bacterial infections when overexpressing RELISH. In the last part of my thesis, I'll describe a collaborative project unrelated to immunity, whereby we showed two miRNAs in *Drosophila*, dme-miR-263a and -263b, are regulated by the circadian clock.

Chapter 2. Circadian regulation in the ability of *Drosophila* to combat pathogenic infections

Summary

In this chapter, we sought to determine if the innate immune response is under circadian regulation and whether this impacts overall health status. To this end, we used infection of *Drosophila* with the human opportunistic pathogenic bacteria *Pseudomonas aeruginosa* as our model system [64]. We show that the survival rates of wild-type flies vary as a function of when during the day they are infected, peaking in the middle of the night. Although this rhythm is abolished in clock mutant flies, those with an inactive *period* gene are highly susceptible to infection, whereas mutants with impairment in other core clock genes exhibit enhanced survival. After an initial phase of strong suppression, the kinetics of bacterial growth correlates highly with time-of-day and clock mutant effects on survival. Expression profiling revealed that night-time infection leads to a clock-regulated transient burst in the expression of a limited number of innate immunity genes. Circadian modulation of survival was also observed with another pathogen, *Staphylococcus aureus*. Our findings suggest that medical intervention strategies incorporating chronobiological considerations could enhance the innate immune response, boosting the efficacy of combating pathogenic infections.

Introduction

One of the well documented circadian rhythm in mammals is the daily oscillations in immune parameters. For instance, the levels of human pro-inflammatory cytokines in response to *E. Coli* LPS vary across a day, depending on the time of stimulation [65]. The innate immune response [32, 33] and circadian clock mechanisms [5] are both highly conserved between *Drosophila* and mammals. In light of the recent interest in chronotherapy and output rhythms in *Drosophila*, we set out to determine if a circadian clock regulates the humoral immune response in *Drosophila*.

We initially focused on the humoral systemic immune response at the level of induction of AMP genes because it is the best characterized immune response in *Drosophila*. I also chose to use a bacterial infection model as opposed to fungal one, considering it takes several days to a week to induce anti-fungal immune response. During early investigations, the levels of induced AMP genes and the kinetics of bacterial growth were used as the only read-outs to evaluate possible time-of-day effects on innate immunity, using nonpathogenic bacteria. However, initial attempts to get reproducible daily patterns of these read-outs from infections with nonpathogenic bacteria were not successful, suggesting a possibility that time-of-day effects may be limited to a subset of innate immunity responsible for fighting pathogenic infections. Therefore, I tested a range of pathogenic bacteria and scored the survival rates of infected flies as a primary read-out to evaluate the reproducibility of the circadian pattern of the innate immune response in *Drosophila*. *Pseudomonas aeruginosa* and *Staphylococcus aureus* were chosen

for further study because not only they provided a reproducible circadian pattern of survival rates in optimized conditions but studies using them may also add more insights into understanding these human opportunistic pathogens commonly found in hospital-acquired infections [34, 64].

Here we show that the survival rates of wild-type flies vary as a function of when during the day they are infected, peaking in the middle of the night. Also the kinetics of bacterial growth and the expression of a limited number of innate immunity genes correlate with time-of-day effects on survival. Our findings provide a *Drosophila* model system where the link between circadian clock and innate immunity can potentially be characterized in detail.

Results

Time-of-day and clock mutant effects on the survival rates of *Drosophila* infected with *P. aeruginosa*

To test if the circadian system modulates the ability of *D. melanogaster* to combat a pathogenic infection, we first entrained control rhythmic flies (*yw*) under standard 12 hr light/12 hr dark cycles [LD; where zeitgeber time 0 (ZT0) is defined as lights-on] for 2 days and on the third day inoculated them at different times of day with the PA14-isogenic mutant strain of *P. aeruginosa*, which is defective in *phospholipase C* (PA14 *plcs*) [66] (Figure 2.1A and B). The PA14 *plcs* strain is a less virulent strain than PA14 and was chosen in our studies because although infection with this attenuated strain evokes rapid mortality (between 1-2 days) of many flies, a sizable proportion survives throughout an extended post-infection observation period (at least 1 week in our standard experimental setup; termed ‘survivors’) (Figure 2.1A and B), as previously reported [66]. By establishing conditions that yielded a mixed population response with individuals that succumbed quickly to the infection and those that survived over an extended period of time, this allowed us to better evaluate whether the clock modulates the ability of flies to successfully combat a pathogenic infection. Adult flies were infected by the standard method of lightly stabbing their abdomens with a fine needle dipped in a concentrated liquid culture containing PA14 *plcs*. We also included control groups that were contemporaneously mock-treated with needles placed in just the growth media (on average, 90-100% of the flies stabbed

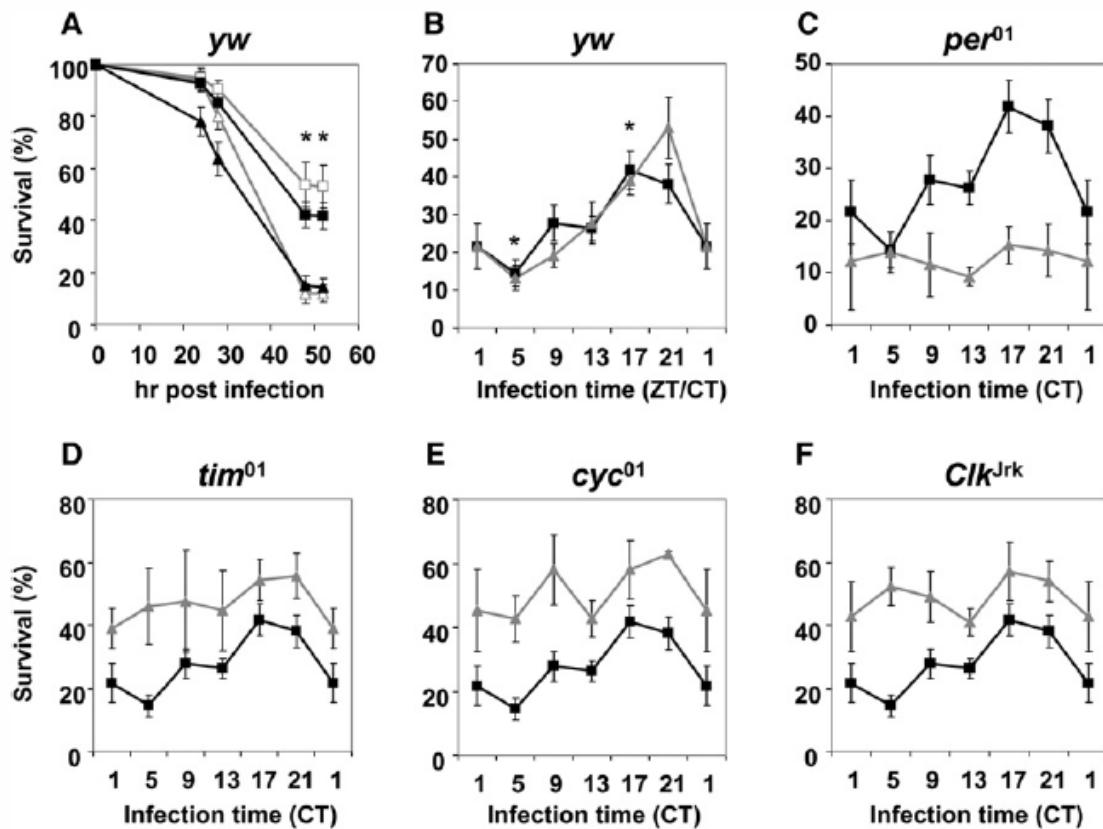


Figure 2.1. Time of infection during a daily cycle and mutations in clock genes modulate the survival outcomes of flies infected with *P. aeruginosa*

(A) Time course in the proportion of *yw* flies surviving after infection with PA14 *plcs* at ZT5 (open triangles, *n* = 251; indicates total number of flies from several independent experiments that were infected and used to calculate the average survival data shown) and ZT21 (open squares, *n* = 249) during LD, or CT5 (filled triangles, *n* = 321) and CT17 (filled squares, *n* = 321) during DD. Asterisks indicate significantly higher survival rates for the ZT21- or CT17-groups compared to the ZT/CT5-groups (two-tailed Student's *t*-test; * denotes *p* < 0.005).

Figure Legend 2.1 Continued

(B) Survival rates of *yw* flies infected with PA14 *p/lcs* at different times of day during either LD (grey triangles, $n = 246-253$; i.e., indicates the range in the total number of flies from several independent experiments that were infected at the different times in a daily cycle) or DD (black squares, $n = 315-323$). Survival profiles were evaluated by one-way ANOVA followed by Tukey-Kramer HSD analysis with the following results; (1) in LD, the ZT21-group survived better than the ZT1-, ZT5-, or ZT9- groups (one-way ANOVA, $p < 0.0005$; Tukey-Kramer HSD, $\alpha = 0.01$). At $\alpha = 0.001$, only the ZT5-group died significantly more than the ZT21-group; (2) in DD, the CT17- and CT21-groups have higher survival rates compared to the CT5-group (one-way ANOVA, $p < 0.005$; Tukey-Kramer HSD, $\alpha = 0.05$). At $\alpha = 0.01$, only the CT17-group exhibited significantly higher survival compared to the CT5-group (*). (C-F) Survival rates of clock mutant flies (grey triangles) infected with PA14 *p/lcs* during DD compared to control *yw* flies (black squares). Results reflect the average of at least three independent experiments. Error bars indicate S.E.M.

with control needles survived to the end of the test period; Table 2.1). Control (yw) flies exhibit a diurnal profile in their survival rates (one-way ANOVA, $p < 0.0005$ for Figure 2.1A and B). Tukey-Kramer HSD analysis indicated that control flies infected at ZT21 have significantly higher rates of survival than those infected at ZT1, 5, or 9 (when $\alpha = 0.01$; see also legend to Figure 2.1). Flies infected at ZT21 survived approximately 4-fold better compared to the trough values at ZT5 (two-tailed Student's *t*-test, $p < 0.005$ at 48 hrs post infection and thereafter) (Figure 2.1A and B). We observed a similar daily pattern in survival rates when inoculating flies with bacterial titers 5- to 20-fold lower compared to our standard conditions (compare Figures 2.1A and 2.1B to 2.2), demonstrating that the time-of-day effects on survival are observed over a broad range of initial bacterial doses.

To determine if the survival rhythm is endogenously driven, flies were entrained by three LD cycles and subsequently maintained in constant darkness (DD) followed by inoculation on the second day of DD. In addition, we also infected the well-characterized *per*⁰¹, *tim*⁰¹, *Clk*^{Jrk} and *cyc*⁰¹ arrhythmic clock mutants that carry inactivated *period* (*per*), *timeless* (*tim*), *clock* (*Clk*) and *cycle* (*cyc*) genes, respectively [5]. To minimize genetic background effects, the clock mutants were evaluated in the same yw background as the control strain.

Daily changes in the survival rates of control rhythmic flies were also observed in DD (Figure 2.1B; one-way ANOVA, $p < 0.005$; statistical analysis summarized in legend to Figure 2.1 and Table 2.2). The profile in constant darkness was almost identical to that observed in LD except that flies infected at

Table 2.1. Percent survival of mock-injury groups

Cycle	Genotype	n	Infection time (ZT/CT)	Survival (%) (Mean \pm SEM)	Independent experiments
LD3	<i>yw</i>	125	1	96.0 \pm 0.0	5
LD3	<i>yw</i>	125	5	100.0 \pm 0.0	5
LD3	<i>yw</i>	125	9	97.3 \pm 1.3	5
LD3	<i>yw</i>	125	13	98.7 \pm 1.3	5
LD3	<i>yw</i>	125	17	100.0 \pm 0.0	5
LD3	<i>yw</i>	125	21	97.3 \pm 1.3	5
DD2	<i>yw</i>	150	1	97.5 \pm 1.2	6
DD2	<i>yw</i>	150	5	97.0 \pm 1.9	6
DD2	<i>yw</i>	150	9	98.5 \pm 1.0	6
DD2	<i>yw</i>	149	13	98.0 \pm 0.9	6
DD2	<i>yw</i>	150	17	96.7 \pm 1.1	6
DD2	<i>yw</i>	150	21	96.7 \pm 1.2	6
DD2	<i>per</i> ⁰¹	69	1	89.3 \pm 7.1	3
DD2	<i>per</i> ⁰¹	70	5	93.0 \pm 2.5	3
DD2	<i>per</i> ⁰¹	70	9	95.7 \pm 0.3	3
DD2	<i>per</i> ⁰¹	69	13	90.0 \pm 5.8	3
DD2	<i>per</i> ⁰¹	70	17	79.3 \pm 8.4	3
DD2	<i>per</i> ⁰¹	70	21	81.0 \pm 10.7	3
DD2	<i>tim</i> ⁰¹	70	1	91.3 \pm 4.7	3
DD2	<i>tim</i> ⁰¹	70	5	94.3 \pm 1.2	3
DD2	<i>tim</i> ⁰¹	70	9	97.3 \pm 2.7	3
DD2	<i>tim</i> ⁰¹	70	13	94.7 \pm 1.3	3
DD2	<i>tim</i> ⁰¹	69	17	95.7 \pm 2.3	3
DD2	<i>tim</i> ⁰¹	70	21	92.0 \pm 4.6	3
DD2	<i>cyc</i> ⁰¹	75	1	93.3 \pm 1.3	3
DD2	<i>cyc</i> ⁰¹	75	5	98.7 \pm 1.3	3
DD2	<i>cyc</i> ⁰¹	75	9	100.0 \pm 0.0	3
DD2	<i>cyc</i> ⁰¹	75	13	97.3 \pm 1.3	3
DD2	<i>cyc</i> ⁰¹	75	17	98.7 \pm 1.3	3
DD2	<i>cyc</i> ⁰¹	75	21	98.7 \pm 1.3	3
DD2	<i>Clk</i> ^{Jrk}	65	1	95.3 \pm 0.3	3
DD2	<i>Clk</i> ^{Jrk}	65	5	90.7 \pm 0.7	3
DD2	<i>Clk</i> ^{Jrk}	65	9	93.7 \pm 4.5	3
DD2	<i>Clk</i> ^{Jrk}	65	13	92.3 \pm 4.3	3
DD2	<i>Clk</i> ^{Jrk}	65	17	90.7 \pm 5.8	3
DD2	<i>Clk</i> ^{Jrk}	65	21	86.7 \pm 10.9	3

Table 2.2. Power analysis of the survival rates for *yw* and clock mutant flies infected at 6 different times in DD

Genotype	n	Independent experiments	p-value ^a of one-way ANOVA	Power ^b	LSN ^c	Number of observations	LSE ^d
<i>yw</i>	321	6	0.0029	0.9460	22	36	4
<i>per</i> ⁰¹	155-160	3	0.9739	0.0741	259	18	44
<i>tim</i> ⁰¹	137-140	3	0.8825	0.1051	123	18	21
<i>cyc</i> ⁰¹	147-151	3	0.4178	0.2621	41	18	7
<i>Clk</i> ^{Jrk}	125-139	3	0.6614	0.1690	65	18	11

^a P-value represents the probability to get the current data set when the survival rates of flies do not vary as a function of infection time.

^b Power represents the probability to obtain significance at or below a given p-value for a given situation.

^c LSN (Least Significant Number) represents the total number of observations that would give rise to a specified p-value (0.05 in this power analysis) given that the data has the same form.

^d LSE (Least Significant Experiment) represents the total number of experiments that would give rise to a specified p-value (0.05 in this power analysis) given that the data has the same form. Each experiment involves 6 observations (survival rates of flies infected at 6 different times; see Figure 2.1).

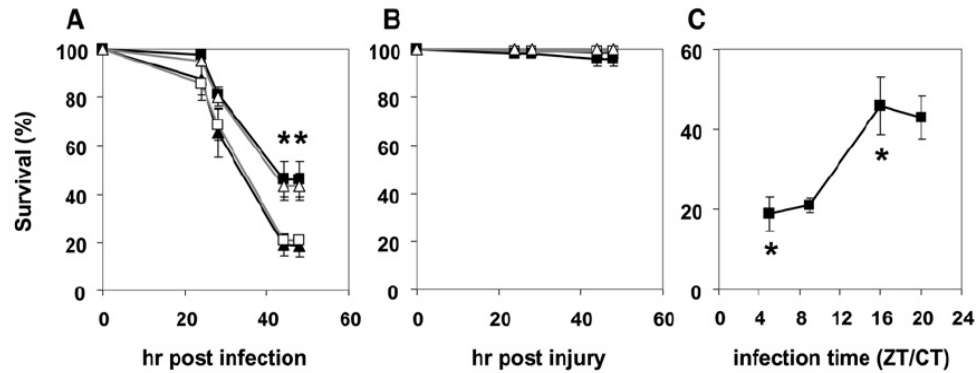


Figure 2.2. Time-of-day differences in the survival rates of *yw* flies infected with *P. aeruginosa* are observed over a wide range of bacterial doses

(A) Time course for the survival rates of *yw* flies infected with PA14 *plcs* at ZT5 (filled triangles, $n = 235$), ZT9 (open squares, $n = 234$), ZT16 (filled squares, $n = 230$), or ZT20 (open triangles, $n = 233$) during LD when the initial bacterial dose was 5- to 20-fold less than the standard amount used in figures 2.1, 2.3, 2.4 and 2.6-2.8 (A_{600} reading of the final bacterial solution ranged between 5 and 20). Asterisks indicate significantly higher survival rates for the ZT16- and 20-groups compared to the ZT5- and 9-groups (one-way ANOVA, $p < 0.005$; Tukey-Kramer HSD, $\alpha = 0.05$). At $\alpha = 0.01$, only the ZT5-group died significantly more than the ZT16-group. Results reflect the average of five independent experiments, one of which was performed on the first day of DD and produced similar results (data not shown). Error bars indicate S.E.M. (B) Time course for the survival rates of control *yw* flies that were treated with clean needles at ZT5 (filled triangles, $n = 195$), ZT9 (open squares, $n = 194$), ZT16 (filled squares, $n = 194$), or ZT20 (open triangles, $n = 194$). (C) Survival rates of *yw* flies infected with PA14 *plcs* at ZT5, 9, 16, or 20. The corresponding data at 48 hrs post-infection shown in panel A was plotted to better show the daily rhythm in survival rates.

circadian time 17 (CT17; in this manuscript we use the term CT as equivalent to ZT, which is a reasonable approximation given the near 24 hr behavioural rhythms of *Drosophila*) showed the best survival rates (Tukey-Kramer HSD when $\alpha = 0.01$). Flies infected at CT17 survived approximately 3-fold better compared to the trough values observed at CT5 (two-tailed Student's *t*-test, $p < 0.005$ at 48 hrs post infection and thereafter) (Figure 2.1A and B; Table 2.2). Importantly, similar results whereby survival rates are significantly higher at CT17 compared to CT5 were also observed when using rhythmic flies with different genetic backgrounds, including the *Canton-S* (CS) and *Oregon R* (OR) wild-type strains (Fig. 2.3A; two-tailed Student's *t*-test, $p < 0.05$; and data not shown).

In contrast to rhythmic control and wild-type strains, a daily survival rhythm was not observed in the four arrhythmic clock mutant strains tested (Figure 2.1C-F; one-way ANOVA, $p > 0.05$, Table 2.2). More extensive analysis comparing CT5 and CT17 groups did not reveal significant time-of-day differences in the survival rates of *per*⁰¹ or *Clk*^{Jrk} flies (Table 2.3). Although we cannot rule out the possibility of small but real time-of-day variations in the survival rates of the clock mutants (Tables 2.2 and 2.3), our data indicate that the robust daily rhythm observed in control and wild-type flies is either abolished or greatly attenuated in the mutants. In addition, close inspection of the survival patterns of the clock mutants suggests the possibility of low amplitude cycles that peak twice per day (Figure 2.1C-F). Intriguingly, in many cases higher frequency 'ultradian' rhythms are more readily observed or enhanced when circadian systems are severely compromised [67].

Although we do not observe robust daily rhythms in survival for the different

Table 2.3. Power analysis of the survival rates of *per*⁰¹ and *Clk*^{Jrk} flies infected at CT5 or CT17

Genotype	n	Independent experiments	p-value of two-tailed Student's t-test	power	LSN	Number of observations	LSE ^a
<i>per</i> ⁰¹	366	8	0.6593	0.0705	306	16	153
<i>Clk</i> ^{Jrk}	315	7	0.6071	0.0776	196	14	98

^a LSE (Least Significant Experiment) represents the total number of experiments that would give rise to a specified p-value (0.05 in this power analysis) given that the data has the same form. Each experiment involves 2 observations in this analysis (survival rates of flies infected at CT5 or CT17).

arrhythmic clock mutants analyzed, *per*⁰¹ flies manifested relatively higher mortality rates compared to control flies, whereas *tim*⁰¹, *Clk*^{Jrk} and *cyc*⁰¹ flies showed overall enhanced survival compared to control flies (Figure 2.1C-F). Similar results were also obtained when examining the survival patterns of the clock mutants in LD, except that mortality of all the clock mutants tested was overall slightly higher during the daytime, suggesting that in these mutants the light/dark conditions have direct effects on the ability to survive the infection (data not shown). While our manuscript was under review, Shirasu-Hiza et al. (2007) reported that *per*⁰¹ flies were more susceptible to *Streptococcus pneumoniae* and *Listeria monocytogenes* compared to wild-type flies [68] consistent with our findings. However, in that study *tim*⁰¹ flies also succumbed to death faster than wild-type flies when infected with the same pathogens. The possible discrepancy between the two studies with regards to the ability of *tim*⁰¹ flies to survive pathogenic infections is presently unclear and might be due to the use of different bacteria and/or the mode of pathogenicity. Although the reasons underlying the differential effects of clock mutations are not known, the collective findings suggest that *per* function plays a protective role in *Drosophila* infected with pathogenic bacteria. Future studies will be required to better evaluate the roles of the different clock genes in innate immunity.

To expand our observations we also inoculated wild-type flies with another human pathogenic bacteria, *Staphylococcus aureus* (*S. aureus*), which unlike *P. aeruginosa* is gram-positive. As with *P. aeruginosa*, the CT17-group exhibited higher rates of survival compared to the CT5-group (Figure 2.3B; two-tailed

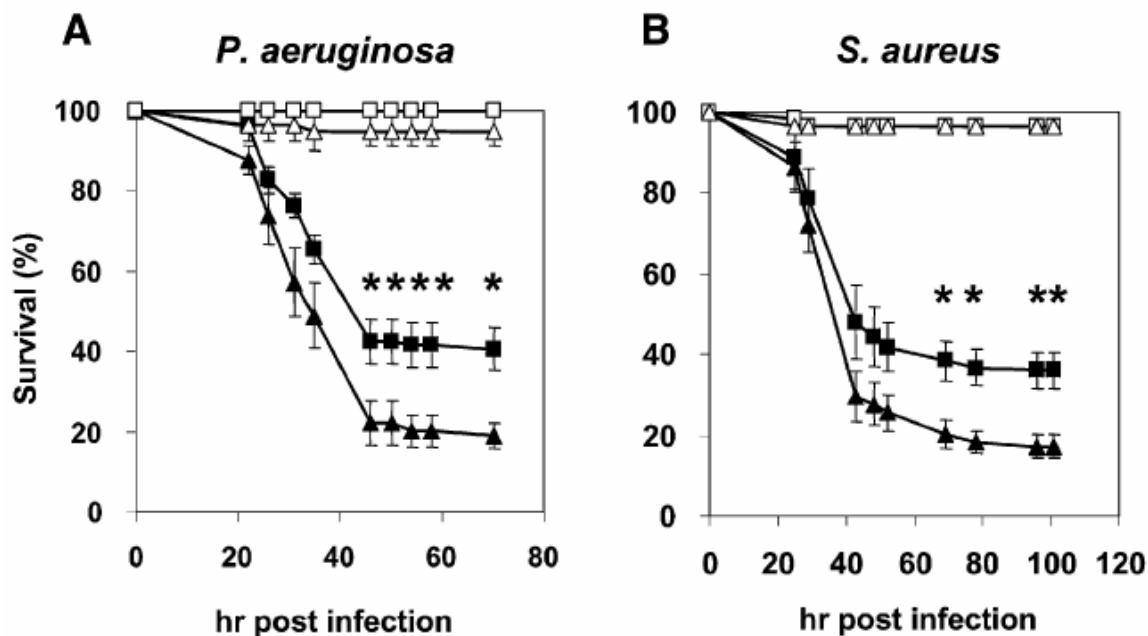


Figure 2.3. Night-time infections lead to higher survival rates in a variety of wild-type *D. melanogaster* strains infected with either *P. aeruginosa* or *S. aureus*

(A) Time course depicting the survival rates of wild-type flies (*Canton-S* and *Oregon R*) infected with PA14 *plcs* at CT5 (filled triangles) and CT17 (filled squares) on the second day of DD; also shown, mock-injury groups pricked at CT5 (open triangles) and CT17 (open squares). Very similar survival curves were obtained for *Canton-S* and *Oregon R* flies (data not shown), and hence the data were pooled. Results are the average of four independent experiments and indicate significantly higher survival rates for flies infected at CT17 compared to CT5 (two-tailed Student's t-test; CT5 vs. CT17, *denotes $p < 0.05$). Error bars indicate S.E.M. The number of flies analyzed is as follows: $n = 151$ for the infected CT5-group, $n = 154$ for the infected CT17-group, $n = 70$ for the mock injury CT5- or CT17- groups. (B) Time course depicting the survival rates of wild-type flies

Figure Legend 2.3 Continued

(*Canton-S* and *Oregon R*) infected with *S. aureus* at CT5 (filled triangles) and CT17 (filled squares); also shown, mock-injury groups pricked at CT5 (open triangles) or CT17 (open squares). Results are the average of four independent experiments and indicate significantly higher survival rates for flies infected at CT17 compared to CT5 (two-tailed Student's *t*-test; CT 5 vs. CT 17, *denotes $p < 0.05$). Error bars indicate S.E.M. The number of flies analyzed is as follows: $n = 160$ for the infected CT5- or CT17-group, $n = 80$ for the mock injury CT5- or CT17-group.

Student's *t*-test, $p < 0.05$). Taken together, the findings indicate that *Drosophila* survive night-time infections significantly better than day-time ones.

Bacterial growth kinetics correlate with survival rates in rhythmic and clock mutant flies

To determine whether the kinetics of bacterial growth correlate with the survival patterns observed, we infected control, *per*⁰¹ and *Clk*^{Jrk} flies on the second day of DD at either CT5 or 17, the trough and peak times for survival rates, respectively (Figure 2.1). Live flies were collected at several times post-inoculation and bacterial titers measured (Figure 2.4). In each experiment, all three genotypes were contemporaneously treated and the results from multiple experiments pooled. Also, a subset of flies were not processed for the bacterial assays but were scored for survival and in rare cases where anomalous survival results were obtained (e.g., little or no mortality) the bacterial data from that experiment was not used. Irrespective of the infection time, all genotypes showed strong decreases in bacterial titers during the first 5 hr post-infection (Figure 2.4A-C). However, in control *yw* flies, the CT5-group had significantly higher bacterial loads at 10 and 23 hr post-infection compared to the CT17-group (two-tailed Student's *t*-test, $p < 0.05$ for 10 hr, $p = 0.01$ for 23h), whereas *per*⁰¹ and *Clk*^{Jrk} flies did not exhibit significant differences in bacterial loads as a function of infection time (Figure 2.4A-D). Nonetheless, the titer of PA14 *plcS* in *per*⁰¹ flies increased between 5 to 10 hr post-infection but remained very low in *Clk*^{Jrk} flies (Figure 2.4B and C). Indeed, pair-wise comparisons indicated significantly higher levels of bacteria in *per*⁰¹ flies

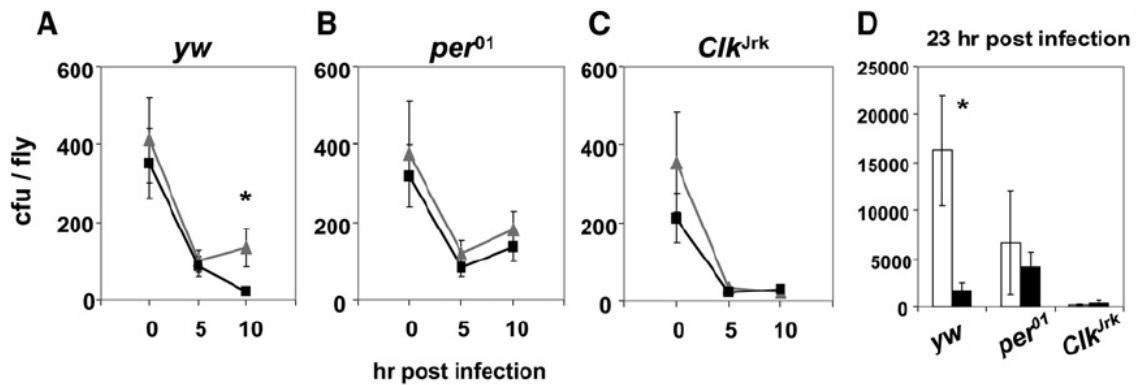


Figure 2.4. Bacterial growth correlates with time of infection and clock mutant effects on survival rates

(A-D) Flies of the indicated genotype were infected at either CT5 (grey triangles or open bars) or CT17 (black rectangles or filled bars) and collected at the indicated times. Asterisks indicate significantly higher bacterial titer for the control CT5-group compared to the CT17-group (two-tailed Student's *t*-test, $p < 0.05$). Results from at least three independent experiments were combined. Mean \pm S.E.M. and values obtained from at least 60 flies per collection time are displayed ($n = 60-128$, $95-130$, $67-90$ for *yw*, *per⁰¹*, and *ClkJrk* flies, respectively).

at 10 and 23 hr post-infection compared to *Clk^{Jrk}* flies (Table 2.3), consistent with its relatively lower survival rates (Figures 2.1 and 2.5).

To further demonstrate that *per⁰¹* flies have higher mortality rates compared to *Clk^{Jrk}* flies, we infected *per⁰¹* flies with approximately half the number of bacteria as *Clk^{Jrk}* flies (Figure 2.5A) and compared their survival rates (Figure 2.5B). Despite the lower bacterial load used in the infection, significantly more *per⁰¹* flies died compared to *Clk^{Jrk}* flies (two-tailed Student's *t*-test, $p < 0.01$ after 52 hrs post infection, $\alpha = 0.05$; Figure 2.5B). These results are consistent with the observation that similar survival rhythms are observed in control flies over a wide range of initial bacterial doses (Figure 2.2). Thus, the time-of-day differences observed in rhythmic flies, and the enhanced survival of *Clk^{Jrk}* compared to *per⁰¹* flies cannot be accounted by possible experimental variations in the amount of bacteria used during inoculation.

In summary, after an initial phase of bacterial clearance, there is a tight correlation between bacterial loads and survival outcomes, both for wild-type flies as a function of circadian time and when comparing clock mutants. Indeed, the early bacterial growth pattern in *per⁰¹* flies mimics that observed in the wild-type CT5-group, increasing after 5 hr post-infection, whereas the *Clk^{Jrk}* response is more similar to the wild-type CT17-group, which declines or remains low at 10 hr post-infection. Thus, our findings suggest that the ability to suppress bacterial growth during the first 10 hr after infection is causally linked to better prognosis for survival.

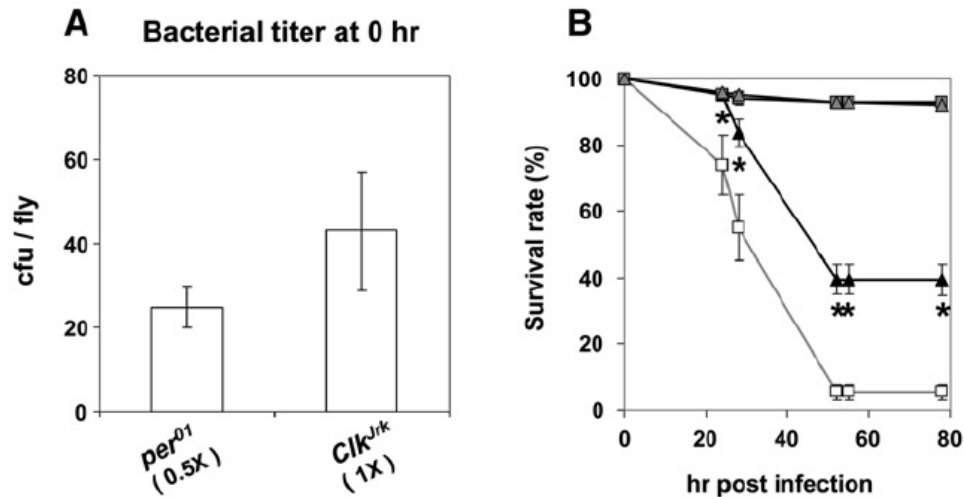


Figure 2.5. *Clk*^{Jrk} flies exhibit higher survival rates compared to *per*⁰¹ flies even when infected with approximately twice the bacterial dose as that used for *per*⁰¹ flies

(A) The average titer of PA14 *plcs* present in *per*⁰¹ or *Clk*^{Jrk} flies immediately after infection. Approximately half the amount of bacteria was used to infect *per*⁰¹ flies (n = 30) compared to *Clk*^{Jrk} flies (n = 20). Results are the average of two independent experiments. Error bars indicate S.E.M. (B) Time course for the percent survival of *per*⁰¹ or *Clk*^{Jrk} flies infected with PA14 *plcs* at CT5 during the second day of DD. *Clk*^{Jrk} flies (filled triangles, n = 414) have higher survival rates compared to *per*⁰¹ flies (open squares, n = 120) despite the higher average bacterial dose used to infect *Clk*^{Jrk} flies (two-tailed Student's *t*-test, *p* < 0.005 at 24 hrs, *p* < 0.05 at 28 hrs, *p* < 0.01 after 52 hrs post infection, α = 0.05). Mock-injury groups are also shown (gray triangles, *Clk*^{Jrk}, n = 185; gray squares, *per*⁰¹, n = 161). Results are the average of nine and two independent experiments for *Clk*^{Jrk} and *per*⁰¹ flies, respectively. Error bars indicate S.E.M.

Clock regulation in the induced profiles of innate immunity genes is highly selective and restricted to the early phase of the infection

The best-studied defense effectors in innate immunity are antimicrobial peptide genes (AMPs) that are rapidly induced following microbial infection [32]. In *Drosophila*, AMPs are primarily induced via activation of the Toll (mainly responding to fungi or gram-positive bacteria) and/or Imd (mainly responding to gram-negative bacteria) pathways [32]. As an initial attempt to understand the molecular mechanisms underlying the circadian pattern of survival rates and bacterial growth kinetics, we largely focused on the expression patterns of several key players in the Toll and Imd innate immune signalling pathways activated by microbial infection. This included measuring the post-inoculation expression kinetics of several peptidoglycan recognition proteins (PGRP) shown to play central roles as microbial receptors and/or scavengers (e.g., PGRP-SA, -LC and -LB), AMPs [i.e. *attacin A* (*attA*), *defensin* (*def*), *diptericin* (*dipt*), *drosocin* (*drc*) and *drosomycin* (*drs*)], and some key signalling components such as *imd*. Control *yw*, *per*⁰¹ and *Clk*^{Jrk} flies were infected during the second day of DD and collected at different times post-infection. We used real-time quantitative RT-PCR to measure RNA levels in head extracts of adult flies because we noted that the induced levels of many immune relevant genes attain higher values in heads compared to isolated bodies or whole flies (e.g., compare Figures 2.5 and 2.6; data not shown). Expression of immune genes in the head has been described elsewhere [69, 70] (data not shown). For each genotype and gene surveyed we compared the RNA values obtained at the same post-infection time point for the CT5 and

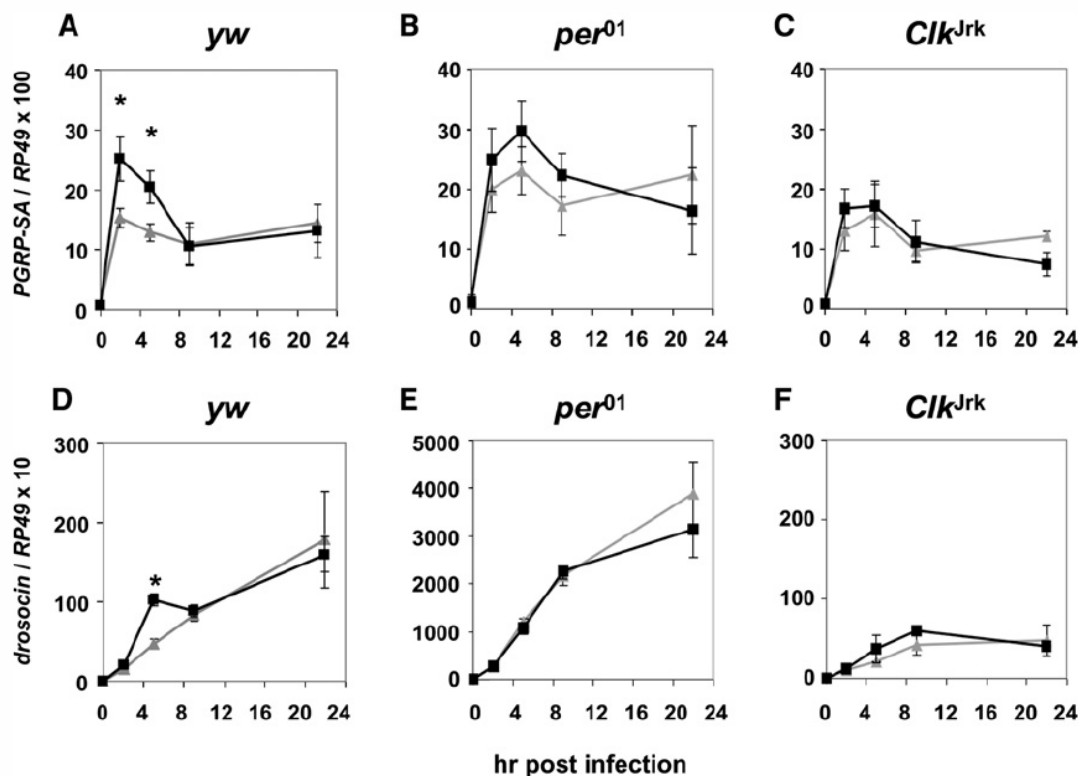


Figure 2.6. Night-time infection leads to early and transient clock-regulated increases in the mRNA induction profiles of a limited number of immune response genes

(A-F) Flies were infected at either CT5 (grey triangles) or CT17 (black squares), collected at the indicated times and RNA levels measured. For each genotype we compared the RNA values for the CT5 and CT17 groups that were obtained at the same post-infection time point. Asterisks indicate significantly higher mRNA levels for the *yw* CT17-group compared to the *yw* CT5-group (two-tailed Student's *t*-test, $p < 0.0005$ for *drosocin*, $p < 0.05$ for *PGRP-SA*). Results from at least three independent experiments were averaged except that *ClkJrk* data were derived from two experiments. Error bars indicate S.E.M.

CT17 infected groups.

Intriguingly, although many immune relevant genes are induced following infection with *Pseudomonas* [71], the post-inoculation expression patterns of only *PGRP-SA* and *drc* showed differences as a function of infection time in control flies, which were abolished in the clock mutants, indicative of *bona-fide* circadian regulation (Figures 2.6 and 2.8). For *PGRP-SA*, its mRNA levels at 2 and 5 hr post-infection are significantly higher in the CT17-group compared to the values obtained at the same post-infection time points in the CT5-group (Figure 2.6A), whereas for *drc* higher mRNA levels were observed at 5 hr post-infection in the CT17-group compared to the same post-infection time point in the CT5-group (Figure 2.6D). Similar circadian patterns in the induction profiles for *PGRP-SA* and *drc* were also obtained when analyzing extracts prepared from isolated bodies (Figure 2.7).

Besides *imd*, none of the immune relevant genes we probed exhibit circadian fluctuations in basal levels (data not shown; e.g., endogenous levels of *imd* are higher at CT17 compared to CT5 in control flies, Figure 2.8M, compare values at 0 hr post-infection). This is consistent with prior work using microarrays to probe daily patterns of gene expression in head extracts [72]. However, we did not observe time-of-day differences in the induced levels of *imd* following infection (Figure 2.8M). Thus, whether the basal expression of an immune response gene is constitutive or circadian is not *necessarily* linked to how the clock regulates its expression post-infection. Although it is not clear why the induced profile of *drc* and not other AMP genes exhibits circadian differences as a function of infection

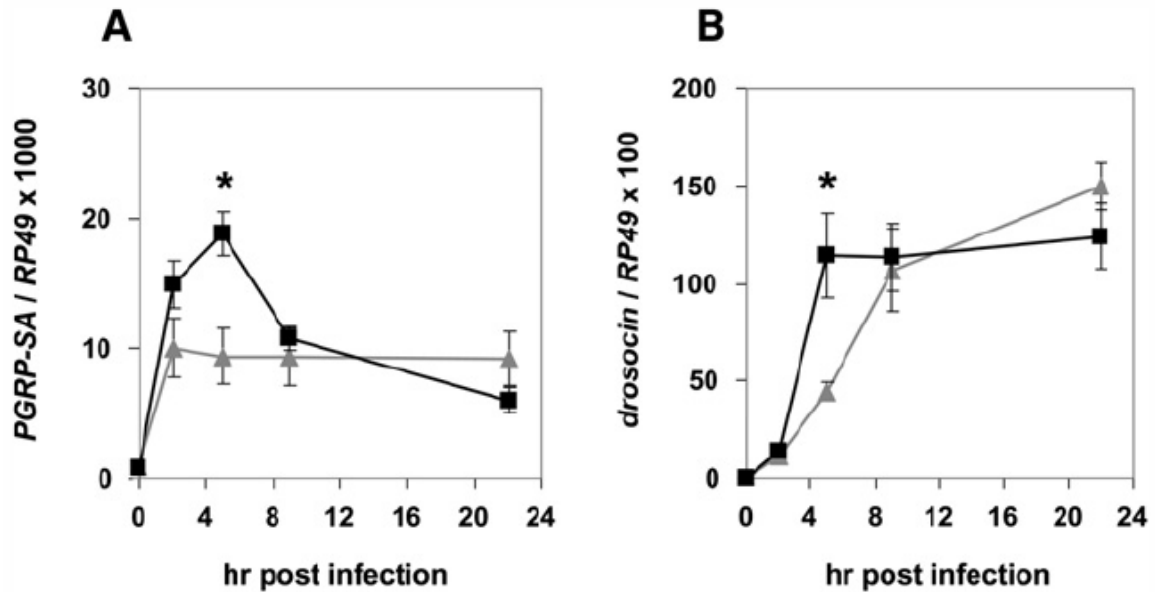


Figure 2.7. Time-of-day effects on the post-infection profiles for *PGRP-SA* and *drosocin* are also observed in the body

Control *yw* flies were infected at either CT5 (grey triangles) or CT17 (black squares), collected at the indicated times and RNA levels measured. Asterisks indicate significantly higher mRNA levels for the *yw* CT17-group compared to its CT 5-group (two-tailed Student's *t*-test, $p < 0.01$). Results reflect the average of four independent experiments. Error bars indicate S.E.M.

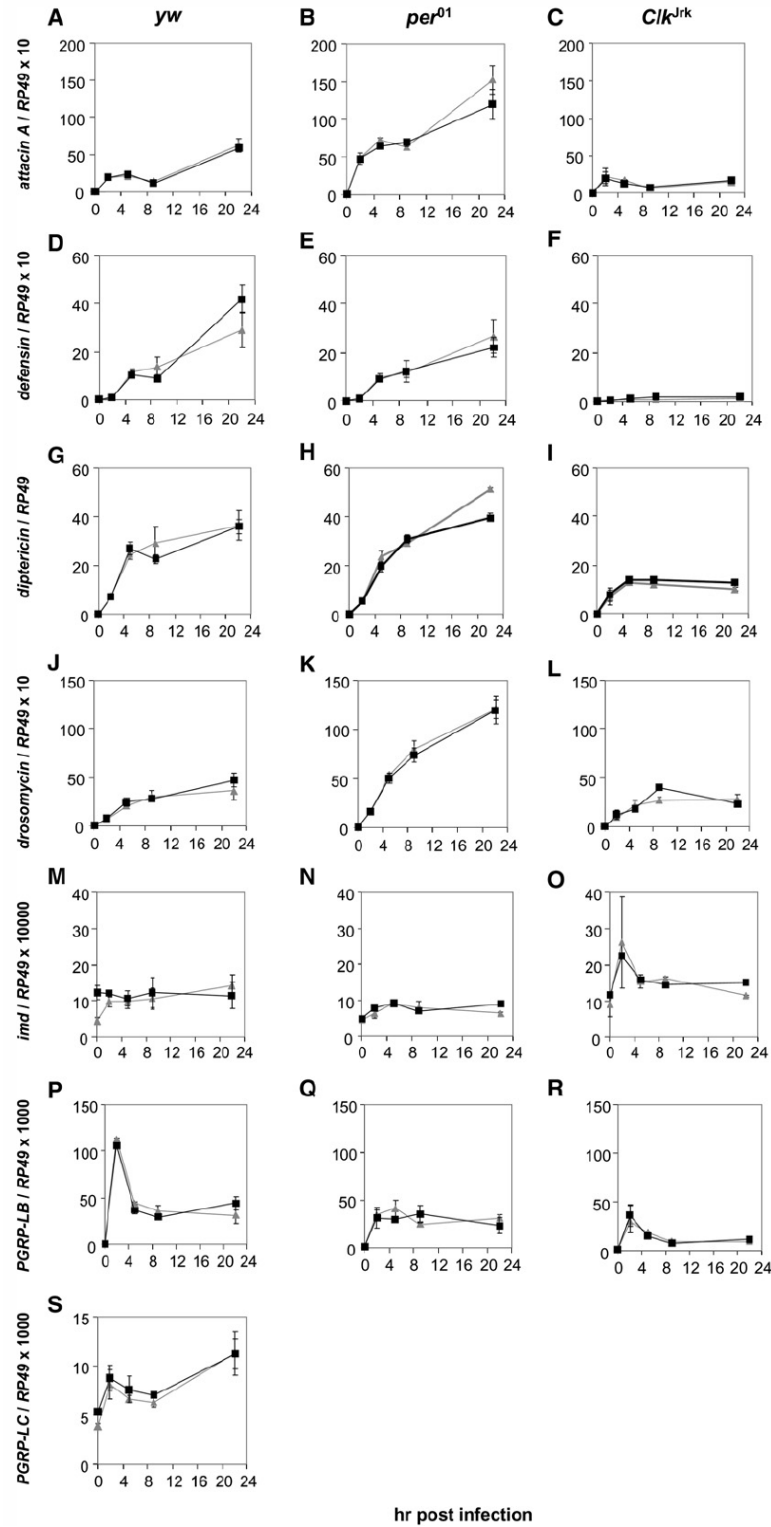


Figure 2.8. No time-of-day effects on the induction kinetics for *attacin A*, *defensin*, *dipthericin*, *drosomycin*, *imd*, *PGRP-LC*, and *PGRP-LB*

Figure Legend 2.8 Continued

(A-S) Control *yw* and clock mutant flies (as indicated) were infected at either CT5 (grey triangles) or CT17 (black squares), collected at the indicated times post-infection and mRNA levels were measured via real-time RT-PCR. For each gene, none of the RNA values measured at a particular time post-infection showed statistically significant differences between the CT5- and CT17-groups (two-tailed Student's *t*-test, $p > 0.05$). Results from at least three independent experiments were averaged, except that *Clk*^{Jrk} data were derived from two experiments. Error bars indicate S.E.M.

time (compare Figures 2.6 and 2.8), Drosocin kills gram-negative bacteria [32] and has been demonstrated to be one of only a few AMPs that when overexpressed can protect flies infected with *P. aeruginosa* [71]. In this context it is interesting to note that although PGRP-SA has a characterized role as a receptor in the Toll pathway [73], it has recently been implicated in phagocytosis as well [74].

Discussion

Together, our findings suggest the following scenario for how the clock in *Drosophila* might influence the progression of an infection with *P. aeruginosa*. Early in the infection a robust immune response (perhaps both cellular and humoral) is mounted, which is effective in pathogen clearance irrespective of when during a daily cycle the flies are infected, as indicated by the rapid drop in bacterial titer during the first 5 hr post-infection (Figure 2.4). However, the clock regulates the induced levels of a limited subset of innate immunity players, such as *PGRP-SA* and *drc*, whereby infections in the mid-night result in a transient burst early during the infection (Figure 2.6A and 2.6D). Higher levels of a few key immune players over a certain threshold may contribute to keeping the titer of pathogenic bacteria low after the initial rapid declining phase (Figure 2.4A). By prolonging the suppression of bacterial growth during a critical window of the infection, this might provide an opportunity to mount or recruit additional host defenses in addition to AMPs, resulting in improved survival (Figure 2.1A and 2.1B). Thus, our results suggest that the clock modulates the strength or responsiveness of immune activation in a time-of-day dependent manner but only during a critical early phase in the infection process that has physiological consequences on the ability of the host to survive pathogenic infections. Indeed, it is noteworthy that *P. aeruginosa* eludes host defenses by the early suppression of antimicrobial peptide gene expression [71]. It will be of interest to determine why the post-infection expression profiles of only certain immune response genes exhibit circadian regulation and how this is apparently restricted to a particular

phase of the immune response.

Although the time-of-day differences in the levels of induced *PGRP-SA* and *drc* are clearly consistent with the survival rates of wild-type flies infected at different times of day, this is not the case for the *per*⁰¹ and *Clk*^{Jrk} mutants where the overall levels of *drc* are much lower in *Clk*^{Jrk} compared to *per*⁰¹ flies (Figure 2.6; a trend observed for other AMP genes surveyed, Figure 2.8 and data not shown). Although seemingly paradoxical, this is not unanticipated as there are precedents in the literature showing that flies can be more susceptible to bacterial infection despite elevated levels of AMP expression, indicating that excessive or inappropriate immune activation can be deleterious [41, 75, 76]. In this context it is important to consider that besides the production of AMPs, innate immunity in adult *Drosophila* includes a proteolytic cascade leading to melanization and a cellular immune response characterized by phagocytosis [77]. It is possible that inactivation of *per* might affect other host defense mechanisms that cannot be compensated by a potentially hypersensitive humoral immune response. Conversely, *Clk*^{Jrk} and other clock mutant flies (Figure 2.1) might have a heightened activity of cellular immunity. Presently, our results based on probing the expression profiles of several immune response genes (Figures 2.6 and 2.8) would seem to demand that the molecular mechanisms governing the time-of-day differences in survival for flies with functional clocks are different from those affecting survival rates in *per*⁰¹ and *Clk*^{Jrk} flies. Otherwise stated, it does not appear likely that the survival rates of *per*⁰¹ and *Clk*^{Jrk} flies are simply due to their 'clocks' being pegged or held at a phase that is similar to either ZT/CT5 or

ZT/CT17 in wild-type flies, respectively. While future work will be required to resolve the molecular underpinnings governing the differential clock mutant effects on survival, these considerations suggest that core clock genes have ‘non-circadian’ related roles (i.e., roles not solely limited to their functions in timekeeping) in fighting microbial infections. Indeed, our findings add to a growing list of physiological and behavioral pathways that are differentially regulated in different clock mutants; e.g., mutations in *per* but not *tim*, *Clk* or *cyc* play a key role in long-term memory formation in *Drosophila* [78].

If the ability to evoke a stronger response at night enhances the efficacy of fighting a microbial infection, why restrict it to the night? It is widely thought that maintaining an optimal immune system is metabolically costly, competing for limited metabolic resources with other energetically demanding activities such as foraging or mating [79]. Within this framework we suggest that the clock might function as a temporal sieve to ensure the proper allocation of metabolic resources at biologically desirable times. On a more medical perspective, our results suggest that the innate immune system is a prime target for interventions based on chronobiological considerations in the hopes of boosting the ability to combat pathogenic infections.

Materials and Methods

Fly strains

The *Canton-S*, *Oregon R*, *yw* and clock mutant strains used in this study were descendents of stocks that were maintained in our lab for several years. *Oregon-R* flies were a gift from S. Kurata and all the clock mutant strains used in this study are in a *yw* background; i.e., *yw per*⁰¹ (a gift from A. Sehgal), *yw; tim*⁰¹ (a gift from A. Sehgal), *yw;; cyc*⁰¹ (a gift from J. Hall), and *yw;; Clk*^{Jrk} (a gift from R. Allada).

P. aeruginosa culture

The PA14 *plcs* strain used in this study was obtained from L. Rahme (Harvard Medical School) [66]. For every experiment, a glycerol stock was freshly streaked onto an LB/gentamycin plate. After an overnight incubation, a single colony was picked and grown in 1ml of LB/gentamycin until this seed culture reached a logarithmic phase. Subsequently, the culture was diluted in 25ml of LB/gentamycin and grown until the desired A₆₀₀ concentration was reached (see below). Finally, the bacterial culture was centrifuged and the pellet resuspended in LB media to obtain an A₆₀₀ reading of 100 and kept on ice during infection. Needles were directly placed in this concentrated bacterial solution and used for the infection.

***S. aureus* culture**

For every experiment, a glycerol stock of *S. aureus* (ATCC 10390) was freshly streaked onto an LB plate. Subsequently, a single colony was picked and grown in 2ml of LB overnight. This seed culture was diluted in 10ml of LB and grown until its A_{600} value reached 5.0. Finally, the bacterial culture was centrifuged and the pellet resuspended in LB media to obtain an A_{600} reading of between 10 and 50. Needles were dipped into the concentrated bacterial cultures and used to infect adult wild-type flies (*Canton-S* or *Oregon R*) at CT5 and CT17, as described for *P. aeruginosa*. Similar daily rhythms in percent survival were observed for *Canton-S* and *Oregon R* flies (data not shown), and the data from several independent experiments combined to generate the profiles shown in Figure 2.3.

Survival experiment

We used female flies to avoid potential complications due to sexual dimorphism in immunity [80-82]. For each survival experiment, approximately 100 young adult female flies (2-4 days old) of the same genotype were placed in a bottle and entrained under 12 hr light:12 hr dark cycles [LD; where zeitgeber time 0 (ZT0 is defined as lights-on] at 25°C for 2 days. Infections were performed on either the third day of LD or second day of constant darkness (DD), as indicated in the text. For a given genotype and infection time, approximately 40-60 flies were infected with PA14 *plcs* and 20 flies were treated as a contemporaneous mock-injury group to assess the impact of injury on survival (Table 2.1). To infect flies, we used

standard procedures whereby individuals were anesthetized with CO₂ and lightly pricked in the abdomen with a chemically sharpened tungsten needle dipped into a concentrated bacterial solution or LB media (mock-injury). After infection or mock-injury, flies were distributed into groups of about 20 individuals and placed in fresh vials, followed by a return to the same lighting and temperature condition where they had been housed before treatment. Because the virulence of *P. aeruginosa* is proportional to its population density [64], we optimized infection conditions such that the phase of the bacterial culture harvested had an A₆₀₀ value between 3.0–3.2 for LD infections and 3.45–3.57 for DD infections. Also, in our standard conditions we delivered approximately 200–400 bacteria per fly (Figure 2.4). This combination of both the phase of the bacterial culture and the number of bacteria delivered resulted in a mixed response with flies that exhibited rapid death and those that survived throughout the testing period. In our experimental setting, flies that survived the first 48 hr did not die for the rest of the observation period (at least one week) and were considered ‘survivors’ (Figures 2.1A, 2.2A, 2.3A and 2.5B). To better compare genotypes, clock mutant and the control *yw* flies were treated together. The entire procedure of infection, collection and counting was performed under a dim red light (Kodak safelight lamp) for night-time or DD infections.

Bacterial growth assay

At 0, 5, 10 and 23 hr post-infection, flies were put in ice-cold 70% ethanol and rinsed once to remove any bacteria remaining on the surface. Then, ice-cold LB

media was added and flies were homogenized, individually or as a pool of 10 individuals, with a motorized pestle. Serial dilutions of each fly extract was plated onto LB/gentamycin plates and incubated at 37°C overnight. Visible colonies from the serially diluted homogenates were counted and averaged to calculate the bacterial titer in each group of flies. To attain more reliable comparisons, each experiment included control and clock mutant flies (*yw*, *per*⁰¹ and *Clk*^{Jrk}) infected at CT5 and CT17 (Figure 2.4). For each time point and genotype, data from at least 3 independent experiments were pooled. For each experiment, a portion of flies representing each genotype and time of infection were not homogenized but monitored for at least one week to ensure that the survival rates were as anticipated. In rare cases where anomalous survival data were obtained (e.g., little to no mortality of infected flies throughout the week-long observation period), we did not use the corresponding results obtained from the bacterial assays.

Quantitative RT-PCR

In each experiment, at least 20 infected or mock-injured flies treated at either CT5 or CT17 were frozen on dry ice at 0, 2, 5, 9, or 22 hr post-infection and kept at -80°C until ready to process. Fly heads were separated from their bodies with sieves and crushed in 200 µl of TRI Reagent (Sigma) with a motorized pestle [83]. Total RNA was prepared according to the manufacturer's instruction and the final RNA pellet was resuspended in 12 µl or 100 µl of DEPC-treated water for head or body extract, respectively. 5 µl of total RNA solution were used for reverse

transcription (Omniscript RT, Qiagen). The resulting cDNAs were diluted 10-fold in 10 μ M of Tris (pH 8.0). Subsequently, 2 μ l of cDNA solution were added to a total of 30 μ l and PCR reactions performed in triplicate (QuantiTect SYBR Green PCR, Qiagen). Real-time PCR was performed in a 96-well plate on an ABI prism (Applied Biosystems) with the following conditions: a cycle of 15 min at 95°C to activate HotStarTaq DNA polymerase, followed by 40 cycles of 15 s at 94°C, 30 s at 60°C, and 30 s at 72°C. The standard curve was generated for every run and the absolute copy number of the gene of interest was calculated based on Ct (threshold cycle) values. Finally, the values were normalized to the copy number of the *rp49* gene. The efficiency of all the PCR reactions was at least 90%. The sequences of the PCR primers used in this study are provided in Table 2.4). As above for the bacterial growth assays, a portion of flies representing each genotype and time of infection were monitored for at least one week to ensure that the survival rates were as anticipated and results from experiments with anomalous survival data were not used. For each genotype, the values for RNA levels obtained at the same post-infection collection time were compared for the CT5 and CT17 groups.

Statistical analysis

Survival rates of flies infected at different times of a day were evaluated by one-way ANOVA to determine if they show statistically significant differences as a function of infection time. Comparison between all pairs of groups was performed

by Tukey-Kramer HSD (Honestly Significant Difference) analysis to determine the lowest and highest survival rates in cases where the survival rates varied among groups. Power analysis was also done to assess the adequateness of the sample size (Fig. 2.1B-F, and Tables 2.2 and 2.3). For pair-wise comparisons between CT5- and CT17-groups for a given genotype or between two genotypes, two-tailed Student's *t*-test was used. All the statistical analysis described above was carried out with JMP6 software (SAS).

Table 2.4. Sequences of the primers used for quantitative RT-PCR

Gene	Forward primer (5' – 3')	Reverse primer (5' – 3')
<i>attacin A</i>	TCCTTGACGCACAGCAACTTC	GGCGATGACCAGAGATTAGCAC
<i>defensin</i>	TCTCGTGGCTATCGCTTTTGC	CCACATCGGAAACTGGCTGA
<i>diptericin</i>	GACGCCACGAGATTGGACTG	CCCACTTTCCAGCTCGGTTC
<i>drosocin</i>	TGTCCACCACTCCAAGCACAA	CATGGCAAAAACGCAAGCAA
<i>drosomycin</i>	TCCTGATGCTGGTGGTCCTG	TCCCTCCTCCTTGCACACAC
<i>imd</i>	CCGAGCAATGTGAGTTGATTTTCG	CGTGCGTTCTGCCTTCCAATAG
<i>PGRP-LB</i>	CGGCGATGGCATGATTTACA	CGGCAGTTCGGTTCTCCAAT
<i>PGRP-LC</i>	CCTACCCGCCCAACAGTTC	GTGGTACTGCCGCCTCACCT
<i>PGRP-SA</i>	CGGATCTCCTTGGATTATGG	TAGTGGAGTCCCAACGAAGG
<i>rp49</i>	CCCACCGGATTCAAGAAGTTCC	TCGACAATCTCCTTGCGCTTC

Chapter 3. The immune response in the pericerebral fat body is sufficient to protect the animals from bacterial infections

Summary

In *Drosophila*, the fat body, a homolog of the mammalian liver, is thought to be the center of the systemic immune response and mainly located in the thorax and abdomen. In addition, there is some fat body surrounding the brain, termed the pericerebral fat body. Although it was shown that the pericerebral fat body can also mount an immune response, no systematic analysis comparing the fat body in different body parts has been undertaken and it is not clear if the pericerebral fat body contributes to survival over bacterial infections. In this study we show that similar if not identical pathways underlie innate immunity in the head and the body. Also, our data suggest that innate immunity genes are induced more rapidly in the head, compared with the body. To investigate a possible functional role for the pericerebral fat body in host defense, we used inducible tissue specific promoters to drive expression of selective immune response genes in flies with immune-compromised genetic backgrounds. Using this approach we show that the pericerebral fat body is sufficient to induce innate immunity genes and combat bacterial infections, independent of the abdominal fat body. Our findings suggest that the pericerebral fat body provide a fast and local immune response in the head, improving the survival outcome of the whole animal in *Drosophila*.

Introduction

The innate immunity of adult flies consists of cellular and humoral parts: phagocytosis performed by haemocytes (blood cells) is on the cellular arm whereas on its humoral side is the activation of proteolytic cascades leading to melanization and the synthesis of a battery of antimicrobial peptides (AMP) [32]. AMPs are primarily induced via activation of the Toll (mainly responding to fungi or gram-positive bacteria) and/or Imd (mainly responding to gram-negative bacteria) pathways. Relish and Dif/Dorsal, *Drosophila* NF- κ B homologues, are key regulators of the Imd and Toll pathways respectively [32].

AMPs are thought to suppress the growth of invading microbes in the haemolymph (blood) by permeabilizing their membranes [30]. Being a hallmark of humoral immune response and under the regulation of NF- κ B homologues, AMPs serve as a typical readout for *Drosophila* innate immune responses. Several lines of transgenic flies containing a reporter gene under the promoter of one of the AMPs were generated in an attempt to localize the corresponding immune response in flies or dissect the signal pathways leading to their activation. Among them, *Dipt2.2-lacZ* flies report the promoter activity of *diptericin* gene, a typical AMP active against gram-negative bacteria [69]. In that paper, Reichhart et al showed that the fat body in the head, thorax, and abdomen is the site of *diptericin* induction in response to *E.coli*. This is in agreement with another study done by Samakovlis et al, where *cecropinA*, another AMP, mRNAs were localized to the same tissue in addition to 5-10% of haemocytes [70]. These studies established that the fat body is the main tissue where AMP gene expression is induced in

Drosophila.

A recent study suggests that the pericerebral fat body has different functions compared to the abdominal fat body, such as during insulin signaling [84]. However, in the case of the immune response, no systematic analysis has been done, comparing the pericerebral and abdominal fat bodies. We were motivated to compare the host defense functions of both groups of fat body cells because during the process of studying circadian regulation of the *Drosophila* immune response (Chapter 2), the head immune response appeared more robust compared with the rest of the body (compare Figure 2.6 and Figure 2.7). Moreover, manipulation of insulin signaling in the pericerebral fat body affected the endogenous levels of insulin signaling in the abdominal fat body and the expression level of *Drosophila* insulin-like peptide *dilp-2* in neurons, suggesting a hierarchical relationship between the pericerebral and abdominal fat body [84]. This chapter will address some preliminary findings on characterizing the immune response in the head. The data presented in this chapter have been collected discontinuously over several years from different studies, but put together here as related results. The entire data set of chapter 3 can be categorized into two parts: (1) Faster posttranscriptional modification of Relish in the head compared with the body and (2) The pericerebral fat body is sufficient in protecting the animals from bacterial infections. The results regarding the former issue are mainly preliminary and further studies will be required.

Results

RELISH activation in the head follows a similar pathway as that in the body

To better characterize the head immune response, we began with asking the following question; is the head antibacterial immune response regulated by the same players in the Imd pathway previously established using whole flies, which mostly reported the abdominal fat body? The general approach we took was to infect mutants in the Imd pathway, then separate heads and bodies, followed by measuring the molecular innate immune response.

In response to bacterial infection, *Drosophila* caspase-8 homologue DREDD cleaves RELISH to generate two fragments: the N-terminal REL-68, which contains a DNA-binding Rel homology domain, translocates to the nucleus, and activates its target genes such as AMPs, and the C-terminal REL-49, which includes an I κ B-like domain and remains in the cytosol [55].

As a marker for the RELISH processing event in the Imd pathway, we monitored the C-terminal REL-49 fragment by Western analysis using head or body extract (Figure 3.1). In control *yw* and *Rel^{F23}* flies where P element used to generate *relish* mutations has been precisely excised [85], production of REL-49 was evident 4hrs post infection in the head (Figure 3.1, upper panel, lanes 1 and 2, lanes 5 and 6) whereas it was barely visible in the body (Figure 3.1, lower panel, lanes 1 and 2, lanes 5 and 6). On the other hand, *dredd* or *relish* null mutants (*Rel^{F20}*) did not show any significant signal for the correspondingly sized protein (Figure 3.1, upper and lower panels, lanes 3 and 4, lanes 7 and 8), illustrating that

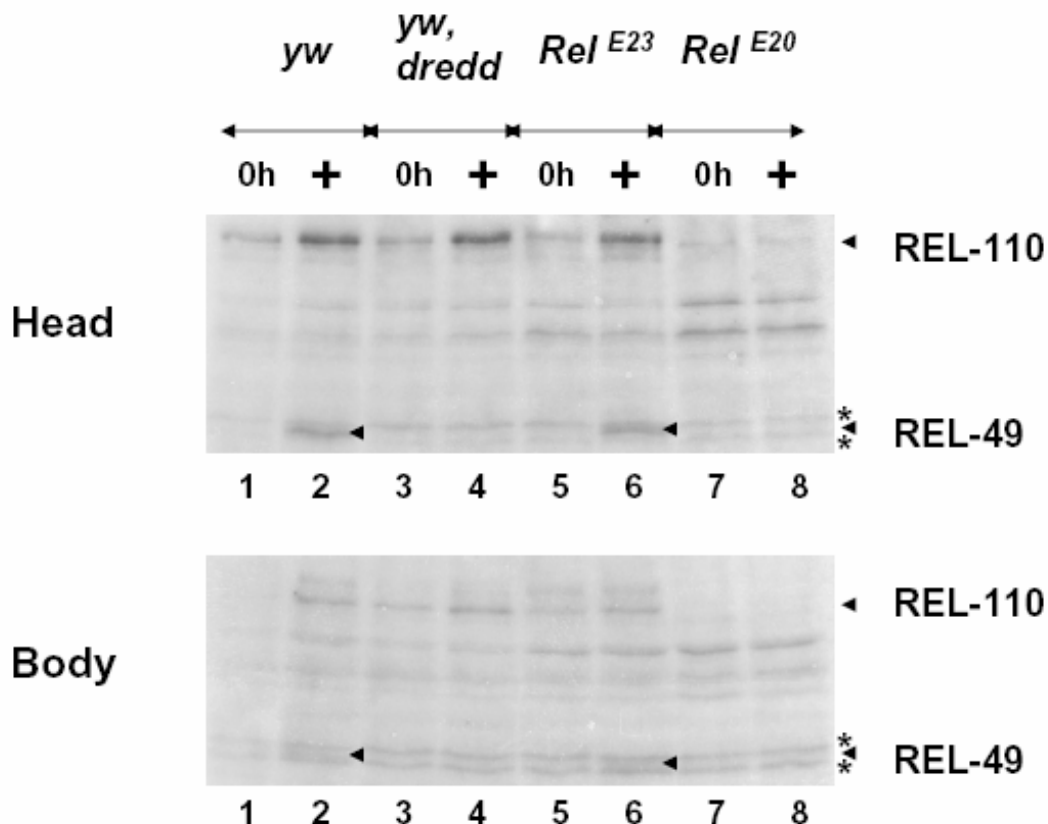


Figure 3.1. Cleavage of RELISH in the head depends on *dredd*

Adult flies were entrained under 12 hr light:12 hr dark cycles (LD) at 25°C for 2 days, infected with a mixture of *E. coli* and *Micrococcus luteus* between ZT17 and ZT18 on the third day of LD cycle, and collected at time 0hr or 4hrs post infection (+). Head (upper panel) or body (lower panel) extracts were analyzed by Western blotting and blots were incubated with antibody against the c-terminal 107 aa of RELISH [55]. Precursor form of RELISH is designated as REL-110 and its c-terminal cleavage product as REL-49. Note that the band of REL-49 (arrowhead) runs right between two nonspecific bands (*). Genotypes of the flies used are shown on top of the upper panel.

DREDD is required to process RELISH in the head as well as in the body [53].

Microbial signals lead to the transcriptional activation of *relish* as well as other target genes, forming a positive feedback loop [85]. In Figure 3.1, upon bacterial infection, the amount of unprocessed form of RELISH, REL-110, also increased in *dredd* mutants as well as in control flies (upper panel, compare lanes 3 and 4), demonstrating that *dredd* mutation did not affect the transcriptional activation of *relish* in the head as expected from its specific role in processing RELISH [56].

The C-terminal fragment of RELISH accumulates faster in the head, which correlates with the extent of posttranscriptional modification

To investigate the head immune response further, we took advantage of the Gene-Switch system to induce immune response genes in a temporally regulated manner [86]. The Gene-Switch system relies on a GAL4-progesterone receptor chimera activated by the ligands of progesterone receptor. One can induce a gene of interest at a desirable time by feeding the flies with food containing RU486 (mifepristone), a progesterone receptor antagonist. Among the P{Switch} lines, S₁106 Gene-Switch GAL4 driver seems to express its target gene in both the pericerebral and abdominal fat body [87] (Figure 3.2; data not shown).

Since the abundance of RELISH was always much lower in the body than in the head (Figure 3.1, compare upper and lower panel), we upregulated *relish* both in the pericerebral and abdominal fat body with the S₁106 driver and compared the RELISH processing step between head and body (Figure 3.2). We focused on

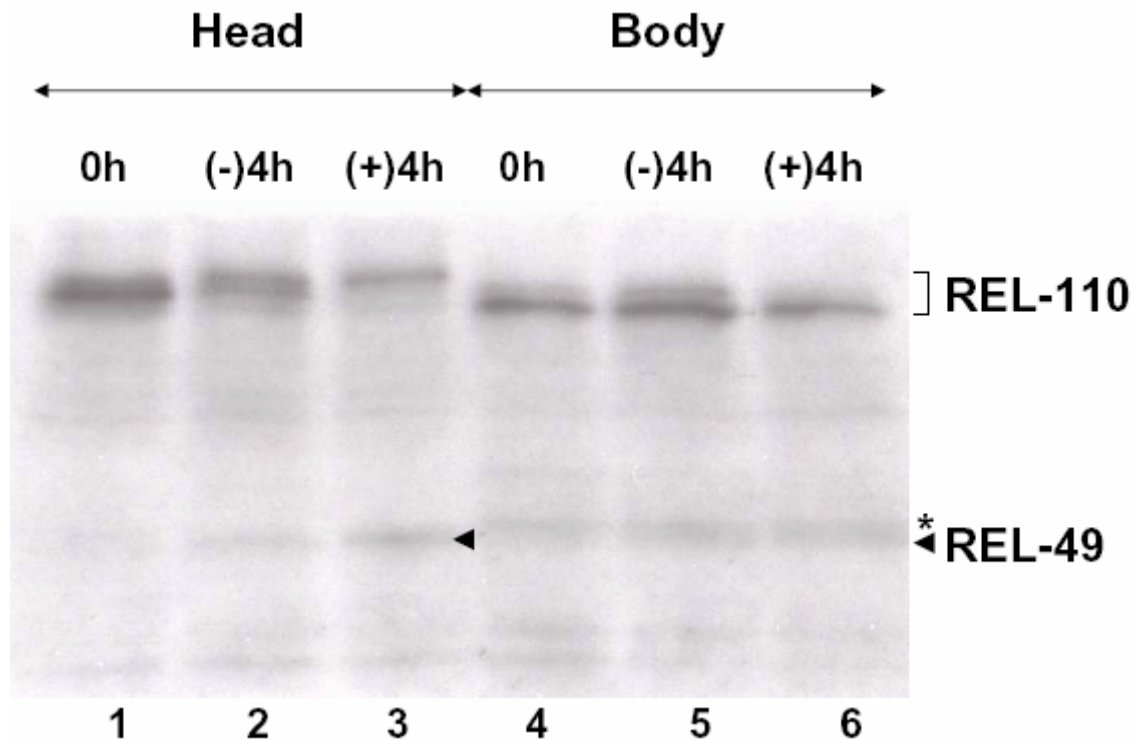


Figure 3.2. Comparison of RELISH in the head and body following bacterial infection

Female adult flies overexpressing *relish* under S₁106 Gene-Switch GAL4 driver [88] were entrained in the presence of 200μM of RU486, infected with a mixture of *E. coli* and *M. luteus* at ZT18 on the third day of LD cycle, and collected at time 0hr or 4hrs post mock-injury (-) or infection (+). Protein samples were treated in the same way as in Figure 3.1 for Western blotting. Note that the band of REL-49 (arrowheads) runs right beneath a nonspecific band (*) in the body.

female flies because they induce much stronger immune response than males (data not shown) despite the presence of ovaries in the body, which could potentially skew the comparison of the head and body immune response per cell. Flies were entrained in LD cycles at 25°C for 2 days. On the third day of LD, they were infected or mock-treated at ZT18 (ZT0 is defined as lights-on). We chose this particular infection time of a day to maximize the immune response induced by bacterial infection (Figure 2.6).

From the Western blot analysis targeting RELISH, we noted two major differences between head and body immune response: (1) Earlier accumulation of REL-49 in the head; (2) Head-specific higher mobility REL-110 isoforms that are likely due to phosphorylation. I κ B kinase (IKK) complex as well as DREDD participate in activating RELISH [49, 50]. Interestingly, in the head, REL-110 displayed progressive shifts toward slower mobility isoforms in response to bacterial infection, positively correlated with the amount of REL-49 (Figure 3.2, compare lanes 1, 2, and 3). However, in the body, we did not see the corresponding change in the proportion of RELISH isoforms displaying differential mobility (Figure 3.2, compare lanes 4, 5, and 6). This contrast reached its peak at 4hrs post infection, when most of REL-110 showed the slowest mobility in the head and the fastest one in the body (Figure 3.2, compare lanes 3 and 6). In addition, there was no significant difference in the amount of body REL-49 between the flies pricked with aseptic needle (mock treatment) and the ones infected with bacteria (Figure 3.2, compare lanes 5 and 6). Together, this result suggests that RELISH may be posttranscriptionally modified more rapidly upon bacterial infection,

resulting in a faster accumulation of REL-49 in the head compared with the body.

A more robust induction of *PGRP-SA* and *drosocin* mRNAs in the head, compared with the body

Since REL-49 accumulated more rapidly in the head than in the body during night time infection (Figure 3.2), we were curious to find out if there is a similar trend at the level of induction of RELISH target genes. To this end, the data used to generate Figure 2.6 were reanalyzed (Table 3.1) and the results of this analysis are presented in Table 3.2 where two downstream target genes of RELISH were compared in their induction fold for the first 2hrs after PA14 *p/ics* was delivered during day or night time (Table 3.2). It should be noted that Figure 3.2 was derived from an experiment using *E.coli* and *M.luteus* and cannot be directly related to the results presented in Tables 3.1 and 3.2. Although follow-up experiments using the same experimental conditions as used in Figure 3.2 have to be done to draw a fair conclusion, the data suggest a general trend where there is a higher amplitude response in the head. Irrespective of the infection time, both *PGRP-SA* and *drosocin* mRNA increased more steeply in the head, compared with the body, although the difference in the induction fold of *drosocin* mRNA did not reach statistical significance due to the high standard deviation in its levels at time 0hr (Tables 3.1 and 3.2). *PGRP-SA* mRNA levels at time 0hr in the head were comparable to those in the body. In case of *drosocin*, mRNA levels in the head were either higher or lower than those in the body at time 0hr, but consistently higher in the head than in the body at 2hrs post infection. Therefore, higher

Table 3.1. Relative *PGRP-SA* and *drosocin* mRNA levels at time 0hr and 2hrs post infection in response to PA14 *plcs*

Gene	<i>PGRP-SA</i>				<i>drosocin</i>			
Infection time	CT5		CT17		CT5		CT17	
Collection time	0hr	2hr	0hr	2hr	0hr	2hr	0hr	2hr
Head	0.82±0.1	15.3±1.6	0.71±0.1	25.2±3.7	0.54±0.4	15.2±2.8	0.07±0.0	19.9±5.1
Body	0.96±0.2	10.1±2.3	0.84±0.2	15.0±1.8	0.24±0.1	11.6±2.0	0.16±0.1	14.2±1.7

Shown are the average normalized mRNA levels \pm SEM, using the data derived from the same experiment as in Figure 2.6.

Table 3.2. Induction fold^a of *PGRP-SA* and *drosocin* mRNAs between 0hr and 2hrs post infection in response to PA14 *plcs*

Gene	<i>PGRP-SA</i>		<i>drosocin</i>	
Infection time	CT5	CT17	CT5	CT17
Head	20 \pm 2.6	36 \pm 4.2	92 \pm 39	272 \pm 95
Body	11 \pm 1.4	18 \pm 3.5	57 \pm 15	91 \pm 22
Head vs. body ^b	0.024*	0.029*	0.472	0.083

^a Induction fold was calculated by dividing the normalized mRNA level at 2hrs post infection with the one at time 0hr, using the data derived from the same experiment as in Figure 2.6. Shown is the average induction fold \pm SEM.

^b p-value of two-tailed Student's *t*-test. An asterisk (*) indicates significantly higher induction fold of *PGRP-SA* mRNA in the head, compared with that in the body (**P* < 0.05).

induction folds of *PGRP-SA* and *drosocin* mRNAs in the head did not result from their consistently lower basal mRNA levels, compared with the body. When the results of Figure 3.2 and Tables 3.1 and 3.2 are taken together, it raises a possibility that RELISH may go through posttranscriptional modification more rapidly in the head, leading to a faster accumulation of REL-49 and transactivation of its target genes in the head, compared to the body.

Processing of RELISH in *tim*-expressing cells of the head

In an attempt to optimize the conditions of detecting RELISH by Western blotting, we used a *tim(UAS)GAL4* driver line and observed the production of REL-49 in *tim*-expressing cells in the head in response to bacterial infection (data not shown). Since there has not been a systematic analysis addressing what tissues are responsible for the head immune response other than the pericerebral fat body, we were curious to find out the tissue specificity of head immune response. To this end, a side-by-side experiment was performed, using two GAL4 driver lines: *tim(UAS)GAL4* whose expression is limited to clock neurons, photoreceptor cells in the compound eyes, brain glia and fat body [89, 90] whereas *GMR-GAL4* induces its target genes only in the photoreceptors in the compound eyes.

When *relish* was driven under *tim* promoter, significant amounts of REL-49 were produced in response to bacterial infection (Figure 3.3, compare lanes 3 and 4). On the contrary, when using the *GMR-GAL4* driver, the amount of REL-49 produced in response to bacterial infection was no more than that from the parental line (Figure 3.3, compare lanes 2 and 6) even though the amount of

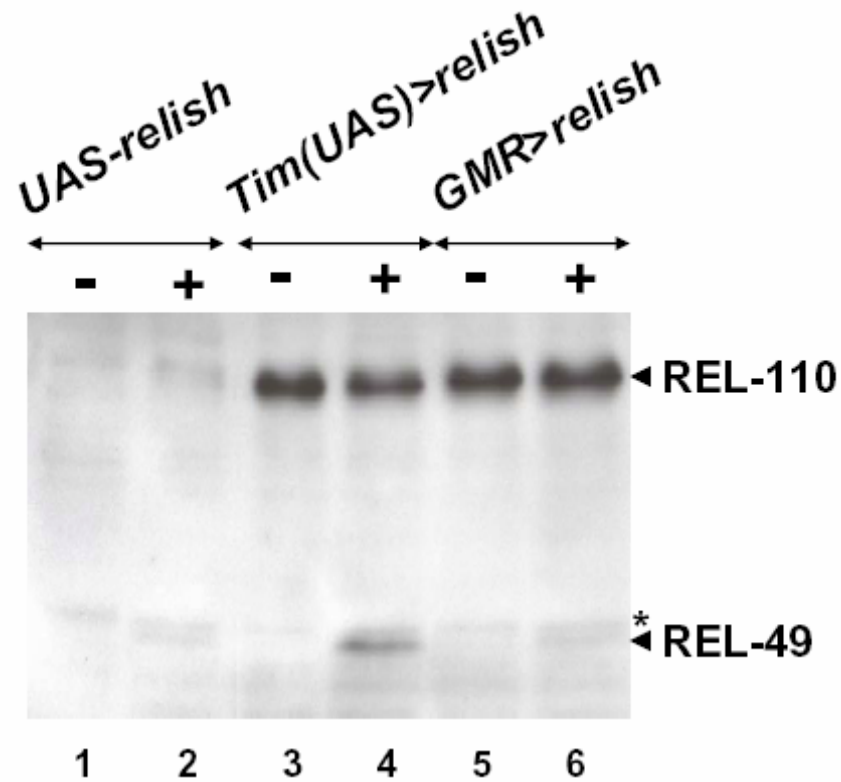


Figure 3.3. *tim*-expressing cells are capable of processing RELISH in the head.

Parental line (e.g. *UAS-relish*) and progeny with a driver and *UAS-relish* transgenes [e. g. *Tim(UAS)>relish* and *GMR>relish*] were entrained, infected with a mixture of *E. Coli* and *M. luteus* between ZT16 and ZT17 on the third day of LD cycle, and collected 4hrs post mock-injury (-) or infection (+). Protein samples were treated in the same way as in Figure 3.1 for Western blotting. Note that the band of REL-49 (arrowhead) runs right beneath a nonspecific band (*).

REL-110 mainly coming from photoreceptors was comparable to that from *tim*-expressing cells. Therefore, this result suggests that a subset of *tim*-expressing cells such as the pericerebral fat body, clock neurons and/or brain glia is capable of processing RELISH in the head but not the photoreceptors.

RELISH overexpressed mainly in the pericerebral fat body is sufficient to improve the survival of *relish* null mutants in response to bacterial infections

Based on the descriptions in the previous studies regarding the AMP expression or reporter activities driven by AMP promoter [69, 70], we focused on the pericerebral fat body as a potential target tissue for the head immune response. Among the P{Switch} lines whose Gene-Switch GAL4 expression is limited in the head, S₁32 showed a pericerebral fat body-specific expression when driving a reporter gene [84, 88]. Therefore, we used S₁32 to overexpress immune response genes in the pericerebral fat body and S₁106 in the entire fat body as a positive control.

Motivated by a faster accumulation of REL-49 and higher induction fold of downstream target genes of RELISH in the head compared with the body, we asked if the immune response mounted by pericerebral fat body is sufficient to protect the animals from bacterial infections. To this end, we overexpressed *relish* in the pericerebral fat body, the entire fat body, or pan-neuronal cells in *relish* nullmutant background (*Rel*^{E20}) by using S₁32, S₁106, or ELAV Gene-Switch GAL4 lines [91], respectively. Flies were entrained in LD cycles at 25°C for 2 days. On the third day of LD, they were infected or mock-treated between ZT5 and ZT8. We

chose this particular infection times of a day to maximize the survival difference between the flies overexpressing *relish* and their control group, considering that *Rel^{E20}* mutant flies survive much better when infected during night time, compared with the day time infections, in the same way as the wild-type flies do (data not shown; Figure 2.3).

When infected with *Enterobacter cloacae* β 12, nonpathogenic gram-negative bacteria, the flies overexpressing *relish* mainly in the pericerebral fat body rescued the survival phenotype of *Rel^{E20}* mutant to a level comparable to those overexpressing *relish* in the entire fat body (Figure 3.4A and 3.4B). Interestingly, *relish* overexpression in pan-neuronal cells also improved the survival of *Rel^{E20}* mutants significantly albeit to a less extent (Figure 3.4C). The ability of flies overexpressing *relish* in the pericerebral fat body to boost the survival of *Rel^{E20}* mutants was also confirmed with pathogenic gram-negative bacteria PA14 *p/lcs* mutant (Figure 3.4D). Taken together, the pericerebral fat body is able to mount a sufficient immune response to protect *Rel^{E20}* mutants from bacterial infections.

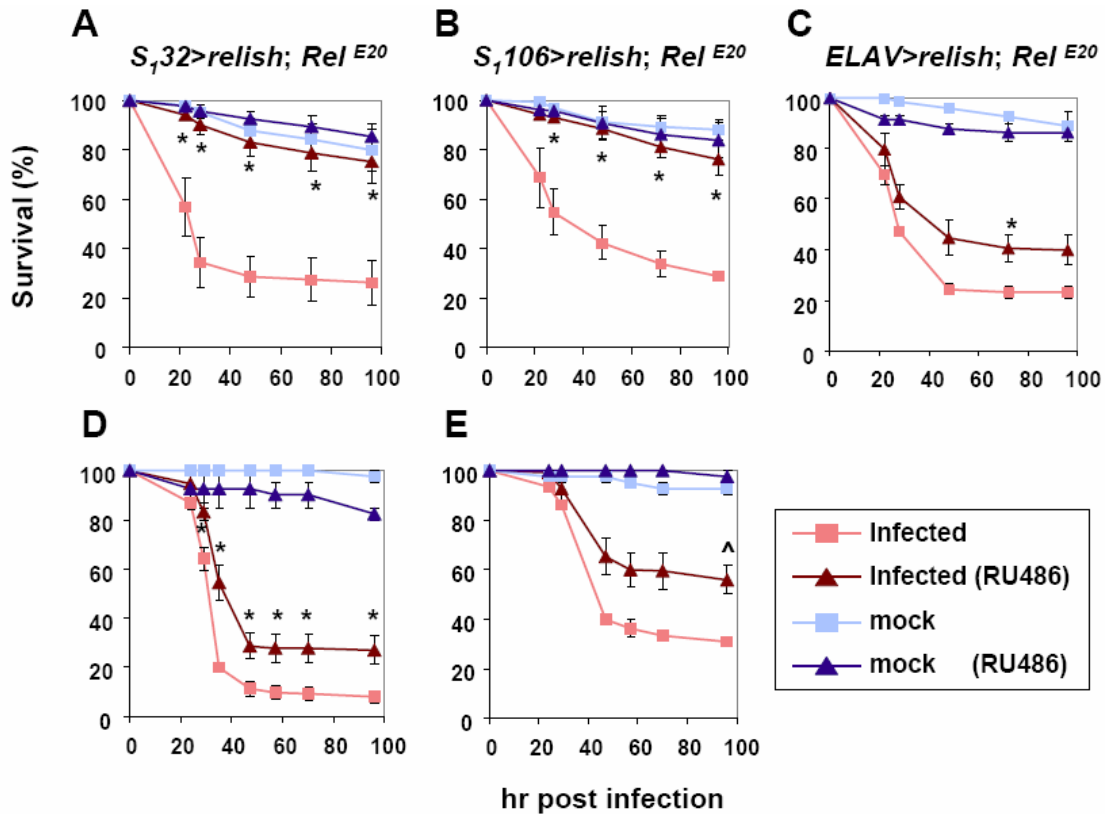


Figure 3.4. RELISH overexpressed mainly in the pericerebral fat body is sufficient to rescue *relish* null mutant (*Rel^{E20}*) in response to *E. cloacae* β 12 or PA14 *plcs*.

Adult female flies that harbor UAS-*relish* and *S₁32*, *S₁106*, or *ELAV* Gene-Switch drivers in *relish* mutant background were entrained with or without 400 μ M of RU486, infected with *E. cloacae* β 12 (A-C) or PA14 *plcs* (D-E) between ZT5 and ZT8, and the number of survivors was scored over time. Shown are the average results of four (A-B), three (C-D), or two (E) independent experiments. Mean \pm SEM and values obtained from 40-80 animals per experiment are displayed. Asterisks (*) indicate significantly higher survival rates of flies fed with RU486, compared with the ones fed with vehicles (two-tailed Student's *t*-test, **P* < 0.05, \wedge *P*=0.054).

Discussion

In this chapter, we presented preliminary data based on biochemical and genetic strategies, suggesting that the pericerebral fat body mounts a powerful immune response sufficient to protect the host animals from bacterial infections. In the first series of experiments, we investigated RELISH, a key player in the Imd pathway and found that the processing of RELISH in the head requires *dredd* (Figure 3.1). Also, our data suggest the possibility that processing of RELISH in the head is more efficient compared to the body (Figure 3.2). Although we do not have evidence to support that the slower migrating isoforms of RELISH in the head are due to phosphorylation, it is tempting to speculate that the level of IKK or efficiency of its activation might be higher in the head, sensitizing RELISH to bacterial signals and leading to its more rapid processing and induction of downstream target genes. It is also intriguing that REL-49 accumulates faster and some of RELISH downstream target genes tend to be induced more steeply in the head compared with the body even though the exogenous bacteria are delivered into the abdomen, implying existence of a rapid signaling mechanism to give a warning for the invading bacteria to the head. Kim et al reported that the mRNA level of *caspar*, an inhibitor targeting DREDD-dependent cleavage of RELISH, is much lower in the head in comparison with the abdominal fat body [57]. Differential expression of *caspar* could also contribute to the faster accumulation of REL-49 in the head upon bacterial signals.

Of note, in order to substantiate our tentative conclusions, follow-up experiments should be done: first, it is necessary to infect the flies overexpressing

relish both in the pericerebral and abdominal fat body with S₁106 Gene-Switch GAL4 driver in *Rel^{E20}* background, monitor the RELISH processing step and the induction fold of RELISH target genes, and compare them in the head and the body. Second, evaluation of the magnitude of the head immune response demands either immunohistochemistry targeting the N-terminal fragment of RELISH or in situ hybridization scoring the AMP mRNA levels per fat body cell.

Previous studies showed some expression of immune response genes in the head, presumably the pericerebral fat body. However, to date, there is no evidence that the pericerebral fat body can mount a functional immune response. The possibility of a faster processing of RELISH and higher induction fold of its downstream target genes in the head suggests that the pericerebral fat body provides the head a fast and local immune response. Considering that it is sufficient to protect the animals from bacterial infections (Figure 3.4), by inducing an immune response promptly, the pericerebral fat body could suppress the bacterial growth in the head and preserve the neuronal functions longer, resulting in better survival outcome of the whole animal.

Although it is very likely that the pericerebral fat body is mainly responsible for the head immune response, we cannot rule out the possibility that there may be other immune-competent tissues in the head. In fact, neuronal cells were also sufficient to improve the survival of *Rel^{E20}* mutants upon bacterial infection (Figure 3.4C), suggesting that neurons may be capable of mounting a functional immune response, perhaps of a smaller magnitude than the fat body. The significance of neuronal immune response is not clear at this point, but it is noteworthy that NF- κ B

activity has been reported to keep central neurons alive in mammals [92] and the mammalian nervous system can produce neuropeptides and peptide hormones with antimicrobial properties [93].

Taken together, the innate immune response centered at RELISH follows the same regulatory rule in the head as in the body. However, it appears more sensitive to bacterial stimuli and shows a sharp initial increase in the head compared with the body. By taking a prompt antibacterial action in the head, the pericerebral fat body and possibly neurons may serve neuroprotective roles cooperatively and increase the chance of survival of the whole animal.

Materials and Methods

Fly strains

yw flies used in this study were descendents of a stock that was maintained in our lab for several years. The following stocks were gifts from other laboratories: *yw, dredd^{B118}* (B. Lemaitre), *Rel^{E20}*, *Rel^{E23}*, *w; UAS-relish; +/TM3, Sb* and *w; UAS-relish; Rel^{E20}* (D. Hultmark), *S₁32* and *S₁106* Gene-Switch GAL4 (R. Davis), ELAV Gene-Switch GAL4 with second chromosome insertion (H. Keshishian), *tim(UAS)GAL4* (M. Young), *GMR-GAL4* (K. Irvine).

Bacterial culture

The PA14 *plcs* strain was prepared in the same way as described in Chapter 2 except that the bacterial pellet was resuspended in LB media to obtain a desired A_{600} reading as described below. The A_{600} value of the bacterial culture used to generate the Figure 3.4E was 20 whereas the survival data over the bacterial culture whose A_{600} value was 20, 40, or 120 gave similar results and were pooled to generate the Figure 3.4D.

E. cloacae β 12 strain was a gift from D. Hultmark (Umea University). It was cultured in the same way as for PA14 *plcs* except that the phase of the bacterial culture harvested had an A_{600} value of 3.0 and the bacterial pellet was resuspended in LB media to obtain an A_{600} reading of 200.

As for *M. luteus* (a gift from D. Hultmark) and *JM109* (*E.coli* strain, Promega), a glycerol stock was freshly streaked onto an LB plate for every

experiment. Subsequently, a single colony was picked and grown in 1ml of LB overnight. This bacterial culture was centrifuged and the pellet resuspended in LB media to obtain an A_{600} reading of 200. Finally, equal amounts of concentrated *M. luteus* and *JM109* were mixed right before infection.

Western blot analysis

Flies were entrained in LD cycles at 25°C for 2 days. On the third day of LD, flies were infected or mock-treated between ZT16 and ZT18. They were collected on dry ice at indicated times and kept at -80°C until ready to process. Fly heads were separated from their bodies with sieves and crushed in 30 or 200µl of extraction buffer 1 (EB1) for heads or bodies, respectively, with a protease inhibitor cocktail (Roche) as described previously [94]. The samples were centrifuged for 15 minutes at 14000 rpm at 4°C and their supernatant was recovered. This step was repeated twice. The protein concentration of the samples was measured by Bradford assay (Coomassie Plus, Pierce) with BSA standards. 40µg of total protein per sample (except for the body samples in Figure 3.2: 60 µg) was mixed with 4X SDS sample buffer, resolved in 10% polyacrylamide gel, and blotted onto nitrocellulose (Figure 3.1 and 3.2) or polyvinylidene difluoride membrane (Hybond-P, Amersham; Figure 3.3). The primary and secondary antibodies were used at the following dilutions: 1:10 or 50 for anti-RELISH antibody targeting the c-terminal 107 aa of RELISH (a gift from D. Hultmark) [55] and 1:20,000 for anti-mouse HRP (Amersham). Signals were detected with ECL Advance (Amersham).

Survival experiment

We used female flies to avoid potential complications due to sexual dimorphism in immunity [80-82]. Young adult female flies were entrained in LD cycles at 25°C for 2 days with the food containing either vehicle or 400µM of RU486. On the third day of LD, flies were infected or mock-treated between ZT5 and ZT8. Right after infection or mock treatment, the flies were transferred to vials with fresh food containing either vehicle or 400µM of RU486 and kept in the same condition as entrained. The number of survivors was scored over time up to 4 days post infection.

Chapter 4. Circadian regulation of a limited set of conserved microRNAs in *Drosophila*

Summary

MicroRNAs (miRNAs) are short non-coding RNA molecules that target mRNAs to control gene expression by attenuating the translational efficiency and stability of transcripts. They are found in a wide variety of organisms, from plants to insects and humans. Here, we use *Drosophila* to investigate the possibility that circadian clocks regulate the expression of miRNAs. We used a microarray platform to survey the daily levels of *D. melanogaster* miRNAs in adult heads of wild-type flies and the arrhythmic clock mutant *cyc*⁰¹. We find two miRNAs (dme-miR-263a and -263b) that exhibit robust daily changes in abundance in wild-type flies that are abolished in the *cyc*⁰¹ mutant. dme-miR-263a and -263b reach trough levels during the daytime, peak during the night and their levels are constitutively elevated in *cyc*⁰¹ flies. A similar pattern of cycling is also observed in complete darkness, further supporting circadian regulation. In addition, we identified several miRNAs that appear to be constitutively expressed but nevertheless differ in overall daily levels between control and *cyc*⁰¹ flies. The circadian clock regulates miRNA expression in *Drosophila*, although this appears to be highly restricted to a small number of miRNAs. A common mechanism likely underlies daily changes in the levels of dme-miR-263a and -263b. Our results suggest that cycling miRNAs contribute to daily changes in mRNA and/or protein levels in *Drosophila*. Intriguingly, the mature forms of dme-miR-263a and -263b are very similar in

sequence to several miRNAs recently shown to be under circadian regulation in the mouse retina, suggesting conserved functions.

Introduction

Circadian rhythms (approx. 24 hr) are governed by cellular "clocks" or pacemakers that can be synchronized to the daily and seasonal changes in external time cues (zeitgebers), most notably visible light and ambient temperature (reviewed in, [95]). This endogenously driven timing system enables life forms to anticipate environmental transitions, perform activities at biologically advantageous times during the day and undergo characteristic seasonal responses. An important challenge is to gain a better understanding of the biochemical and cellular bases underlying clocks.

Despite the wide variety of overt rhythms manifested by different species (e.g., from flowering in plants to wake-sleep cycles in humans), there is remarkable similarity in the underlying timing mechanisms. A core feature is based on species or tissue specific sets of 'clock' genes, whose RNA and protein products participate in interconnected positively and negatively acting transcriptional-translational feedback loops [96, 97]. As a result of the design principles inherent in these autoregulatory molecular loops, one or more of the core clock RNA and protein products manifest 'self-sustained' daily rhythms in abundance that are instrumental for normal clock progression. The central clock transcription factors that participate in their own cyclical expression and that of other core clock genes also either directly or indirectly drive daily oscillations in the expression of many downstream effector genes. Microarray profiling studies indicate that ~1-10% of the genes expressed in a particular animal cell type undergo circadian fluctuations, demonstrating the strong influence of clocks in

global gene expression [98-100]. Indeed, malfunctions in mammalian clock function have been linked to many diseases including cancer, metabolic syndromes and affective disorders [101-103].

Our understanding of clock mechanisms in general and mammalian ones in particular have been strongly based on findings using *Drosophila melanogaster* as a model system [95]. Key components of the intracellular clock mechanism in this species include PERIOD (*Drosophila* PER; *dPER*), TIMELESS (TIM), CLOCK (CLK) and CYCLE (CYC). CLK and CYC are transcription factors of the basic-helix-loop-helix (bHLH)/PAS (*Per-Arnt-Sim*) superfamily that heterodimerize to stimulate the daily transcription of *dper* and *tim*, in addition to other clock and downstream genes. After a time delay, *dPER* and TIM enter the nucleus where the association of *dPER* with the CLK-CYC heterodimer leads to the inhibition of CLK-dependent transcriptional activity. After several hours the levels of TIM and *dPER* undergo sharp decreases, relieving autoinhibition and initiating another round of CLK-CYC-dependent transcription. Mutations that either inactivate or severely impair the activities of *dper* (e.g., *per*⁰¹), *tim* (e.g., *tim*⁰¹) *cyc* (e.g., *cyc*⁰¹), or *Clk* (e.g., *Clk*^{Jrk}), abolish molecular and behavioral rhythms [104].

MicroRNAs (miRNAs) are single-stranded RNA species of ~22 nucleotides that are derived by processing from a larger precursor and are found in a wide variety of organisms, from plants to insects and humans (recently reviewed in [105]). In animals, miRNAs usually have imperfect complementarity to elements in the 3' untranslated regions (UTRs) of mRNA targets, leading to post-transcriptional regulation of the target mRNA by inhibition of translation and/or stimulation of

degradation [106-108]. It is thought that miRNAs mainly function to fine-tune the levels of key proteins. At present, estimates suggest there are about 100 miRNA encoding genes in insects, and over 400 in mammals [<http://microrna.sanger.ac.uk/cgi-bin/sequences/browse.pl>]. Although a comprehensive list of mRNAs targeted by miRNAs is still lacking in any organism, computational analysis suggests that a single miRNA could target 100s of genes [109]. Recent studies indicate that miRNAs have diverse physiological roles, such as apoptosis, homeobox regulation, viral infection, and development [105, 110]. *Drosophila* has provided a powerful genetic and genomic model system to understand the biological roles of miRNAs [111, 112]. Herein, we show that several miRNAs in *Drosophila* are clock-regulated, raising the possibility that they play fundamental roles in circadian systems.

Results

A limited number of miRNAs exhibit circadian regulation in *Drosophila* heads

To determine whether miRNAs exhibit daily changes in abundance we entrained control *D. melanogaster* flies (*yw*) to standard 12 hr light/12 hr dark cycles [12:12LD; where zeitgeber time 0 (ZT0) is defined as beginning of the light phase] at 25°C and collected flies at 6 hr intervals during the third LD cycle (i.e., ZT1, 7, 13 and 19). In addition, we analyzed the well-characterized *cyc*⁰¹ arrhythmic mutant [113]. The wild-type control and mutant *cyc*⁰¹ flies used here are in the same *yw* genetic background and were treated contemporaneously. RNA was prepared from adult heads, which contain the key pacemaker neurons driving rhythmic behavior [114] and are routinely used to evaluate cycling profiles of mRNAs in *Drosophila* (e.g., [99, 115]). We used the miRMAX microarray platform with the Array900 miRNA Direct Labeling System [116] that features dimer probes complementary to mature or abridged miRNA sequences of all the identified miRNAs of *Drosophila* according to the miRBase version 5.1 [<http://www.sanger.ac.uk/Software/Rfam/>]. For each time point, three independent experiments were analyzed and data pooled (Figure 4.1).

To identify clock-regulated miRNAs we applied several criteria. First, there had to be at least a statistically significant difference between the lowest and highest signal intensity of the four time points analyzed in wild-type flies. We applied the stringent test of ANOVA with FDR (5%) to compare within each

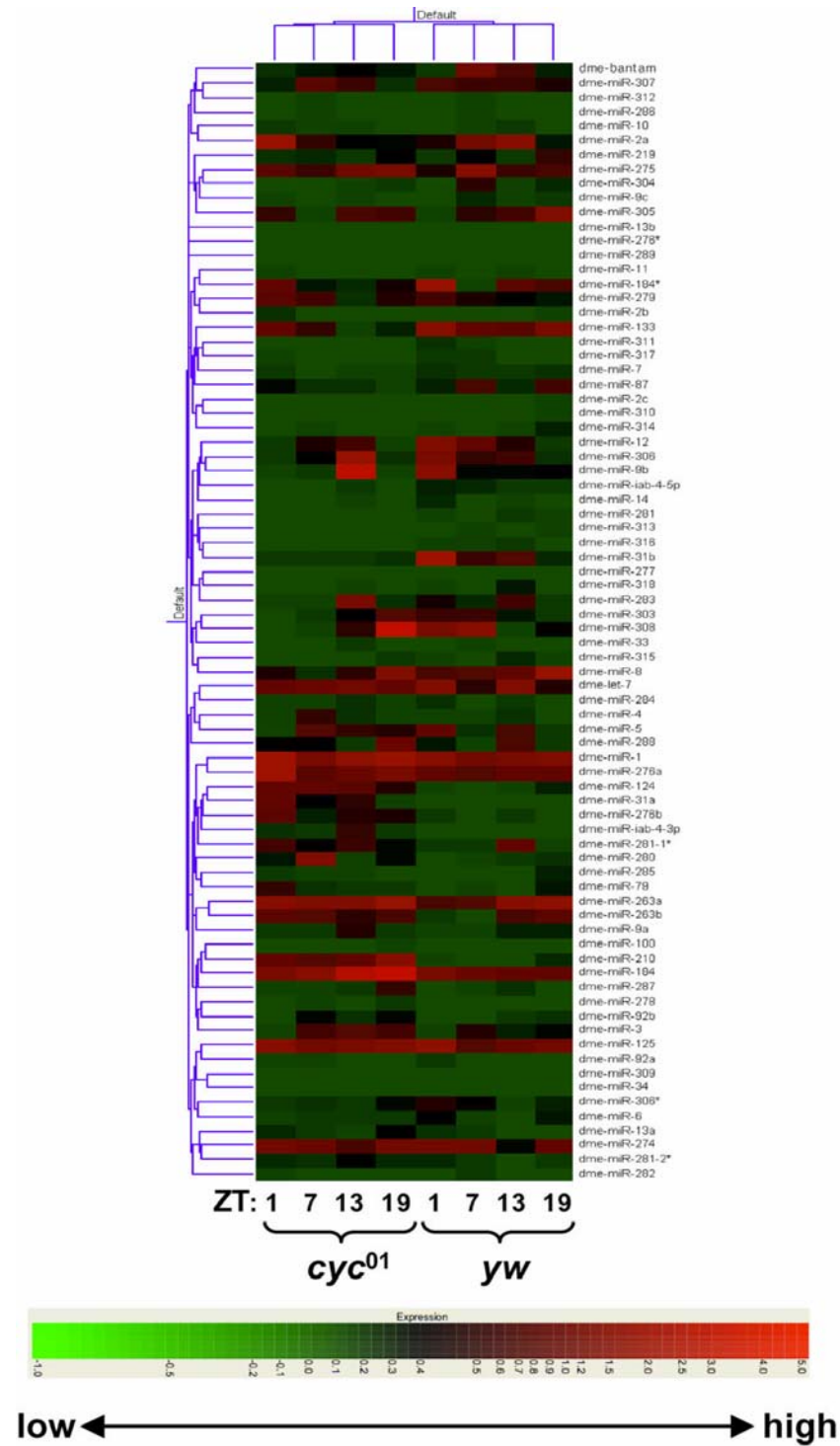


Figure 4.1. Heatmap of *Drosophila* miRNA expression as a function of daily time and in *cyc*⁰¹ flies.

Figure Legend 4.1 Continued

Colorgram depicts the relative levels of miRNAs (high, red; average, black; low, green—as indicated by color bar, bottom) and summarizes hierarchical clustering of daily light-dark patterns of miRNAs in control (*y w*) and mutant (*y w;;cyc⁰¹*) flies using Genespring GX (Agilent, Santa Clara, CA). Flies were collected at ZT1, 7, 13 and 19, as indicated (bottom of panel).

genotype as a function of time, and between the *yw* control and *yw;; cyc⁰¹* (herein, more simply referred to as *cyc⁰¹*) mutant groups. Second, a bona-fide clock-regulated miRNA should not exhibit statistically significant difference between the four time points in *cyc⁰¹* flies; i.e., levels should remain constant throughout a daily cycle—as is observed for clock-controlled mRNAs in this mutant [113, 117]. Finally, we required a minimum difference of 50% between peak and trough values in wild-type flies.

We obtained significant signals from 78 *Drosophila melanogaster* miRNAs (Figure 4.1). Of these, only two miRNAs (dme-miR-263a and -263b) in wild-type control flies exhibited daily abundance changes that were statistically significant using the ANOVA with 5% FDR test (Figure 4.2A and 4.2B). Importantly, the levels of miR-263a and -263b were constant throughout a daily cycle in the *cyc⁰¹* mutant, indicative of bona-fide circadian regulation (Figure 4.2A and 4.2B). Intriguingly, both miRNAs attain trough levels during the daytime hours and have constitutively elevated levels in the *cyc⁰¹* mutant, suggesting a common mechanism underlying their clock regulation (see Discussion). We confirmed that both dme-miR-263a and -263b cycle using quantitative RT-PCR (qRT-PCR) and also showed that these oscillations persist in constant dark conditions (Figure 4.2C and 4.2D). Although it is not clear why the daily profiles are slightly different when comparing results obtained using the microarray platform or qRT-PCR, the combined results clearly indicate circadian regulation in the levels of dme-miR-263a and -263b.

No miRNAs that we evaluated showed significant differences in levels as a function of time in *cyc⁰¹* flies, suggesting that (at least in the absence of a

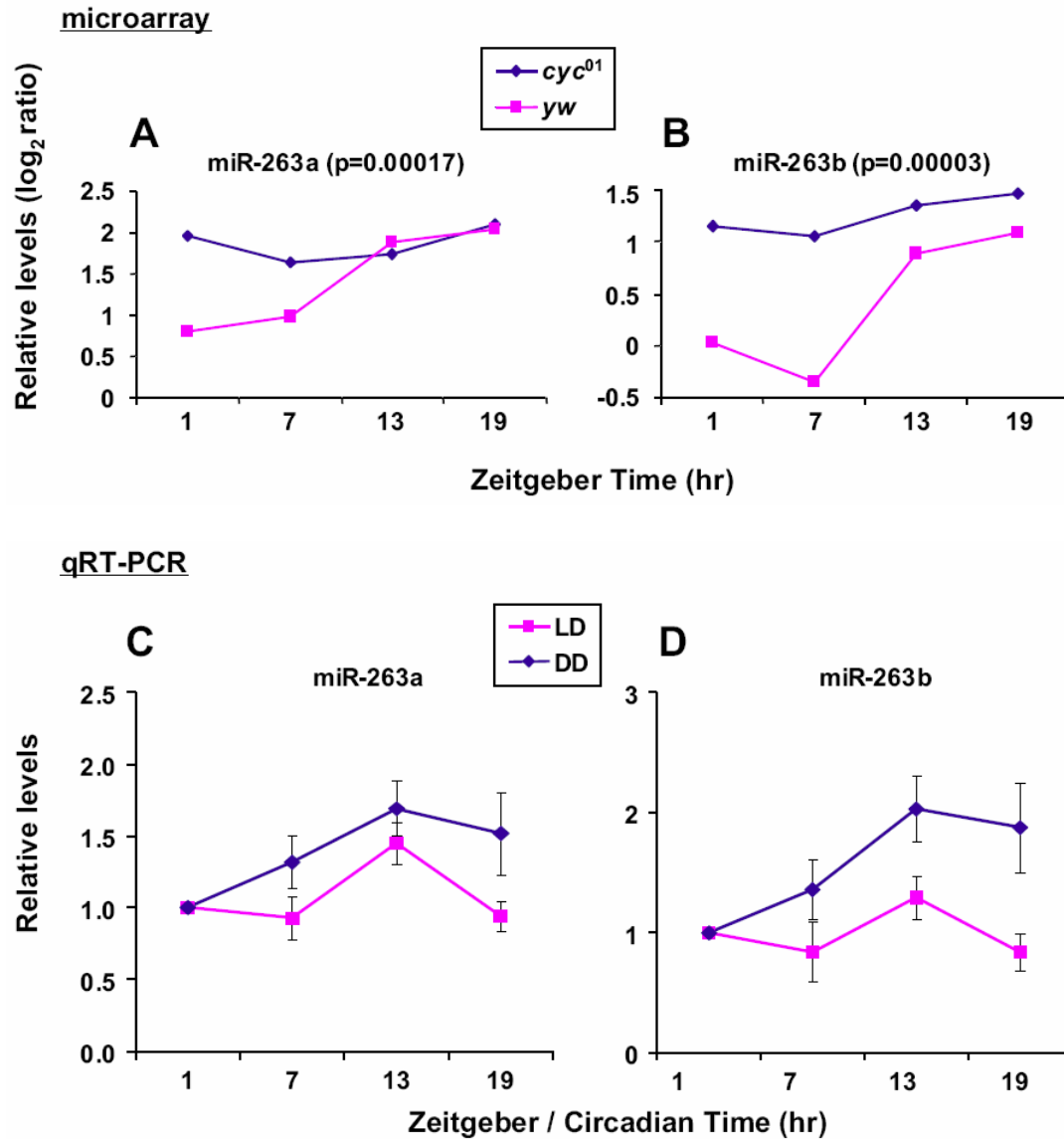


Figure 4.2. MiRNAs showing significant differences in levels as a function of daily time within the *yw* control group

(A, B) *yw* or *yw*; *cyc*⁰¹ flies were collected at the indicated times during the third LD cycle. LMW RNA was prepared from head extracts and subjected to miRNA microarray profiling. Shown are the miRNAs with statistically different levels as a function of time within the *yw* group but not within the *yw*; *cyc*⁰¹ group. P values

Figure Legend 4.2 Continued

are indicated for each miRNA. (C, D) *Canton-S* flies were collected at the indicated times during either the third LD or the first day of DD. Total RNA was prepared from head extracts and subjected to quantitative RT-PCR (qRT-PCR). Results reflect the average of four replicates from two independent experiments. Error bars are S.E.M.

functional clock) the light-dark cycle has little to no direct effect on the expression of miRNAs in *Drosophila* heads. We also identified miRNAs that do not exhibit statistically significant changes throughout a daily cycle in wild-type flies but nonetheless show differences in average daily levels when compared to *cyc*⁰¹ flies (Figure 4.3). In most cases, the average daily values in *cyc*⁰¹ flies were higher compared to control flies. Of these, dme-miR-124 showed a pattern very similar to that of dme-miR-263a and -263b, exhibiting trough levels during the mid-day that were followed by increases during the early to late-night in wild-type flies and constantly elevated levels in the *cyc*⁰¹ mutant (Figure 4.3B). Although the differences in daily levels for miR-124 in wild-type flies do not reach significance even when less stringent criteria was applied ($p=0.0813$, ANOVA without FDR), it is possible that miR-124 undergoes low amplitude circadian oscillations in abundance. Likewise, miR-31a (Figure 4.3F) might also exhibit low amplitude cycling similar to that of miR-124.

Possible circadian-relevant targets of dme-miR-263a and 263b

Experimental and computational studies have shown that several hundred different mRNAs can be targeted by each miRNA [109, 118]. As an initial attempt to identify possible targets for the miRNAs that either show circadian regulation or differences in overall daily levels between control and *cyc*⁰¹ flies (Figures 4.2 and 4.3) we used four readily available web-based prediction programs that contain information on *D. melanogaster* (i.e., PicTar [<http://pictar.bio.nyu.edu>], miRBase [<http://microrna.sanger.ac.uk>], TargetScan [<http://www.targetscan.org>] and

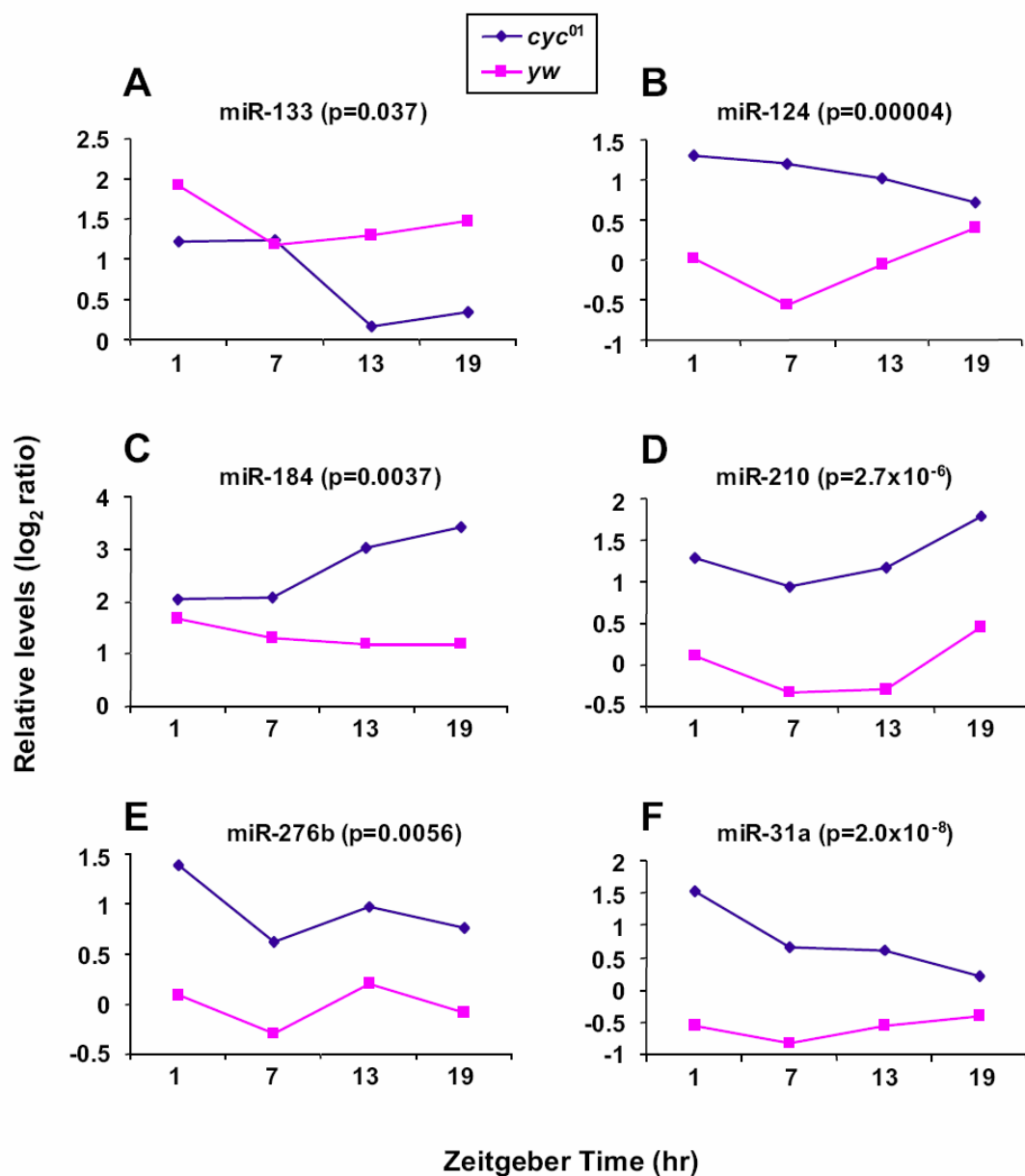


Figure 4.3. MiRNAs showing significant differences in overall daily levels between *yw* and *cyc*⁰¹ flies

yw or *yw*;; *cyc*⁰¹ flies were collected at the indicated times during the third LD cycle. LMW RNA was prepared from head extracts and subjected to miRNA microarray profiling. Shown are the miRNAs with statistically different overall daily levels between the *yw* and *yw*;; *cyc*⁰¹ groups. P values are indicated for each miRNA.

EMBL [<http://www.russell.embl.de/miRNAs>]).

Cycling mRNAs that were previously identified based on whole genome expression profiling (e.g., [72, 119-123]) are found among the predicted targets of the clock-regulated miRNAs we detected in this study (data not shown). This is to be expected based simply on the many clock regulated genes reported to date, the possibility that a single miRNA can target many different transcripts and the use of multiple prediction programs. However, although hundreds of circadian regulated mRNAs have been identified in *Drosophila* using microarray-based strategies, there is little overlap between the different studies, except for the high-amplitude core clock transcripts (e.g., [99, 121, 124]). In addition, miRNAs apparently function in animals by mainly regulating translational efficiency [107, 108], suggesting that constitutively expressed mRNAs are equally good targets of miRNAs to generate daily fluctuations in protein levels. Thus, we limited our focus of possible targets to genes that function within the central clock mechanism or with characterized roles in the *Drosophila* circadian timing system (Table 4.1).

Using this more limited search, we noted that *Clk* might be a target of both miR-263a and -263b (Table 4.1). However, this was only predicted by TargetScan and might be an artefact of using a *Clk* sequence with a premature translation stop codon (i.e., the region in question lies upstream to the normal translation stop codon). In addition, although *Clk* RNA levels cycle [125], the total abundance of the protein is constant throughout a daily cycle [17, 18]. Perhaps a more promising candidate is *clockwork orange* (*cwo*), which is a transcriptional repressor recently shown to modulate circadian rhythms in *Drosophila* [126-128]. Two independent

Table 4.1. Predicted clock-relevant targets for miRNAs identified in this study

miRNA	Target ^a
dme-miR-263a	<i>Clk</i> [T] ^b , <i>dbt</i> [P], <i>twi</i> [T], <i>slo</i> [S]
dme-miR-263b	<i>Clk</i> [T], <i>cwo</i> [P, E]
dme-miR-31a	-
dme-miR-124	<i>jet</i> [S]
dme-miR-133	<i>CklIα</i> [S], <i>slo</i> [S]
dme-miR-184	-
dme-miR-210	<i>per</i> [S], <i>CklIβ</i> [S]
dme-miR-276b	<i>tim</i> [S, T], <i>CklIβ</i> [S]

^aThe predicted targets were limited to the following clock relevant genes (annotation symbol); *dper* (CG2647), *tim* (CG3234), *Clk* (CG7391), *cyc* (CG8727), *vri* (CG14029), *Pdp1* (CG17888), *cwo* (CG17100), *dbt* (CG2048), *CklIα* (CG17520), *CklIβ* (CG15224), *sgg* (CG2621), *slmb* (CG3412), *twi* (CG6235), *wdb* (CG5643), *mts* (CG7109), *jet* (CG8873), *cry* (CG3772), *slo* (CG10693) and *pdf* (CG6496).

^bThe following abbreviations are used: P, Pictar; S, miRBase (Sanger); T, TargetScan; E, EMBL.

search programs (Pictar and EMBL) predict that *cwo* might be targeted by miR-263b. Expression of *cwo* is directly driven by CLK-CYC and exhibits daily RNA cycles that peak in the early night with trough values attained during the late night/early day [126-128]. miR-263b has a similar RNA profile as *cwo*, raising the possibility that it functions to attenuate translation of *cwo* transcripts as they accumulate during the night.

Other possible targets of miR-263a and miR-263b include *doubletime* (*dbt*) and *twins* (*tw*s), respectively. DBT is the *Drosophila* homolog of casein kinase 1 ϵ (CK1 ϵ), whereas TWS is a protein phosphatase type 2A regulator. Both play important but presumably opposing or balancing roles in the *Drosophila* circadian system by targeting key clock proteins, such as dPER and CLK (reviewed in, [6]). Prior work has shown that at least one isoform of the *tw*s transcripts cycles in abundance, rising during the late day and decreasing during the night, while remaining constitutively low in the *cyc*⁰¹ mutant [15]. Intriguingly, miR-263b expression is essentially anti-phase to that of the cycling *tw*s transcript and is constantly high in *cyc*⁰¹ flies (Figure 4.2). Thus, miR-263b could amplify daily oscillations in the levels or translational efficiency of *tw*s RNA. While speculation is tempting, just one out of the four prediction programs identified *dbt* and *tw*s. Finally, the physiological significance of targeting *dbt* expression in a circadian manner by miRNAs is suspect because neither *dbt* mRNA nor protein levels cycle [129].

With regards to the other class of miRNAs that show differences in overall daily levels between wild-type and *cyc*⁰¹ flies (Figure 4.3), we noted several

clock-relevant genes as putative targets (Table 4.1). A possibly noteworthy finding is that casein kinase 2 (CKII), which has a role in the *Drosophila* clock [13, 14], is predicted to be a target of miR-133, miR-210 and miR-276b. It is thought that the presence of multiple miRNA interaction sites allows for exquisite control of target mRNA expression [130]. Nonetheless, only a single prediction program (in this case, Sanger) identified *CkII* as a potential target of these miRNAs. Besides *cwo*, the only clock gene that was predicted by more than one program as a potential target of a single miRNA was *tim*, a candidate target of miR-276b (Table 4.1). Clearly, future studies will be required to verify if any of the miRNAs identified in this study play roles in the clock and/or rhythmic expression.

Discussion

Our results indicate that the levels of a limited number of miRNAs in *D. melanogaster* exhibit robust circadian regulation. Of the 78 miRNAs that we probed by expression profiling, only dme-miR263a and -263b displayed strong evidence of circadian regulation (with possible weak cycling for dme-miR-124). Importantly, the daily cycles in dme-miR263a and -263b were abolished in the *cyc*⁰¹ mutant, and persisted in constant dark conditions (Figure 4.2). These results indicate that changes in the amounts of miR-263a and -263b are not merely driven by daily light-dark cycle but are dependent on a functional clock. Moreover, we did not detect other miRNAs that display robust cycling profiles in daily light-dark cycles, suggesting that the expression of miRNAs in *D. melanogaster* is largely insensitive to photic signals. However, we cannot rule out transient effects of light. In addition, it is possible that highly stable miRNAs, despite circadian regulation in expression, would not exhibit daily cycles in abundance. Also, as an initial foray into determining whether miRNA expression in *Drosophila* is under circadian regulation we used total head extracts as a source for miRNA isolation, which could mask cell or tissue specific temporal regulation. Despite these caveats the limited number of cycling miRNAs strongly suggests that these molecular rhythms mainly arise at the level of transcriptional regulation and not oscillations in the miRNA-processing machinery.

At least two interconnected transcriptional feedback loops operate within the core clock mechanism in *Drosophila* [131]. In the ‘major’ loop, CLK and CYC form a heterodimer that binds E-box containing elements found in 5’ regulatory

regions of *dper*, *tim* and *vrille* (*vri*), in addition to numerous other downstream effector genes. While dPER and TIM cooperate to negatively regulate CLK-CYC transactivation, VRI functions in an interacting transcriptional loop by binding to 5' upstream regulatory elements on *Clk*, an event that inhibits *Clk* expression. As a result of the molecular logic underlying the intertwined transcriptional circuitry, *dper*, *tim* and *vri* mRNA levels follow a similar temporal profile peaking in the early night, whereas *Clk* transcripts exhibit essentially anti-phase cycling [125].

MiR-263a and -263b have similar daily profiles, with peak levels in the early to mid-night (between ZT/CT13 and ZT/CT19) and trough amounts reached during the early to mid-day (ZT/CT1-7) (Figure 4.2). Moreover, both miRNAs are constitutively expressed at peak levels in the *cyc*⁰¹ mutant, suggesting a common mechanism is controlling daily changes in the levels of miRs -263a and -263b. The daily patterns of changes in the levels of miR-263a and -263b are somewhat reminiscent of mRNA targets directly regulated by CLK-CYC. However, whereas the levels of *bona-fide* direct targets of CLK-CYC, such as *dper* and *tim*, are reduced in *cyc*⁰¹ flies [113, 117], the abundance of miR-263a and -263b are pegged at peak amounts (Figure 4.2). These considerations raise the possibility that the circadian expression of miR-263a and -263b is not directly driven by core clock transcription factors. For example, CLK-CYC might stimulate the rhythmic expression of a transcriptional inhibitor that blocks transcription of miR-263a and -263b during the day.

Besides targeting individual genes, clusters of genes can be coordinately regulated by the circadian clock in *Drosophila*, presumably as a result of temporal

changes in chromatin remodelling [72]. In a somewhat analogous manner, recent evidence shows that multiple unique miRNAs can be generated and co-regulated from a single primary miRNA (pri-miRNA) transcript [132, 133]. However, even though miR-263a and -263b are paralogous genes in the same family (miR-263) with very similar mature sequences (Figure 4.4A), they are found on the second and third chromosomes, respectively. The fact that these two miRNAs have closely related target sites and undergo similar circadian regulation suggests that they have parallel functions in contributing to rhythms in the expression of an overlapping set of genes. Nonetheless, recent work comparing 12 *Drosophila* genomes suggest that some of the miRNA sequences currently in use need to be revised, which could result in marked changes in predicted targets [134]. This could be especially relevant to this study as evolutionary evidence suggests a different 5' end for miR-263a [134].

Although we also identified several (apparently) non-cycling miRNAs with statistically different overall daily levels between wild-type and *cyc*⁰¹ mutants (Figure 4.3), the physiological significance of these results is presently not clear. Nonetheless, whole genome microarray profiling in *Drosophila* has shown that mutations in core clock transcription factors not only abolishes rhythmic expression but can lead to changes in the basal levels of many constitutively expressed mRNAs (e.g., [123]). Future work will be instrumental in identifying *in vivo* targets of the miRNAs identified in this study and evaluate their putative roles in the *Drosophila* circadian system.

While this manuscript was under preparation, evidence of miRNA cycling

Shown are the alignments between miRNAs identified in this study and possible mammalian orthologs that were recently described by Xu et al. (2007) as cycling in the mouse retina. The entire sequences of the mature forms of *Drosophila* miRNA are shown in different colors, whereas mouse sequences are shown in black. The identity of the miRNA is shown at left; number in brackets signifies the nucleotide position of the mature mouse miRNA starting from left (5') to right (3'). Sequences used were those in the Sanger miRBase as of December 2007.

and roles in the clock were shown in mammals. One study identified miR-132 and miR-219 as being clock regulated in the suprachiasmatic nucleus (SCN), the ‘master clock’ in mammals [135]. In addition, they also showed that miR-132 plays a role in circadian photic entrainment, whereas miR-219 modulates period length. In another study, several miRNAs specifically expressed in the mouse retina exhibited daily oscillations in levels [133]. Among the subgroup of miRNAs showing circadian regulation in the retina were members of the miR-183/96/182 cluster. We used the miRBase database to determine if any of the miRNAs we identified are similar to the recently described cycling miRNAs in mammals. We used the mature sequences of the *D. melanogaster* miRNAs as queries to search the database for vertebrate miRNAs with similar sequences. Although potentially coincidental, the mature sequence for miR-183 in vertebrates is very similar to that of both *D. melanogaster* dme-miR-263a and miR-263b (Figures 4.4B and 4.4C). The *D. melanogaster* dme-miR-263b is also similar to the vertebrate miR-182 (three mismatches over the length of 20 aligned nucleotides). Finally, the *D. melanogaster* dme-miR-124 is similar to vertebrate miR-124a (Figure 4.4D), which also cycled in the mouse retina [133]. Because we probed whole heads where the majority of the clocks reside in the compound eyes [136], this might have contributed to the surprising overlap in cycling miRNAs between our study and those identified in the mouse retina. Of the miRNAs we identified only miR-276b appears not to be conserved in vertebrates. Thus, our results raise the interesting possibility that similar miRNAs have conserved functions in the circadian systems of vertebrates and insects, perhaps in a tissue-specific manner.

A small proportion of miRNAs in *Drosophila* exhibit robust clock-regulated rhythms in abundance. Our results suggest that for some proteins, daily changes in their levels are modulated by miRNA-mediated post-transcriptional regulation. It is likely that the action of miRNAs in rhythmic expression is to provide a fine-tuning mechanism that coordinates with transcriptional and post-translational pathways to generate an oscillatory system that can adjust the levels of specific proteins to values that are appropriate for a given time of day.

Materials and Methods

Fly strains and treatment

Drosophila strains used were descendants of *Canton-S*, *yw* and *yw;; cyc⁰¹* strains previously described [113]. Flies were maintained in standard media at 25°C. For collections, approximately 30-100 young (2-5 day old) flies were placed in vials that were incubated at 25°C for three to four days in standard 12hr light-12hr dark cycles [LD; where zeitgeber time 0 (ZT0) is defined as lights-on], and in some cases followed by complete darkness [DD; where circadian time 0 (CT0) is defined as subjective lights-on]. Flies were collected by freezing in dry ice during the third or fourth LD cycle or the first DD cycle at the following times; ZT/CT1, 7, 13 and 19. Subsequently, heads were isolated from the frozen flies and kept at -70°C until further processed, as described below.

RNA preparation and labelling

Adult fly heads were flash frozen and ground into fine powder in liquid nitrogen for miRNA microarray analysis. Low molecular weight (LMW) RNA was purified using the mirVana™ miRNA extraction kit (Ambion, Austin, TX, USA). About 250 ng of LMW RNA was used as the input for miRNAs labelling using the Array900 miRNA Direct kit (Genisphere Inc., Hatfield, PA, USA), a tagging method that allows direct labeling of mature miRNAs without PCR amplification. All samples were labelled with Cy5 dye. A pooled control was labelled with Cy3 and equal amount of the tagged Cy3 was hybridized to every chip. The fluorescent (Cy5/ Cy3) signal of

each labelled miRNA was amplified about 850-900 times after being tagged with 3DNA dendromer in hybridization [116].

MiRNA microarrays

For microRNA expression evaluation, we used miRMAX microarray technology [116] that features tandem dimer probes complementary to mature microRNA sequences (or abridged sequence) of all the identified miRNAs of *Drosophila* according to the miRNA registry VERSION 5.1 [<http://microrna.sanger.ac.uk/sequences>]. The total number of miRNAs on the chip is 1231, which includes 1087 miRNAs from miRbase 5.1 and 144 predicted human miRNAs. The chip contains several subarrays for all miRNAs from *Drosophila*, *C. elegans*, human, mouse, and rat so it can be used for probing various organisms. We only extracted data from the *Drosophila* subarray. The miRMAX microarray can detect miRNA expression with only 100 ng LMW RNA input. Three independent RNA samples for each time point were hybridized and analyzed. Microarray chips were hybridized in Hybex Microarray Incubation System (SciGene, Sunnyvale, CA) and processed according to the protocol of the Array900 miRNA Direct kit (Genisphere Inc., Hatfield, PA, USA). A GenePix 4000B scanner (Axon Instruments, Union City, CA, USA) was used to scan individual chips and median spot intensities were generated using GenePix 4.0 (Axon Instruments).

Statistical analysis for microarrays

Scanned microarray raw data were processed and normalized using a GeneTraffic Duo server on campus (Stratagene, La Jolla, CA, USA). We used the Cy3 labelled *cyc*⁰¹ ZT1 samples (About 200 ng LMW RNA input for each chip) for normalization, so that we could compare ratios of a given miRNA relative to the same sample. Data were transformed into log₂ ratio and were further analyzed by using the Genespring GX software (Agilent, Santa Clara, CA). First, miRNAs from all genes were tested with Welch ANOVA among the following groups based on time points ZT1, 7, 13, and 19 in both *yw* and *cyc*⁰¹ origin; p-value cutoff 0.05, multiple testing correction: Benjamini and Hochberg False Discovery Rate (FDR). Then, Welch t-test was used to identify significantly differentially expressed miRNAs between "origin *yw*" and "origin *cyc*⁰¹" from the Volcano Plot built. Multiple Testing Correction: Benjamini and Hochberg False Discovery Rate. Which Genes were differentially expressed was defined by Fold Difference, 1.5 and a P-value Cutoff, 0.05.

Quantitative RT-PCR

Approximately 30 to 40 adult flies were frozen on dry ice at the indicated times during either LD or DD and kept at -80°C until further processing. Fly heads were isolated and crushed in 200 µl of TRI Reagent (Sigma) with a motorized pestle, as previously described [83, 137]. Total RNA was prepared according to the manufacturer's instruction and the final RNA pellet was resuspended in 12-15 µl of DEPC-treated water. For the analysis of miR-263a and miR-263b, 4 µl of total

RNA solution were subjected to reverse transcription in the presence of miRNA-specific primers as supplied by the manufacturer (TaqMan MicroRNA Assay, Applied Biosystems). The resulting cDNAs were diluted 15-fold in 1 mM Tris-HCl (pH 8.0). Subsequently, 2 μ l of cDNA solution were added to a total of 20 μ l and PCR reactions performed in triplicate using either the miR-263a or miR-263b specific primers, according to the manufacturer's instructions (TaqMan MicroRNA Assay, Applied Biosystems). We used oligo-dT primed cDNA synthesis to measure the levels of the internal controls, *rp49* or *cbp20*, as previously described [83, 137]. Briefly, 2 μ l of total RNA solution was used for reverse transcription (Omniscript RT, Qiagen). The resulting cDNAs were diluted 10-fold in 1 mM Tris-HCl (pH 8.0). Subsequently, 2 μ l of cDNA solution were added to a total of 30 μ l and PCR reactions performed in triplicate (QuantiTect SYBR Green PCR, Qiagen) with the following conditions: an initial step of 15 min at 95°C to activate HotStarTaq DNA polymerase, followed by 40 cycles of 15 s at 94°C, 30 s at 60°C, and 30 s at 72°C. All PCR reactions were performed in 96-well plates using an ABI prism 7600 system (Applied Biosystems). Standard curves were generated with serially diluted cDNA samples for every run and the relative copy number of the gene of interest was calculated based on Ct (threshold cycle) values. The values for miR-263a and miR-263b were normalized to the relative copy number of *rp49* or *cbp20* cDNAs. Finally, the relative levels of miR-263a and miR-263b at ZT/CT1 were set to 1.0 and the other values normalized. The efficiency of all the PCR reactions was at least 90%.

Chapter 5. Summary

Circadian regulation in the ability of *Drosophila* to combat pathogenic infections

Predictable daily cycles of environmental changes likely underlie timing systems that can anticipate such changes and hence enable organisms to perform their physiological activities at biologically advantageous times.

Our immune system adds to a growing list of examples that are regulated by circadian clock. Numerous immunological parameters show time-of-day effects: the counts and functions of lymphoid cells, the levels of pro-inflammatory cytokines, interferon- γ production stimulated by *E. coli* LPS, and antibody titer after immunization [65]. The findings described in chapter 2 indicate that in *Drosophila*, the circadian clock can even modulate the survival outcomes, depending on the time of pathogenic infections.

LPS, a component in the outer cell layer of gram-negative bacteria, serves as one of the main signals in the pathogenesis of sepsis in mammals. Sepsis results from the uncontrolled activation of host-derived factors such as pro-inflammatory cytokines in response to bacteria or bacterial products, leading to multi-organ failure, cardiovascular collapse and death [138]. Mammals are sensitive to LPS and detect a small amount of infectious microorganisms at an early stage, thus inducing innate immune response and destroying the invading pathogens in a timely manner [139]. Ironically, the efforts of the host to defend it can also be detrimental if they go out of control. For example, when neutrophils

are activated systemically, they mediate microvascular injury by overproducing elastases and reactive oxygen species. They are efficient weapons to destroy bacteria, but also capable of damaging host tissues [140].

It is interesting to notice that the circadian pattern of the lipopolysaccharide (LPS) response in mammals shows a remarkable similarity to that of *Drosophila* survival over pathogenic bacterial infections reported in our study (chapter 2), in a sense that both mammalian LPS response and *Drosophila* immune response tend to be stronger during the resting period. In mice, LPS-induced lethality is at its trough in the middle of the activity period and increases towards the end of the resting period [141]. Also in humans, the fever and hypothalamic-pituitary-adrenocortical (HPA) axis activation in response to LPS is greater in the evening than in the morning [141]. Considering the similar circadian pattern of the LPS-induced lethality in mammals and that of survival to pathogenic infection in *Drosophila*, both of which depend on the level of induced immune response, *Drosophila* may serve as a useful model organism to provide a mechanistic basis for sepsis as well as chronotherapeutic strategies concerning the time-of-administration of cytokines or immunomodulatory drugs.

If the circadian clock governs the magnitude of the induced immune response, then how could they be connected? The clock mutant effects on the survival over pathogenic infections may provide some clues. It was shown that *per*⁰¹ flies succumb to death much faster than wild-type flies whereas *tim*⁰¹ flies are more resistant to pathogenic bacteria (Figure 2.1). In *per*⁰¹ flies, there is no detectable level of PER but significant amount of TIM available [142]. On the other

hand, *tim*⁰¹ flies do not have detectable level of PER or TIM [142]. Therefore, PER may provide protection to the infected flies whereas TIM may suppress the immune response and negate the survival outcomes. This antagonistic relationship between PER and TIM demands non-circadian roles, considering that both PER and TIM inhibit the transcription of CLK/CYC-mediated transcription as central pacemakers [5]. To test this idea, it will be interesting to see if the flies overexpressing *tim* in *tim*⁰¹ background die faster than their control *tim*⁰¹ flies. One can also expect that the flies overexpressing *per* or downregulating *tim* in *per*⁰¹ background would survive better than their control *per*⁰¹ flies.

Another important issue regarding the circadian regulation in the immune response is finding the tissue(s) responsible for it. It is intriguing that *tim* mRNA and PER cycle in the abdominal fat body (K. Xu, unpublished data). It will be informative to overexpress *per* in either the fat body or hemocytes in *per*⁰¹ background and see if the fat body clock or hemocyte clock, if there is any, is sufficient to improve the survival of *per*⁰¹ flies.

The head immune response in *Drosophila*

The mammalian immune system operating in the head has been getting a lot of attention in terms of its regulatory roles in adult neurogenesis [143] and inflammation-associated neurotoxicity implicated in neurodegenerative diseases [144]. On the other hand, studies in the *Drosophila* immunity have been mainly focused on the body immune response. As a result, there is lack of information regarding the functionality and characteristics of head immune response in

Drosophila. Our study shows that the same principles underlying the activation of the innate immune response operate in the *Drosophila* head as those established in the body (Figure 3.1).

However, *Drosophila* head immune response does not seem to be qualitatively identical to the body one in a sense that it appears more sensitive to bacterial stimuli (Table 3.1 and 3.2). It is worth noticing that mammals adopt neural routes to relay information of microbial invasion to the central nervous system (CNS) and send regulatory signals back to the sites of infection to amplify local immune responses quickly [145]. Considering that in our experimental setup bacterial entry sites were in the abdomen, one would not expect to see a faster induction of immune response in the head if the transmission of bacterial signals were to entirely depend on passive diffusion from their entry site. In a preliminary experiment where isolated heads and bodies were incubated with LPS and their immune response was monitored by *dipthericin-lacZ* over time, we observed a significant induction of *dipthericin-lacZ* only from the bodies, suggesting that the head immune response requires an intact physical connection between the head and the body (data not shown). It is tempting to speculate there might be some neuronal innervation relaying the bacterial signal from the body to the head just like the vagus nerve in mammalian system [146]. In this context, it will be interesting to find out if neuronal activities are involved in *Drosophila* head immune response. To this end, one can inhibit synaptic transmission (Tetanus toxin light chain) [147], increase neuronal membrane excitability (NaChBac) [148], or hyperpolarize neurons (Kir_{2.1}) [149] by employing UAS-GeneSwitch systems and analyze the

head and body immune response of the flies whose neuronal activities are disturbed by the manipulations mentioned above.

Although we demonstrated that the pericerebral fat body is sufficient to protect the flies from bacterial infection (Figure 3.4), it is not clear at this point how much it contributes to the overall immune response. To gauge the physiological importance of the pericerebral fat body, we set up a cross to get the flies overexpressing *head involution defective*, an apoptotic effector caspase gene in *Drosophila* [150], in the pericerebral fat body at an adult stage using S₁₃₂ Gene-Switch driver and the analysis of those flies is underway.

Interestingly, RELISH overexpressed only in neurons also contributes to the survival of adult flies over bacterial infections (Figure 3.4). Its underlying mechanisms can be speculated in three aspects: First, neurons may be capable of mounting a functional immune response mediating RELISH, such as the production of AMPs. Second, they may play a regulatory role to enhance humoral or cellular immunity. Third, they may coordinate the overall behavioral response in a way that would maximize the chance of survival in pathogenic infections. For example, it would be more advantageous to the survival of hosts if they could reserve available metabolic resources as much as possible for boosting immune responses by minimizing their usage for physiological functions less critical for the survival over pathogenic infections. Lethargy and decrease in feeding, social interaction and exploration hallmark the sickness behavior of mammals [151]. Shirasu-Hiza et al reported that flies infected with a lethal dose of *S. pneumoniae* sleep for shorter length of time than mock-injury control flies [68]. It will be

interesting to find out if the flies overexpressing RELISH only in neurons sleep more than *relish* null mutant flies in response to bacterial infections, establishing a positive correlation between the amount of sleep after pathogenic infections and the survival outcome.

References

1. Moore-Ede, M.C., Sulzman, F.M., and Fuller, C.A. (1982). *The clocks that time us* (Cambridge: Harvard University Press).
2. Czeisler, C.A., and Gooley, J.J. (2007). Sleep and circadian rhythms in humans. *Cold Spring Harb Symp Quant Biol* 72, 579-597.
3. Sack, R.L., Lewy, A.J., Blood, M.L., Keith, L.D., and Nakagawa, H. (1992). Circadian rhythm abnormalities in totally blind people: incidence and clinical significance. *J Clin Endocrinol Metab* 75, 127-134.
4. Levi, F., Canon, C., Dipalma, M., Florentin, I., and Misset, J.L. (1991). When should the immune clock be reset? From circadian pharmacodynamics to temporally optimized drug delivery. *Ann N Y Acad Sci* 618, 312-329.
5. Stanewsky, R. (2003). Genetic analysis of the circadian system in *Drosophila melanogaster* and mammals. *J Neurobiol* 54, 111-147.
6. Bae, K., and Edery, I. (2006). Regulating a circadian clock's period, phase and amplitude by phosphorylation: insights from *Drosophila*. *J Biochem (Tokyo)* 140, 609-617.
7. Grima, B., Lamouroux, A., Chelot, E., Papin, C., Limbourg-Bouchon, B., and Rouyer, F. (2002). The F-box protein slimb controls the levels of clock proteins period and timeless. *Nature* 420, 178-182.
8. Ko, H.W., Jiang, J., and Edery, I. (2002). Role for Slimb in the degradation of *Drosophila* Period protein phosphorylated by Doubletime. *Nature* 420, 673-678.
9. Koh, K., Zheng, X., and Sehgal, A. (2006). JETLAG resets the *Drosophila* circadian clock by promoting light-induced degradation of TIMELESS. *Science* 312, 1809-1812.
10. Martinek, S., Inonog, S., Manoukian, A.S., and Young, M.W. (2001). A role for the segment polarity gene shaggy/GSK-3 in the *Drosophila* circadian clock. *Cell* 105, 769-779.

11. Naidoo, N., Song, W., Hunter-Ensor, M., and Sehgal, A. (1999). A role for the proteasome in the light response of the timeless clock protein. *Science* **285**, 1737-1741.
12. Stanewsky, R., Kaneko, M., Emery, P., Beretta, B., Wager-Smith, K., Kay, S.A., Rosbash, M., and Hall, J.C. (1998). The cryb mutation identifies cryptochrome as a circadian photoreceptor in *Drosophila*. *Cell* **95**, 681-692.
13. Akten, B., Jauch, E., Genova, G.K., Kim, E.Y., Edery, I., Raabe, T., and Jackson, F.R. (2003). A role for CK2 in the *Drosophila* circadian oscillator. *Nat Neurosci*.
14. Lin, J.M., Kilman, V.L., Keegan, K., Paddock, B., Emery-Le, M., Rosbash, M., and Allada, R. (2002). A role for casein kinase 2alpha in the *Drosophila* circadian clock. *Nature* **420**, 816-820.
15. Sathyanarayanan, S., Zheng, X., Xiao, R., and Sehgal, A. (2004). Posttranslational regulation of *Drosophila* PERIOD protein by protein phosphatase 2A. *Cell* **116**, 603-615.
16. Fang, Y., Sathyanarayanan, S., and Sehgal, A. (2007). Post-translational regulation of the *Drosophila* circadian clock requires protein phosphatase 1 (PP1). *Genes Dev* **21**, 1506-1518.
17. Kim, E.Y., and Edery, I. (2006). Balance between DBT/CKIepsilon kinase and protein phosphatase activities regulate phosphorylation and stability of *Drosophila* CLOCK protein. *Proc Natl Acad Sci U S A* **103**, 6178-6183.
18. Yu, W., Zheng, H., Houl, J.H., Dauwalder, B., and Hardin, P.E. (2006). PER-dependent rhythms in CLK phosphorylation and E-box binding regulate circadian transcription. *Genes Dev* **20**, 723-733.
19. Nitabach, M.N., and Taghert, P.H. (2008). Organization of the *Drosophila* circadian control circuit. *Curr Biol* **18**, R84-93.
20. Grima, B., Chelot, E., Xia, R., and Rouyer, F. (2004). Morning and evening peaks of activity rely on different clock neurons of the *Drosophila* brain. *Nature* **431**, 869-873.

21. Rieger, D., Shafer, O.T., Tomioka, K., and Helfrich-Forster, C. (2006). Functional analysis of circadian pacemaker neurons in *Drosophila melanogaster*. *J Neurosci* 26, 2531-2543.
22. Stoleru, D., Peng, Y., Agosto, J., and Rosbash, M. (2004). Coupled oscillators control morning and evening locomotor behaviour of *Drosophila*. *Nature* 431, 862-868.
23. Yoshii, T., Funada, Y., Ibuki-Ishibashi, T., Matsumoto, A., Tanimura, T., and Tomioka, K. (2004). *Drosophila* cryb mutation reveals two circadian clocks that drive locomotor rhythm and have different responsiveness to light. *J Insect Physiol* 50, 479-488.
24. Giebultowicz, J.M., and Hege, D.M. (1997). Circadian clock in Malpighian tubules. *Nature* 386, 664.
25. Krishnan, B., Dryer, S.E., and Hardin, P.E. (1999). Circadian rhythms in olfactory responses of *Drosophila melanogaster*. *Nature* 400, 375-378.
26. Tanoue, S., Krishnan, P., Krishnan, B., Dryer, S.E., and Hardin, P.E. (2004). Circadian clocks in antennal neurons are necessary and sufficient for olfaction rhythms in *Drosophila*. *Curr Biol* 14, 638-649.
27. Sakai, T., and Ishida, N. (2001). Circadian rhythms of female mating activity governed by clock genes in *Drosophila*. *Proc Natl Acad Sci U S A* 98, 9221-9225.
28. Jiravanichpaisal, P., Lee, B.L., and Soderhall, K. (2006). Cell-mediated immunity in arthropods: hematopoiesis, coagulation, melanization and opsonization. *Immunobiology* 211, 213-236.
29. Pinheiro, V.B., and Ellar, D.J. (2006). How to kill a mocking bug? *Cell Microbiol* 8, 545-557.
30. Hoffmann, J.A., Kafatos, F.C., Janeway, C.A., and Ezekowitz, R.A. (1999). Phylogenetic perspectives in innate immunity. *Science* 284, 1313-1318.
31. Anderson, K.V. (2000). Toll signaling pathways in the innate immune response. *Curr Opin Immunol* 12, 13-19.

32. Hoffmann, J.A. (2003). The immune response of *Drosophila*. *Nature* 426, 33-38.
33. Kimbrell, D.A., and Beutler, B. (2001). The evolution and genetics of innate immunity. *Nat Rev Genet* 2, 256-267.
34. Vodovar, N., Acosta, C., Lemaitre, B., and Boccard, F. (2004). *Drosophila*: a polyvalent model to decipher host-pathogen interactions. *Trends Microbiol* 12, 235-242.
35. Evans, H.E. (1984). *Insect Biology* (Addison-Wesley Publishing Company).
36. Imler, J.L., and Hoffmann, J.A. (2000). Signaling mechanisms in the antimicrobial host defense of *Drosophila*. *Curr Opin Microbiol* 3, 16-22.
37. Ferrandon, D., Jung, A.C., Cricqui, M., Lemaitre, B., Uttenweiler-Joseph, S., Michaut, L., Reichhart, J., and Hoffmann, J.A. (1998). A drosomycin-GFP reporter transgene reveals a local immune response in *Drosophila* that is not dependent on the Toll pathway. *Embo J* 17, 1217-1227.
38. Tzou, P., Ohresser, S., Ferrandon, D., Capovilla, M., Reichhart, J.M., Lemaitre, B., Hoffmann, J.A., and Imler, J.L. (2000). Tissue-specific inducible expression of antimicrobial peptide genes in *Drosophila* surface epithelia. *Immunity* 13, 737-748.
39. Schroder, J.M. (1999). Epithelial peptide antibiotics. *Biochem Pharmacol* 57, 121-134.
40. Kocks, C., Cho, J.H., Nehme, N., Ulvila, J., Pearson, A.M., Meister, M., Strom, C., Conto, S.L., Hetru, C., Stuart, L.M., Stehle, T., Hoffmann, J.A., Reichhart, J.M., Ferrandon, D., Ramet, M., and Ezekowitz, R.A. (2005). Eater, a transmembrane protein mediating phagocytosis of bacterial pathogens in *Drosophila*. *Cell* 123, 335-346.
41. Bischoff, V., Vignal, C., Duvic, B., Boneca, I.G., Hoffmann, J.A., and Royet, J. (2006). Downregulation of the *Drosophila* immune response by peptidoglycan-recognition proteins SC1 and SC2. *PLoS Pathog* 2, e14.
42. Zaidman-Remy, A., Herve, M., Poidevin, M., Pili-Floury, S., Kim, M.S., Blanot,

- D., Oh, B.H., Ueda, R., Mengin-Lecreulx, D., and Lemaitre, B. (2006). The *Drosophila* amidase PGRP-LB modulates the immune response to bacterial infection. *Immunity* 24, 463-473.
43. Kaneko, T., Yano, T., Aggarwal, K., Lim, J.H., Ueda, K., Oshima, Y., Peach, C., Erturk-Hasdemir, D., Goldman, W.E., Oh, B.H., Kurata, S., and Silverman, N. (2006). PGRP-LC and PGRP-LE have essential yet distinct functions in the *drosophila* immune response to monomeric DAP-type peptidoglycan. *Nat Immunol* 7, 715-723.
 44. Takehana, A., Yano, T., Mita, S., Kotani, A., Oshima, Y., and Kurata, S. (2004). Peptidoglycan recognition protein (PGRP)-LE and PGRP-LC act synergistically in *Drosophila* immunity. *Embo J* 23, 4690-4700.
 45. Bischoff, V., Vignal, C., Boneca, I.G., Michel, T., Hoffmann, J.A., and Royet, J. (2004). Function of the *drosophila* pattern-recognition receptor PGRP-SD in the detection of Gram-positive bacteria. *Nat Immunol* 5, 1175-1180.
 46. Wang, L., Weber, A.N., Atilano, M.L., Filipe, S.R., Gay, N.J., and Ligoxygakis, P. (2006). Sensing of Gram-positive bacteria in *Drosophila*: GGBP1 is needed to process and present peptidoglycan to PGRP-SA. *Embo J* 25, 5005-5014.
 47. Choe, K.M., Lee, H., and Anderson, K.V. (2005). *Drosophila* peptidoglycan recognition protein LC (PGRP-LC) acts as a signal-transducing innate immune receptor. *Proc Natl Acad Sci U S A* 102, 1122-1126.
 48. Vidal, S., Khush, R.S., Leulier, F., Tzou, P., Nakamura, M., and Lemaitre, B. (2001). Mutations in the *Drosophila* dTAK1 gene reveal a conserved function for MAPKKs in the control of rel/NF-kappaB-dependent innate immune responses. *Genes Dev* 15, 1900-1912.
 49. Lu, Y., Wu, L.P., and Anderson, K.V. (2001). The antibacterial arm of the *drosophila* innate immune response requires an IkappaB kinase. *Genes Dev* 15, 104-110.
 50. Rutschmann, S., Jung, A.C., Zhou, R., Silverman, N., Hoffmann, J.A., and Ferrandon, D. (2000). Role of *Drosophila* IKK gamma in a toll-independent antibacterial immune response. *Nat Immunol* 1, 342-347.
 51. Leulier, F., Vidal, S., Saigo, K., Ueda, R., and Lemaitre, B. (2002). Inducible

expression of double-stranded RNA reveals a role for dFADD in the regulation of the antibacterial response in *Drosophila* adults. *Curr Biol* 12, 996-1000.

52. Naitza, S., Rosse, C., Kappler, C., Georgel, P., Belvin, M., Gubb, D., Camonis, J., Hoffmann, J.A., and Reichhart, J.M. (2002). The *Drosophila* immune defense against gram-negative infection requires the death protein dFADD. *Immunity* 17, 575-581.
53. Leulier, F., Rodriguez, A., Khush, R.S., Abrams, J.M., and Lemaitre, B. (2000). The *Drosophila* caspase Dredd is required to resist gram-negative bacterial infection. *EMBO Rep* 1, 353-358.
54. Silverman, N., Zhou, R., Stoven, S., Pandey, N., Hultmark, D., and Maniatis, T. (2000). A *Drosophila* IkappaB kinase complex required for Relish cleavage and antibacterial immunity. *Genes Dev* 14, 2461-2471.
55. Stoven, S., Ando, I., Kadalayil, L., Engstrom, Y., and Hultmark, D. (2000). Activation of the *Drosophila* NF-kappaB factor Relish by rapid endoproteolytic cleavage. *EMBO Rep* 1, 347-352.
56. Stoven, S., Silverman, N., Junell, A., Hedengren-Olcott, M., Erturk, D., Engstrom, Y., Maniatis, T., and Hultmark, D. (2003). Caspase-mediated processing of the *Drosophila* NF-kappaB factor Relish. *Proc Natl Acad Sci U S A* 100, 5991-5996.
57. Kim, M., Lee, J.H., Lee, S.Y., Kim, E., and Chung, J. (2006). Caspar, a suppressor of antibacterial immunity in *Drosophila*. *Proc Natl Acad Sci U S A* 103, 16358-16363.
58. Gottar, M., Gobert, V., Matskevich, A.A., Reichhart, J.M., Wang, C., Butt, T.M., Belvin, M., Hoffmann, J.A., and Ferrandon, D. (2006). Dual detection of fungal infections in *Drosophila* via recognition of glucans and sensing of virulence factors. *Cell* 127, 1425-1437.
59. Jang, I.H., Chosa, N., Kim, S.H., Nam, H.J., Lemaitre, B., Ochiai, M., Kambris, Z., Brun, S., Hashimoto, C., Ashida, M., Brey, P.T., and Lee, W.J. (2006). A Spatzle-processing enzyme required for toll signaling activation in *Drosophila* innate immunity. *Dev Cell* 10, 45-55.
60. Weber, A.N., Tauszig-Delamasure, S., Hoffmann, J.A., Lelievre, E., Gascan,

- H., Ray, K.P., Morse, M.A., Imler, J.L., and Gay, N.J. (2003). Binding of the *Drosophila* cytokine Spatzle to Toll is direct and establishes signaling. *Nat Immunol* 4, 794-800.
61. Tauszig-Delamasure, S., Bilak, H., Capovilla, M., Hoffmann, J.A., and Imler, J.L. (2002). *Drosophila* MyD88 is required for the response to fungal and Gram-positive bacterial infections. *Nat Immunol* 3, 91-97.
 62. Rutschmann, S., Jung, A.C., Hetru, C., Reichhart, J.M., Hoffmann, J.A., and Ferrandon, D. (2000). The Rel protein DIF mediates the antifungal but not the antibacterial host defense in *Drosophila*. *Immunity* 12, 569-580.
 63. Gordon, M.D., Dionne, M.S., Schneider, D.S., and Nusse, R. (2005). WntD is a feedback inhibitor of Dorsal/NF-kappaB in *Drosophila* development and immunity. *Nature* 437, 746-749.
 64. Van Delden, C., and Iglewski, B.H. (1998). Cell-to-cell signaling and *Pseudomonas aeruginosa* infections. *Emerg Infect Dis* 4, 551-560.
 65. Haus, E., and Smolensky, M.H. (1999). Biologic rhythms in the immune system. *Chronobiol Int* 16, 581-622.
 66. Lau, G.W., Goumnerov, B.C., Walendziewicz, C.L., Hewitson, J., Xiao, W., Mahajan-Miklos, S., Tompkins, R.G., Perkins, L.A., and Rahme, L.G. (2003). The *Drosophila melanogaster* toll pathway participates in resistance to infection by the gram-negative human pathogen *Pseudomonas aeruginosa*. *Infect Immun* 71, 4059-4066.
 67. Vitaterna, M.H., King, D.P., Chang, A.M., Kornhauser, J.M., Lowrey, P.L., McDonald, J.D., Dove, W.F., Pinto, L.H., Turek, F.W., and Takahashi, J.S. (1994). Mutagenesis and mapping of a mouse gene, Clock, essential for circadian behavior. *Science* 264, 719-725.
 68. Shirasu-Hiza, M.M., Dionne, M.S., Pham, L.N., Ayres, J.S., and Schneider, D.S. (2007). Interactions between circadian rhythm and immunity in *Drosophila melanogaster*. *Curr Biol* 17, R353-355.
 69. Reichhart, J.M., Meister, M., Dimarcq, J.L., Zachary, D., Hoffmann, D., Ruiz, C., Richards, G., and Hoffmann, J.A. (1992). Insect immunity: developmental and inducible activity of the *Drosophila* dipterin promoter. *Embo J* 11,

1469-1477.

70. Samakovlis, C., Kimbrell, D.A., Kylsten, P., Engstrom, A., and Hultmark, D. (1990). The immune response in *Drosophila*: pattern of cecropin expression and biological activity. *Embo J* 9, 2969-2976.
71. Apidianakis, Y., Mindrinos, M.N., Xiao, W., Lau, G.W., Baldini, R.L., Davis, R.W., and Rahme, L.G. (2005). Profiling early infection responses: *Pseudomonas aeruginosa* eludes host defenses by suppressing antimicrobial peptide gene expression. *Proc Natl Acad Sci U S A* 102, 2573-2578.
72. McDonald, M.J., and Rosbash, M. (2001). Microarray analysis and organization of circadian gene expression in *Drosophila*. *Cell* 107, 567-578.
73. Michel, T., Reichhart, J.M., Hoffmann, J.A., and Royet, J. (2001). *Drosophila* Toll is activated by Gram-positive bacteria through a circulating peptidoglycan recognition protein. *Nature* 414, 756-759.
74. Garver, L.S., Wu, J., and Wu, L.P. (2006). The peptidoglycan recognition protein PGRP-SC1a is essential for Toll signaling and phagocytosis of *Staphylococcus aureus* in *Drosophila*. *Proc Natl Acad Sci U S A* 103, 660-665.
75. Mukae, N., Yokoyama, H., Yokokura, T., Sakoyama, Y., and Nagata, S. (2002). Activation of the innate immunity in *Drosophila* by endogenous chromosomal DNA that escaped apoptotic degradation. *Genes Dev* 16, 2662-2671.
76. Tsichritzis, T., Gaentzsch, P.C., Kosmidis, S., Brown, A.E., Skoulakis, E.M., Ligoxygakis, P., and Mosialos, G. (2007). A *Drosophila* ortholog of the human cylindromatosis tumor suppressor gene regulates triglyceride content and antibacterial defense. *Development* 134, 2605-2614.
77. Hultmark, D. (2003). *Drosophila* immunity: paths and patterns. *Curr Opin Immunol* 15, 12-19.
78. Sakai, T., Tamura, T., Kitamoto, T., and Kidokoro, Y. (2004). A clock gene, period, plays a key role in long-term memory formation in *Drosophila*. *Proc Natl Acad Sci U S A* 101, 16058-16063.

79. Schmid-Hempel, P. (2005). Evolutionary ecology of insect immune defenses. *Annu Rev Entomol* 50, 529-551.
80. Charlet, M., Lagueux, M., Reichhart, J.M., Hoffmann, D., Braun, A., and Meister, M. (1996). Cloning of the gene encoding the antibacterial peptide drosocin involved in *Drosophila* immunity. Expression studies during the immune response. *Eur J Biochem* 241, 699-706.
81. Jung, A.C., Cricqui, M.C., Rutschmann, S., Hoffmann, J.A., and Ferrandon, D. (2001). Microfluorometer assay to measure the expression of beta-galactosidase and green fluorescent protein reporter genes in single *Drosophila* flies. *Biotechniques* 30, 594-598, 600-591.
82. Rolff, J. (2002). Bateman's principle and immunity. *Proc Biol Sci* 269, 867-872.
83. Majercak, J., Chen, W.F., and Edery, I. (2004). Splicing of the period gene 3'-terminal intron is regulated by light, circadian clock factors, and phospholipase C. *Mol Cell Biol* 24, 3359-3372.
84. Hwangbo, D.S., Gershman, B., Tu, M.P., Palmer, M., and Tatar, M. (2004). *Drosophila* dFOXO controls lifespan and regulates insulin signalling in brain and fat body. *Nature* 429, 562-566.
85. Hedengren, M., Asling, B., Dushay, M.S., Ando, I., Ekengren, S., Wihlborg, M., and Hultmark, D. (1999). Relish, a central factor in the control of humoral but not cellular immunity in *Drosophila*. *Mol Cell* 4, 827-837.
86. McGuire, S.E., Mao, Z., and Davis, R.L. (2004). Spatiotemporal gene expression targeting with the TARGET and gene-switch systems in *Drosophila*. *Sci STKE* 2004, pl6.
87. Giannakou, M.E., Goss, M., Jacobson, J., Vinti, G., Leivers, S.J., and Partridge, L. (2007). Dynamics of the action of dFOXO on adult mortality in *Drosophila*. *Aging Cell* 6, 429-438.
88. Roman, G., Endo, K., Zong, L., and Davis, R.L. (2001). P[Switch], a system for spatial and temporal control of gene expression in *Drosophila melanogaster*. *Proc Natl Acad Sci U S A* 98, 12602-12607.

89. Blau, J., and Young, M.W. (1999). Cycling *vrille* expression is required for a functional *Drosophila* clock. *Cell* 99, 661-671.
90. Kaneko, M., and Hall, J.C. (2000). Neuroanatomy of cells expressing clock genes in *Drosophila*: transgenic manipulation of the period and timeless genes to mark the perikarya of circadian pacemaker neurons and their projections. *J Comp Neurol* 422, 66-94.
91. Osterwalder, T., Yoon, K.S., White, B.H., and Keshishian, H. (2001). A conditional tissue-specific transgene expression system using inducible GAL4. *Proc Natl Acad Sci U S A* 98, 12596-12601.
92. Bhakar, A.L., Tannis, L.L., Zeindler, C., Russo, M.P., Jobin, C., Park, D.S., MacPherson, S., and Barker, P.A. (2002). Constitutive nuclear factor-kappa B activity is required for central neuron survival. *J Neurosci* 22, 8466-8475.
93. Brogden, K.A., Guthmiller, J.M., Salzet, M., and Zasloff, M. (2005). The nervous system and innate immunity: the neuropeptide connection. *Nat Immunol* 6, 558-564.
94. Kim, E.Y., Ko, H.W., Yu, W., Hardin, P.E., and Edery, I. (2007). A DOUBLETIME kinase binding domain on the *Drosophila* PERIOD protein is essential for its hyperphosphorylation, transcriptional repression, and circadian clock function. *Mol Cell Biol* 27, 5014-5028.
95. Edery, I. (2000). Circadian rhythms in a nutshell. *Physiol Genomics* 3, 59-74.
96. Dunlap, J.C. (1999). Molecular bases for circadian clocks. *Cell* 96, 271-290.
97. Gallego, M., and Virshup, D.M. (2007). Post-translational modifications regulate the ticking of the circadian clock. *Nat Rev Mol Cell Biol* 8, 139-148.
98. Duffield, G.E. (2003). DNA microarray analyses of circadian timing: the genomic basis of biological time. *J Neuroendocrinol* 15, 991-1002.
99. Etter, P.D., and Ramaswami, M. (2002). The ups and downs of daily life: profiling circadian gene expression in *Drosophila*. *Bioessays* 24, 494-498.

100. Vitalini, M.W., de Paula, R.M., Park, W.D., and Bell-Pedersen, D. (2006). The rhythms of life: circadian output pathways in *Neurospora*. *J Biol Rhythms* 21, 432-444.
101. Fu, L., and Lee, C.C. (2003). The circadian clock: pacemaker and tumour suppressor. *Nat Rev Cancer* 3, 350-361.
102. McClung, C.A. (2007). Circadian genes, rhythms and the biology of mood disorders. *Pharmacol Ther* 114, 222-232.
103. Staels, B. (2006). When the Clock stops ticking, metabolic syndrome explodes. *Nat Med* 12, 54-55; discussion 55.
104. Hall, J.C. (2003). Genetics and molecular biology of rhythms in *Drosophila* and other insects. *Adv Genet* 48, 1-280.
105. Bushati, N., and Cohen, S.M. (2007). microRNA Functions. *Annu Rev Cell Dev Biol* 23, 175-205.
106. Bagga, S., Bracht, J., Hunter, S., Massirer, K., Holtz, J., Eachus, R., and Pasquinelli, A.E. (2005). Regulation by let-7 and lin-4 miRNAs results in target mRNA degradation. *Cell* 122, 553-563.
107. Jackson, R.J., and Standart, N. (2007). How do microRNAs regulate gene expression? *Sci STKE* 2007, re1.
108. Valencia-Sanchez, M.A., Liu, J., Hannon, G.J., and Parker, R. (2006). Control of translation and mRNA degradation by miRNAs and siRNAs. *Genes Dev* 20, 515-524.
109. Lewis, B.P., Burge, C.B., and Bartel, D.P. (2005). Conserved seed pairing, often flanked by adenosines, indicates that thousands of human genes are microRNA targets. *Cell* 120, 15-20.
110. Ambros, V. (2004). The functions of animal microRNAs. *Nature* 431, 350-355.
111. Gesellchen, V., and Boutros, M. (2004). Managing the genome: microRNAs in *Drosophila*. *Differentiation* 72, 74-80.

112. Jaubert, S., Mereau, A., Antoniewski, C., and Tagu, D. (2007). MicroRNAs in *Drosophila*: The magic wand to enter the Chamber of Secrets? *Biochimie* 89, 1211-1220.
113. Rutila, J.E., Suri, V., Le, M., So, W.V., Rosbash, M., and Hall, J.C. (1998). CYCLE is a second bHLH-PAS clock protein essential for circadian rhythmicity and transcription of *Drosophila* period and timeless. *Cell* 93, 805-814.
114. Helfrich-Forster, C. (2005). Neurobiology of the fruit fly's circadian clock. *Genes Brain Behav* 4, 65-76.
115. Hardin, P.E., Hall, J.C., and Rosbash, M. (1990). Feedback of the *Drosophila* period gene product on circadian cycling of its messenger RNA levels. *Nature* 343, 536-540.
116. Goff, L.A., Yang, M., Bowers, J., Getts, R.C., Padgett, R.W., and Hart, R.P. (2005). Rational probe optimization and enhanced detection strategy for microRNAs using microarrays. *RNA Biol* 2, 93-100.
117. Glossop, N.R., Lyons, L.C., and Hardin, P.E. (1999). Interlocked feedback loops within the *Drosophila* circadian oscillator. *Science* 286, 766-768.
118. Grimson, A., Farh, K.K., Johnston, W.K., Garrett-Engle, P., Lim, L.P., and Bartel, D.P. (2007). MicroRNA targeting specificity in mammals: determinants beyond seed pairing. *Mol Cell* 27, 91-105.
119. Ceriani, M.F., Hogenesch, J.B., Yanovsky, M., Panda, S., Straume, M., and Kay, S.A. (2002). Genome-wide expression analysis in *Drosophila* reveals genes controlling circadian behavior. *J Neurosci* 22, 9305-9319.
120. Claridge-Chang, A., Wijnen, H., Naef, F., Boothroyd, C., Rajewsky, N., and Young, M.W. (2001). Circadian regulation of gene expression systems in the *Drosophila* head. *Neuron* 32, 657-671.
121. Keegan, K.P., Pradhan, S., Wang, J.P., and Allada, R. (2007). Meta-Analysis of *Drosophila* Circadian Microarray Studies Identifies a Novel Set of Rhythmically Expressed Genes. *PLoS Comput Biol* 3, e208.
122. Lin, Y., Han, M., Shimada, B., Wang, L., Gibler, T.M., Amarakone, A., Awad,

- T.A., Stormo, G.D., Van Gelder, R.N., and Taghert, P.H. (2002). Influence of the period-dependent circadian clock on diurnal, circadian, and aperiodic gene expression in *Drosophila melanogaster*. *Proc Natl Acad Sci U S A* 99, 9562-9567.
123. Ueda, H.R., Matsumoto, A., Kawamura, M., Iino, M., Tanimura, T., and Hashimoto, S. (2002). Genome-wide transcriptional orchestration of circadian rhythms in *Drosophila*. *J Biol Chem* 277, 14048-14052.
 124. Wijnen, H., Naef, F., and Young, M.W. (2005). Molecular and statistical tools for circadian transcript profiling. *Methods Enzymol* 393, 341-365.
 125. Bae, K., Lee, C., Sidote, D., Chuang, K.Y., and Edery, I. (1998). Circadian regulation of a *Drosophila* homolog of the mammalian Clock gene: PER and TIM function as positive regulators. *Mol Cell Biol* 18, 6142-6151.
 126. Kadener, S., Stoleru, D., McDonald, M., Nawathean, P., and Rosbash, M. (2007). Clockwork Orange is a transcriptional repressor and a new *Drosophila* circadian pacemaker component. *Genes Dev* 21, 1675-1686.
 127. Lim, C., Chung, B.Y., Pitman, J.L., McGill, J.J., Pradhan, S., Lee, J., Keegan, K.P., Choe, J., and Allada, R. (2007). Clockwork orange encodes a transcriptional repressor important for circadian-clock amplitude in *Drosophila*. *Curr Biol* 17, 1082-1089.
 128. Matsumoto, A., Ukai-Tadenuma, M., Yamada, R.G., Houl, J., Uno, K.D., Kasukawa, T., Dauwalder, B., Itoh, T.Q., Takahashi, K., Ueda, R., Hardin, P.E., Tanimura, T., and Ueda, H.R. (2007). A functional genomics strategy reveals clockwork orange as a transcriptional regulator in the *Drosophila* circadian clock. *Genes Dev* 21, 1687-1700.
 129. Kloss, B., Rothenfluh, A., Young, M.W., and Saez, L. (2001). Phosphorylation of period is influenced by cycling physical associations of double-time, period, and timeless in the *Drosophila* clock. *Neuron* 30, 699-706.
 130. Hobert, O. (2004). Common logic of transcription factor and microRNA action. *Trends Biochem Sci* 29, 462-468.
 131. Hardin, P.E. (2005). The circadian timekeeping system of *Drosophila*. *Curr Biol* 15, R714-722.

132. Venturini, L., Battmer, K., Castoldi, M., Schultheis, B., Hochhaus, A., Muckenthaler, M.U., Ganser, A., Eder, M., and Scherr, M. (2007). Expression of the miR-17-92 polycistron in chronic myeloid leukemia (CML) CD34+ cells. *Blood* 109, 4399-4405.
133. Xu, S., Witmer, P.D., Lumayag, S., Kovacs, B., and Valle, D. (2007). MicroRNA (miRNA) transcriptome of mouse retina and identification of a sensory organ-specific miRNA cluster. *J Biol Chem* 282, 25053-25066.
134. Stark, A., Lin, M.F., Kheradpour, P., Pedersen, J.S., Parts, L., Carlson, J.W., Crosby, M.A., Rasmussen, M.D., Roy, S., Deoras, A.N., Ruby, J.G., Brennecke, J., Hodges, E., Hinrichs, A.S., Caspi, A., Paten, B., Park, S.W., Han, M.V., Maeder, M.L., Polansky, B.J., Robson, B.E., Aerts, S., van Helden, J., Hassan, B., Gilbert, D.G., Eastman, D.A., Rice, M., Weir, M., Hahn, M.W., Park, Y., Dewey, C.N., Pachter, L., Kent, W.J., Haussler, D., Lai, E.C., Bartel, D.P., Hannon, G.J., Kaufman, T.C., Eisen, M.B., Clark, A.G., Smith, D., Celniker, S.E., Gelbart, W.M., Kellis, M., Crosby, M.A., Matthews, B.B., Schroeder, A.J., Gramates, L.S., St Pierre, S.E., Roark, M., Wiley, K.L., Jr., Kulathinal, R.J., Zhang, P., Myrick, K.V., Antone, J.V., Gelbart, W.M., Carlson, J.W., Yu, C., Park, S., Wan, K.H., and Celniker, S.E. (2007). Discovery of functional elements in 12 *Drosophila* genomes using evolutionary signatures. *Nature* 450, 219-232.
135. Cheng, H.Y., Papp, J.W., Varlamova, O., Dziema, H., Russell, B., Curfman, J.P., Nakazawa, T., Shimizu, K., Okamura, H., Impey, S., and Obrietan, K. (2007). microRNA modulation of circadian-clock period and entrainment. *Neuron* 54, 813-829.
136. Zeng, H., Hardin, P.E., and Rosbash, M. (1994). Constitutive overexpression of the *Drosophila* period protein inhibits period mRNA cycling. *Embo J* 13, 3590-3598.
137. Chen, W.F., Majercak, J., and Edery, I. (2006). Clock-gated photic stimulation of timeless expression at cold temperatures and seasonal adaptation in *Drosophila*. *J Biol Rhythms* 21, 256-271.
138. Zuany-Amorim, C., Hastewell, J., and Walker, C. (2002). Toll-like receptors as potential therapeutic targets for multiple diseases. *Nat Rev Drug Discov* 1, 797-807.
139. Beutler, B., and Rietschel, E.T. (2003). Innate immune sensing and its roots:

the story of endotoxin. *Nat Rev Immunol* 3, 169-176.

140. Tsiotou, A.G., Sakorafas, G.H., Anagnostopoulos, G., and Bramis, J. (2005). Septic shock; current pathogenetic concepts from a clinical perspective. *Med Sci Monit* 11, RA76-85.
141. Mathias, S., Schiffelholz, T., Linthorst, A.C., Pollmacher, T., and Lancel, M. (2000). Diurnal variations in lipopolysaccharide-induced sleep, sickness behavior and changes in corticosterone levels in the rat. *Neuroendocrinology* 71, 375-385.
142. Zeng, H., Qian, Z., Myers, M.P., and Rosbash, M. (1996). A light-entrainment mechanism for the *Drosophila* circadian clock. *Nature* 380, 129-135.
143. Rolls, A., Shechter, R., London, A., Ziv, Y., Ronen, A., Levy, R., and Schwartz, M. (2007). Toll-like receptors modulate adult hippocampal neurogenesis. *Nat Cell Biol* 9, 1081-1088.
144. Cotter, R.L., Burke, W.J., Thomas, V.S., Potter, J.F., Zheng, J., and Gendelman, H.E. (1999). Insights into the neurodegenerative process of Alzheimer's disease: a role for mononuclear phagocyte-associated inflammation and neurotoxicity. *J Leukoc Biol* 65, 416-427.
145. Sternberg, E.M. (2006). Neural regulation of innate immunity: a coordinated nonspecific host response to pathogens. *Nat Rev Immunol* 6, 318-328.
146. Tracey, K.J. (2002). The inflammatory reflex. *Nature* 420, 853-859.
147. Sweeney, S.T., Broadie, K., Keane, J., Niemann, H., and O'Kane, C.J. (1995). Targeted expression of tetanus toxin light chain in *Drosophila* specifically eliminates synaptic transmission and causes behavioral defects. *Neuron* 14, 341-351.
148. Luan, H., Lemon, W.C., Peabody, N.C., Pohl, J.B., Zelensky, P.K., Wang, D., Nitabach, M.N., Holmes, T.C., and White, B.H. (2006). Functional dissection of a neuronal network required for cuticle tanning and wing expansion in *Drosophila*. *J Neurosci* 26, 573-584.
149. Baines, R.A., Uhler, J.P., Thompson, A., Sweeney, S.T., and Bate, M. (2001).

Altered electrical properties in *Drosophila* neurons developing without synaptic transmission. *J Neurosci* 21, 1523-1531.

150. Grether, M.E., Abrams, J.M., Agapite, J., White, K., and Steller, H. (1995). The head involution defective gene of *Drosophila melanogaster* functions in programmed cell death. *Genes Dev* 9, 1694-1708.
151. Johnson, R.W. (2002). The concept of sickness behavior: a brief chronological account of four key discoveries. *Vet Immunol Immunopathol* 87, 443-450.

CURRICULUM VITAE

Jung-Eun Lee

Academic Background

Ph. D. – 2008	Joint Graduate Program in Biochemistry, Graduate School - New Brunswick, Rutgers, The State University of New Jersey and Graduate School of Biomedical Sciences, University of Medicine and Dentistry of New Jersey, New Brunswick, NJ
M. S. – 1996	Department of Life Science, Pohang University of Science and Technology, Pohang, Korea
B. S. – 1994	Department of Life Science, Pohang University of Science and Technology, Pohang, Korea

Research Experience

1996	Research scientist, Samsung Biomedical Research Institute, Seoul, Korea
1997 – 1999	Research scientist, Department of Biology, Yonsei University, Seoul, Korea

Publications

1. **Lee, JE**, and Edery, I. (2008). Circadian Regulation in the Ability of *Drosophila* to Combat Pathogenic Infections. *Current Biology* 18, 195-199.
2. Yang, M*, **Lee, JE***, Padgett, RW, and Edery, I. (2008). Circadian regulation of a limited set of conserved microRNAs in *Drosophila*. *BMC Genomics* 9, 83. (***Co-first authors**)
3. Kim, HE, Yoon, SY, **Lee, JE**, Choi, WS, Jin, BK, Oh, TH, Markelonis, GJ, Chun, SY, and Oh, YJ. (2001). MPP(+) downregulates mitochondrially encoded gene transcripts and their activities in dopaminergic neuronal cells: protective role of Bcl-2. *Biochem Biophys Res Commun* 286, 659-665.
4. Gho, YS, **Lee, JE**, Oh, KS, Bae, DG, and Chae, CB. (1997). Development of antiangiogenin peptide using a phage-displayed peptide library. *Cancer Research* 57, 3733-3740.